e-Jurnal Sains Nuklear Malaysia, 2023, Vol. 35 (No.1): 1 – 10
*eISSN: 2232-0946*

# OPTIMIZATION OF GAMMA IRRADIATION DOSE FOR MAS COTEK AS RAW MATERIAL FOR PHYTOPHARMACEUTICAL PRODUCT

***Daryl Jesus Arapoc[1], Rosniza Razali[1], Zainah Adam[1], Azfar Hanif Bin Abd Aziz[1], Nurmaziah Binti Mohammad Shafie[1], Abang Abdul Rahim Ossen[1] and Veshalini Kasiraja[2]***

[1]Medical Technology Group, Malaysian Nuclear Agency,
43000 Kajang, Selangor, MALAYSIA.
[2]Faculty of Medicine, Universiti Sultan Zainal Abidin, Medical Campus,
20400 Kuala Terengganu, Terengganu, MALAYSIA.
*Correspondence author: daryl@nm.gov.my

## *ABSTRACT*

*Microbial contamination in final product prone to occur in herbal raw material due to the presence of microorganisms in the environment. This may cause a shorter shelf life of the products and lead to undesirable effects on consumer. Mas Cotek, scientifically known as Ficus deltoidea is being utilised as a medication for several medical conditions throughout the Malay Archipelago. This study was conducted to identify the optimum gamma irradiation dose for sterilization of Mas Cotek raw material in order to achieve the acceptable microbiological limits without affecting the quality of raw materials. Besides, the content of vitexin in Mas Cotek with different gamma irradiation dose were also evaluated using Ultra High Performance Liquid Chromatography (UHPLC). Controlled exposure of gamma irradiation (0 kGy, 3 Gy, 6 kGy, 9 kGy and 12 kGy) were exposed to the raw material. Moreover, the specified dose is expected to reduce the bioburden to the desired level concurrently minimizing the effect on the product. Upon irradiation process, the raw materials were extracted and assessment such as antioxidant status, phenolic content, total anti-microbial content, and total yeast content were done. The results shown that, there were significant different in phytochemical component and antioxidant activity status in accordance to difference doses of gamma irradiation. Total aerobic microbial count (TAMC) and total yeast microbial count (TYMC) also showed a significantly reduced in irradiated raw material at higher dose. The vitexin content were found varies depending on the gamma irradiation doses respectively. In conclusion, gamma irradiation on raw material of Mas Cotek will decreases the number of microbial burdens. However, gamma irradiation with different dose also have varies impact on the content of vitexin in Mas Cotek.*

**Keywords:** Mas Cotek, Gamma Irradiation, Phytochemical, Antioxidant Activity.

## INTRODUCTION

Herbal medicine usage has expanded globally in recent years due to their efficacy, low toxicity, and few adverse effects (Adu-Gyamfi et al., 2014). The world health organisation (WHO) has claimed that almost 74% of 119 plant-originated medicines are being utilised in modern medicine (Banik et al., 2020). Since the use of herbal medicine grows, there is a serious concern on the microbial contamination that prone to occur at any step of harvest, storage, or herbal medicine preparation (Alijaniha et al., 2021). To support the medical herb industries, medicinal herb preservation management is required to minimise mould and bacterial contamination. Thus, to ensure the availability of hygienic medicinal herbs for the consumer, a treatment is required to minimise bacterial, mould, and yeast contamination (Katrin et al., 2011). Decontamination techniques include steam treatment, microwave heating, and radiofrequency heat therapy. Electron beams, X-rays, and gamma ray's irradiation has also been utilised. Numerous investigations on the effectiveness and efficiency of various approaches have been undertaken (Molnár et al., 2018).

Gamma irradiation is getting prominence as among the most promising and extensively utilised ways of decontaminating foods and herbal materials (Ernawati et al., 2021). Gamma irradiation exposes the target material to light packets (photons) that are so energetic (gamma rays) that they destroy the DNA strands found in microorganisms. Consequently, the impacted bacteria are unable to proliferate and enhance the shelf life of perishable goods in storage packaging (Hazekamp, 2016; Katrin et al., 2011). Gamma irradiation is favoured over other techniques of decontamination as it effectively destroys bacteria while leaving no chemical residues, allowing it hygienic and environmentally friendly. In addition, water radiolysis can be triggered by gamma irradiation, generates reactive oxygen species (ROS). Free radicals, particularly •OH, predominantly damage DNA and other macromolecules, resulting in microorganism destruction. However, these free radicals can influence the plant's ROS and antioxidant levels, degrade or alter bioactive components, and drive phenolic compound accumulation. Nevertheless, the effect of gamma irradiation on phenolic compounds and antioxidant activity will be dose dependent (Ernawati et al., 2021).

*Ficus deltoidea* also commonly known as Mas Cotek, is being utilised as a medicine besides being marketed and produced as capsules, tea, and tonic tea across Malaysia. Mas Cotek has been claimed to have beneficial pharmacological applications as an anti-diabetic, anti-inflammatory, antinociceptive, anti-melanogenic, antiphotoaging, antioxidant, antiulcerogenic, and antibacterial agent (Bunawan et al., 2014). Previous phytochemical study revealed that this plant contains a wide range of secondary metabolites, including saponins, flavonoids, tannins, polyphenols, triterpenoids, and proanthocyanins (Akmalazura et al., 2020). Thus, the aim of this study is to evaluate the optimal gamma irradiation dose for sterilisation of Mas Cotek raw materials in order to meet approved microbiological limits without compromising raw material quality. Specifically, antioxidant capacities, total microbial content, yeast content and phenolic content besides vitexin content will be determined upon the gamma irradiation.

## MATERIALS AND METHO D

### Plant collection and authentication

The fresh Mas Cotek were harvested from Sungai Tengi Selatan, Selangor, Malaysia. The plant taxonomist from the Institute of Bioscience (IBS), Universiti Putra Malaysia authenticated the sample identification with a voucher specimen (SK1467/07).

### Gamma irradiation and plant extract preparation

Mas Cotek was washed with running water and dried at 50$^{O}$C. The samples were then pulverised before being subjected to dosages of 0, 3, 6, 9, and 12 kGy of Cobalt-60 radiation. The sample was then freeze dried at -80$^{O}$C to -20$^{O}$C overnight for 12 hours after being subjected to an accelerated solvent extraction (ASE) for extraction at 60$^{O}$C for 20 minutes.

### Total phenolic content (TPC)

The Folin-Ciocalteu method was used to determine the total phenolic content (TPC) of the Mas Cotek extracts. The double distilled water was used to dilute the test sample. The 0.1mL of Folin-Ciocalteu reagent was added to 0.2mL of 2% sodium carbonate ($Na_2CO_3$) and incubated for 3 hours. The absorbance was measured at 760nm against blank (Yang et al., 2011).

**Total flavonoid content (TFC)**

The total flavonoid concentration (TFC) of the Mas Cotek extract was assessed using the aluminium chloride colorimetric ($AlCl_3$) method. The test samples diluted in ethanol solution was mixed with 150µL of 2% $AlCl_3$ in 96 well plates and incubated for 15 minutes at room temperature. The absorbance was measured at 435nm against blank (Yang et al., 2011).

**DPPH free radical scavenging**

Direct hydrogen donation to the DPPH radical was utilized to quantify hydrogen-donating activity of Mas Cotek extract. The reaction mixtures in the 96-well plates were made up of the sample diluted in ethanol (100µL) and ethanol-dissolved DPPH radical (100 µL, 0.2 mM). After shaking, the mixture was allowed to stand in the dark for 15 minutes. The absorbance was then measured at 517 nm in comparison to a blank (Yang et al., 2011).

**Microbial burden test**

To count the microorganisms in Mas Cotek, TAMC and TYMC were undertaken. Using the surface spread plate method, 50µL of diluted samples were individually plated on tryptic soy agar (TSA) for TAMC and Sabauroud dextrose sugar (SDA) for TYMC and incubated at 37$^{O}$C for 24 hours. After incubation, the distinct colonies that developed on the agar plates were counted and represented as CFU/g, or colony forming units per gramme. The colony counts were recorded as the average of three separate samples, and the plating was carried out in triplicate.

**Vitexin content analysis**

Samples were weighed at 20 g and soaked in 200 mL of water and sonicated for 1 hour at 80ºC. The mixture was then filtered using vacuum filtration with 0.2 µm membrane filter. The filtered extract was dried using personal evaporator with HPLC mode. Vitexin content was analysed using Ultra High Performance Liquid Chromatography (UHPLC).

**Statistical analysis**

All the findings were presented as mean ± SD for a specific number of observations. The Statistical Package for the Social Sciences (SPSS) software was used to conduct the statistical analysis. The significant difference level was set at $p<0.05$.

## RESULTS

The therapeutic plants like herbs and spices are frequently highly contaminated with bacteria, fungus, moulds, and yeasts (Khawory et al., 2020). Both herbs and spices can quickly deteriorate items that influence health and claimed a huge concern on safety issues related to herbal medicines besides having an impact on the economy if left untreated (Hadiati et al., 2021; Khawory et al., 2020). The application of ionizing radiation such as gamma rays, which have been investigated for their efficacy in decontamination and their effects on the herbal ingredients and biological activities, is one of the most contentious approaches (Alijaniha et al., 2021). Mas Cotek has a long history of utilization in Malay traditional medicine to treat conditions including ulcers, wounds, and rheumatism as well as to promote a healthy pregnancy and treat diabetes (Bunawan et al., 2014). It is apparent that evaluating safety and its possible effects on the biological activity of natural products such as Mas

Cotek is of utmost importance given the widespread use of gamma irradiation as an effective way to disinfect and lengthen the shelf life of herbal items and consumables (Alijaniha et al., 2021).

Ionizing radiation such as gamma irradiation has the power to influence alterations in plant matter and secondary compounds on both a quantitative and qualitative level (Ja&rsquo & afar, 2019). The use of gamma irradiation in herbal medicines is now governed by general food irradiation laws because there is no special legislation governing it (Hadiati et al., 2021). According to previous studies, parasites like protozoa and helminths have been rendered inactive in meat products, fresh produce, and vegetables by low doses of gamma irradiation of less than 1 kGy. In the meanwhile, fresh, frozen, and dried foods and spices have been given medium dosages of 1–10 kGy to diminish or eradicate non-viral bacteria and lengthen the product shelf life. Additionally, strong doses of 10-60 kGy have been used to sterilise or reduce the number of bacteria in foods like dry components and meals for astronauts and hospital patients (Ernawati et al., 2021).

Table 1 below demonstrated the total phenolic and flavonoid content in gamma irradiated Mas Cotek extract. The highest phenolic content, 41.74 µg GAE/mg extract and highest flavonoid content, 189.33 µg QE/mg extract were observed in Mas Cotek extract irradiated with the dose of 3kGy, respectively. There was a significant difference between the total phenolic content of non-irradiated and gamma irradiated Mas Cotek sample at irradiation doses of 6 and 9 kGy. In addition, there was significant different between the total flavonoid content of non-irradiated and gamma irradiated Mas Cotek sample at all irradiation doses.

Table 1: Total phenolic and flavonoid content in non-irradiated and gamma irradiated Mas Cotek sample at different irradiation doses (mean ± SD).

| **Irradiation Doses (kGy)** | **Total Phenolic Content µg GAE/mg Extract** | **Total Flavonoid Content µg QE/mg Extract** |
|---|---|---|
| 0 | $39.74 \pm 0.23^{a}$ | $182.67 \pm 0.74^{a}$ |
| 3 | $41.74 \pm 1.26^{a}$ | $189.33 \pm 1.24^{b}$ |
| 6 | $33.74 \pm 1.12^{b}$ | $179.33 \pm 0.87^{c}$ |
| 9 | $35.06 \pm 0.80^{b}$ | $169.33 \pm 0.34^{d}$ |
| 12 | $39.74 \pm 0.70^{a}$ | $176.00 \pm 0.94^{e}$ |

$^{a,b,c,d,e}$: $p<0.05$ as compared between different gamma irradiation doses.

Since phenolic compounds are recognised as natural antioxidants, they have significant effects on lipid peroxidation inhibition, carcinogenesis inhibition, antibacterial activity, direct capillary constriction, naturally occurring phytohormones, and ascorbic acid stability. Based on this study, there were no significant difference of phenolic content between the Mas Cotek irradiated at multiple doses of gamma irradiation and non-irradiated samples. It is hypothesised that the release of phenolic compounds from glycosidic components and the breakdown of larger phenolic compounds into smaller ones may be responsible for the rise in total phenolics content brought on by gamma irradiation (Harrison & Were, 2007). Besides, according to Taheri et al., (2014), acute gamma irradiation at the dose of 20Gy showed higher content of total phenolic content in *Curcuma alismatifolia* leaves. Based on the previous studies, irradiation causes increased in total phenolic content of *Carulluma tuberculate*, almond skin, *Nigella sativa, Thymus vulgaris, Glycyrrhiza glabra*, pistachio green hull, clove, Curcuma alismatifolia, nutmeg, and soybean. However, it is also found that certain plants had lost their overall phenolic content upon gamma irradiation (Hadiati et al., 2021). Thus, the environmental factor, type and portions of the plant, the composition of the phenolic content, solvent and extraction techniques utilised, storage conditions, and the irradiation dose may all have a significant influences on how irradiation impacts total phenolic content (Hadiati et al., 2021; Harrison & Were, 2007; Khattak et al., 2008).

Flavonoid is a significant group of natural products and they are a group of secondary plant metabolites with a polyphenolic structure that are prevalent in vegetables and fruits. Similar to phenolic content, flavonoid content in natural and herbal medicines can be altered significant either by increasing or decreasing upon gamma irradiation (Hadiati et al., 2021). This is because, irradiation may contribute to making molecules more extractable, but it may also cause the breakdown of some less stable chemicals (Pereira et al., 2016). In addition, gamma radiation may interact with atoms and molecules to produce free radicals that have the power to alter crucial plant cell components. Depending on the irradiation dose, it has been shown that these radicals have an impact on the morphology, anatomy, biochemistry, and physiology of plants. The consequences include modifications to the plant's cellular structure and metabolism, such as thylakoid membrane dilatation, altered photosynthesis, altered antioxidant defences, and enhanced phenolic chemicals (Kavitha et al., 2015). According to research by Khatun et al., (2012), the total flavonoids content in bitter gourd increased significantly with increasing radiation dosage as compared to control sample. The increase in total flavonoid may influences the phenylalanine ammonialyase activity, which is one of the significant enzymes responsible in the production of phenolic compounds in plant tissue.

The DPPH scavenging activity of the gamma irradiated Mas Cotek extract irradiated with multiple doses were presented in Figure 1 in form of percentage of DPPH radical inhibition. Based on the result obtained, the highest DPPH radical inhibition with 54.91% was observed in Mas Cotek irradiated at dose of 6kGy, whereas lowest DPPH radical inhibition was obtained at the irradiation dose of 9kGy at 50.75%. This study signified that there was no significant difference between percentage of DPPH radical inhibition among Mas Cotek sample irradiated at different doses. However, there were significant difference between percentage of DPPH radical inhibition of Mas Cotek sample irradiated at different doses and ascorbic acid.

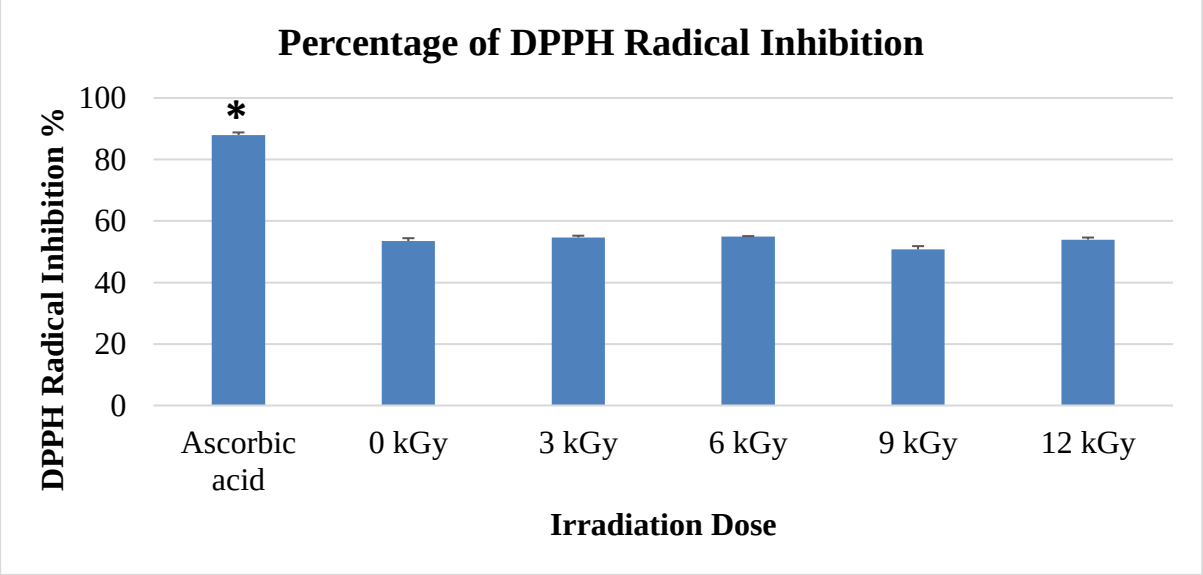


Figure 1: Effect of gamma irradiation dose on the DPPH scavenging activity of Mas Cotek and ascorbic acid (mean ± SD). *: showed a significant highest ($P<0.05$) compared to gamma irradiation dose on the DPPH scavenging activity of Mas Cotek.

The DPPH free radical scavenging assay was utilised to determine the antioxidant activity of both gamma irradiated and non-irradiated sample of Mas Cotek. An antioxidant assay based on electron transfer; the DPPH (2,2-diphenyl-1-picryl-hydrazyl-hydrate) free radical approach generates a violet solution in ethanol. In the presence of an antioxidant molecule, this free radical, which is stable at room temperature, is reduced, producing a colourless ethanol solution (Garcia et al., 2012). As a result, up to the greatest dose, gamma irradiation has no effect on the free radical scavenging capabilities of sample. Based on previous study, it is observed that radiation therapy within a dosage of 10 kGy had no effect on the free radical scavenging activity of tea (Mishra et al., 2006). Besides, the antioxidant activity of methanol extracts from an irradiated plant of *Rosmarinus officinalis* remained the same as in the control in a DPPH test (Gumus et al., 2011). The discrepancies in the effect of gamma irradiation on the free radical scavenging activity of plants might be attributed to changes in their chemical makeup, extraction solvent, and other factors (Gumus et al., 2011).

Table 2 below showed the microbial content in non-irradiated and gamma irradiated Mas Cotek. The total aerobic microbes and yeast/mould content were higher in non-irradiated Mas Cotek sample compared to the gamma irradiated Mas Cotek sample at the irradiation dose of 3kGy. However, both aerobic microbes and yeast were not detected in Mas Cotek samples that have been irradiated at the dose of 6,9 and 12 kGy.

Table 2: Microbial burden measurements in non-irradiated and gamma irradiated Mas Cotek extract at different irradiation doses.

| **Irradiation Doses (kGy)** | **TAMC (CFU/g or CFU/mL)** | **TYMC (CFU/g or CFU/mL)** |
|---|---|---|
| 0 | $7.46x10^{6}$ | $5.14x10^{4}$ |
| 3 | $2.39x10^{2}$ | $1.86x10^{2}$ |
| 6 | NA | NA |
| 9 | NA | NA |
| 12 | NA | NA |

Both the total anaerobic microbes, yeast/ fungi content reduced significantly in irradiated samples and were not detected as the gamma irradiation doses increased. Irradiation has a multitude of physical and biochemical impacts on microorganisms. Microorganisms are destroyed primarily due to the hydroxyl radicals formed within their cells react with the base and sugar moieties of DNA, causing sugar-phosphate bonds to break and lost the replication function. The chromosomal volume of an organism determines its sensitivity to irradiation. This is because, differences in irradiation sensitivity may be attributable to the capacity to repair nucleic acid damage rather than the nucleic acids intrinsic irradiation resistance. The amount of chemical change in radiation-sterilised foods is minimal and uniform *(Gamma Irradiation as a Treatment to Address Pathogens of Animal Biosecurity Concern Final Policy Review*, 2014).

Effect of gamma irradiation doses at doses 0, 3, 6, 9 and 12 kGy on the content of vitexin in Mas Cotek extract were analyzed using UHPLC system. Table 3 presented the concentration of vitexin found in Mas Cotek samples that have been subjected to gamma irradiation of different doses. Results show that the vitexin content are 9.21 ng/mL, 13.19 ng/mL, 18.91 ng/mL, 10.40 ng/mL and 9.48 ng/mL for 0 kGy, 3 kGy, 6 Gy, 9 kGy and 12 kGy gamma irradiation doses respectively. Based on this result, it was found that gamma irradiation with different doses has resulted in varying vitexin content in Mas Cotek extract. Vitexin content shows the highest yield at a dose of 6 kGy compared to other doses.

Table 3: Concentration of vitexin (ng/mL) in non-irradiated and gamma irradiated Mas Cotek sample at different irradiation doses.

| Irradiation Doses (kGy) | Concentration of Vitexin (ng/mL) |
|---|---|
| 0 | 9.21 |
| 3 | 13.19 |
| 6 | 18.90 |
| 9 | 10.40 |
| 12 | 9.48 |

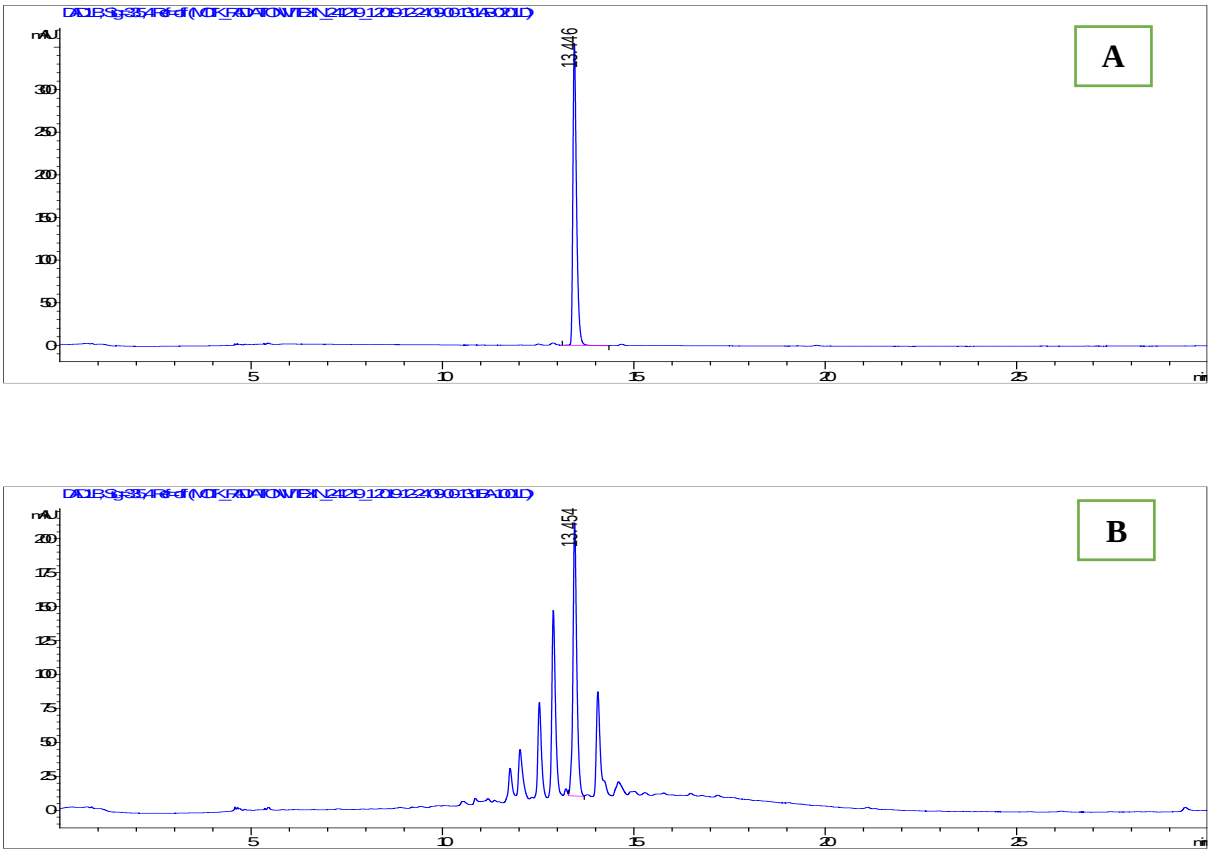


Figure 2: HPLC chromatograms of vitexin concentration (ng/mL) in non-irradiated and gamma irradiated Mas Cotek sample at different irradiation doses. (A) Standard vitexin; (B) Vitexin concentration obtained in non-irradiated and gamma irradiated Mas Cotek sample at different irradiation doses.

Besides, gamma irradiation with different doses has varying vitexin content in Mas Cotek extract. Vitexin is an apigenin flavone glycoside found in ethnomedicinal plants that has antioxidant properties against reactive oxygen species, lipid peroxidation, and other oxidative damages in a number of oxidative stress related disorders, with potential molecular and cellular pathways (Babaei et al., 2020). The varying concentration of vitexin is obtained among different doses of gamma irradiated Mas Cotek because, the micronutrients will be destroyed to varying degrees depending on their capacity to compete for primary radicals with other main components, as well as the irradiation circumstances, including dosage. The irradiation treatment has no effect on the nutritional value or digestibility of macronutrients. Certain micronutrients are vulnerable to irradiation, even though the amount depends on the food's composition as well as processing and storage circumstances (*Gamma Irradiation as a Treatment to Address Pathogens of Animal Biosecurity Concern Final Policy Review*, 2014).

## CONCLUSION

Gamma irradiation, as a food processing technique performed on the Mas Cotek samples did not affect the quality of raw material and reduce the bioburden significantly. However, gamma irradiation affects the content of selected targeted compound, vitexin quantitatively. Thus, this gamma irradiation method can ensure the prolong self-life of the product being exposed at an optimum dosage. However, further studies should be perform to determine the effectiveness of medicinal properties of Mas Cotek upon irradiation and examine the radiolytic by product of irradiation in irradiated Mas Cotek samples.

## ACKNOWLEDGEMENT

The authors would like to acknowledge and wish thanks to the Malaysian Nuclear Agency for providing the facilities besides funding for this study.

## CONFLICTS OF INTEREST

The authors declare no conflict of interest.

## REFERENCES

Adu-Gyamfi, A., Appiah, V., & Nketsia-Tabiri, J. (2014). *Preliminary studies on decontamination of some dried herbal products by gamma irradiation*. *8*(2), 116–120. https://doi.org/10.5897/JMPR10.247

Akmalazura, J., & Nabila A.S., (2020). The antioxidant activities, cytotoxic properties, and identification of water soluble compounds of Ficus deltoidea leaves. 1-20. https://doi.org/ 10.7717/peerj.5694

Alijaniha, F., Emadi, F., Naseri, M., Kamalinejad, M., Motevaseli, E., soodi, M., & Karimi, R. (2021). Effect of gamma irradiation on cytotoxicity, phenolics content and acute toxicity of Cuscuta chinensis L. extract. *Radiation Physics and Chemistry*, *185*, 109508. https://doi.org/10.1016/J.RADPHYSCHEM.2021.109508

Babaei, F., Moafizad, A., Darvishvand, Z., Mirzababaei, M., Hosseinzadeh, H., & Nassiri-Asl, M. (2020). Review of the effects of vitexin in oxidative stress-related diseases. *Food Science & Nutrition*, *8*(6), 2569. https://doi.org/10.1002/FSN3.1567

Banik, B., Das, S., Das, M. K., Malay Das, C. K., & Kumar Das, M. (n.d.). Medicinal Plants with Potent Anti-inflammatory and Anti-arthritic Properties found in Eastern Parts of the Himalaya: An Ethnomedicinal Review. *Pharmacognosy Reviews*, *14*(28), 121–137. https://doi.org/10.5530/phrev.2020.14.16

Bunawan, H., Amin, N. M., Bunawan, S. N., Baharum, S. N., & Mohd Noor, N. (2014). Ficus deltoidea jack: A review on its phytochemical and pharmacological importance. *Evidence-Based Complementary and Alternative Medicine*, *2014*. https://doi.org/10.1155/2014/902734

Ernawati, Suryadi, H., & Mun'im, A. (2021). Effect of gamma irradiation on the caffeoylquinic acid derivatives content, antioxidant activity, and microbial contamination of Pluchea indica leaves. *Heliyon*, *7*(8), e07825. https://doi.org/10.1016/J.HELIYON.2021.E07825

*Gamma irradiation as a treatment to address pathogens of animal biosecurity concern Final policy review*. (2014). Department of Agriculture (2014), Gamma irradiation as a treatment to address pathogens of animal biosecurity concern, Department of Agriculture, Canberra. retrieved from agriculture.gov.au/ba.

Garcia, E. J., Cadorin Oldoni, T. L., de Alencar, S. M., Reis, A., Loguercio, A. D., & Miranda Grande, R. H. (2012). Antioxidant activity by DPPH assay of potential solutions to be applied on bleached teeth. *Brazilian Dental Journal*, *23*(1), 22–27. https://doi.org/10.1590/S0103-64402012000100004

Gumus, T., Albayrak, S., Sagdic, O., & Arici, M. (2011). Effect of Gamma Irradiation on Total Phenolic Contents and Antioxidant Activities of Satureja Hortensis, Thymus Vulgaris, and Thymbra Spicata from Turkey. *Http://Dx.Doi.Org/10.1080/10942910903453397*, *14*(4), 830–839. https://doi.org/10.1080/10942910903453397

Hadiati, S. W., Winarno, H., & Pramono, S. (2021). Gamma irradiation as suitable preservation method on herbal medicine: A review. *Food Research*, *5*(5), 33–42. https://doi.org/10.26656/FR.2017.5(5).494

Harrison, K., & Were, L. M. (2007). Effect of gamma irradiation on total phenolic content yield and antioxidant capacity of Almond skin extracts. *Food Chemistry*, *102*(3), 932–937. https://doi.org/10.1016/J.FOODCHEM.2006.06.034

Hazekamp, A. (2016). Evaluating the effects of gamma-irradiation for decontamination of medicinal cannabis. *Frontiers in Pharmacology*, *7*(APR), 108. https://doi.org/10.3389/FPHAR.2016.00108/BIBTEX

International Atomic Energy Agency (IAEA). (2020). Food irradiation, benefits, use, standards. Retrieved on June 18, 2020, from IAEA Website: https://www.iaea.org/topics/food-irradiation

Ja&rsquo, N.-L., & afar. (2019). Total Antioxidant Activity and Enzymatic Inhibition against Alpha-
Amylase, Alpha-Glucosidase and Pancreatic Lipase of Irradiated Archidendron bubalinum. *Malaysian Journal of Medicine and Health Sciences*, 120–128. http://dx.doi.org/

Kavitha, C., Kuna, A., Supraja, T., Sagar, S. B., Padmavathi, T. V. N., & Prabhakar, N. (2015). Effect of gamma irradiation on antioxidant properties of ber (Zizyphus mauritiana) fruit. *Journal of Food Science and Technology*, *52*(5), 3123. https://doi.org/10.1007/S13197-014-1359-X

Katrin, E., Yulianti, M., & Winarno, H. (2011). Effectiveness of gamma irradiation for decontamination of microbes on tea parasite herb Scurrula atropurpurea (Bl.) dans. *Atom Indonesia*, *37*(3), 107–112. https://doi.org/10.17146/AIJ.2011.77

Khattak, K. F., Simpson, T. J., & Ihasnullah. (2008). Effect of gamma irradiation on the extraction yield, total phenolic content and free radical-scavenging activity of Nigella staiva seed. *Food Chemistry*, *110*(4), 967–972. https://doi.org/10.1016/J.FOODCHEM.2008.03.003

Khatun, A., Hossain, A., Islam, M. S., Hossain, A., Munshi, K., & Huque, R. (2012). Effect of gamma radiation on antioxidant marker and microbial safety of fresh bitter gourd (Momordica charantia L.). *Undefined*.

Khawory, M. H., Amat Sain, A., Rosli, M. A. A., Ishak, M. S., Noordin, M. I., & Wahab, H. A. (2020). Effects of gamma radiation treatment on three different medicinal plants: Microbial limit test, total phenolic content, in vitro cytotoxicity effect and antioxidant assay. *Applied Radiation and Isotopes : Including Data, Instrumentation and Methods for Use in Agriculture, Industry and Medicine*, *157*. https://doi.org/10.1016/J.APRADISO.2019.109013

Molnár, H., Bata-Vidács, I., Baka, E., Cserhalmi, Z., Ferenczi, S., Tömösközi-Farkas, R., Adányi, N., & Székács, A. (2018). The effect of different decontamination methods on the microbial load, bioactive components, aroma and colour of spice paprika. *Food Control*, *83*, 131–140. https://doi.org/10.1016/J.FOODCONT.2017.04.032

Mishra, B. B., Gautam, S., & Sharma, A. (2006). Microbial decontamination of tea (Camellia sinensis) by gamma radiation. *Journal of Food Science*, *71*(6). https://doi.org/10.1111/J.1750-3841.2006.00057.X

Pereira, E., Barros, L., Antonio, A. L., Cabo Verde, S., Santos-Buelga, C., & Ferreira, I. C. F. R. (2016). Infusions from Thymus vulgaris L. treated at different gamma radiation doses: Effects on antioxidant activity and phenolic composition. *LWT*, *74*, 34–39. https://doi.org/10.1016/J.LWT.2016.07.027

Taheri, S., Abdullah, T. L., Karimi, E., Oskoueian, E., & Ebrahimi, M. (2014). Antioxidant Capacities and Total Phenolic Contents Enhancement with Acute Gamma Irradiation in Curcuma alismatifolia (Zingiberaceae) Leaves. *International Journal of Molecular Sciences*, *15*(7), 13077. https://doi.org/10.3390/IJMS150713077

Yang, H., Dong, Y., Du, H., Shi, H., Peng, Y., & Li, X. (2011). Antioxidant Compounds from Propolis Collected in Anhui, China. *Molecules*, *16*(4), 3444. https://doi.org/10.3390/MOLECULES16043444

e-Jurnal Sains Nuklear Malaysia, 2023, Vol. 35 (No.1) : 11 – 21
*eISSN: 2232-0946*

# RADIOACTIVITY CONCENTRATION ASSOCIATED WITH CANCER RISK ARISING FROM THE CONSUMPTION OF PRE-MIX INSTANT PACKAGE BEVERAGE

***Yii Mei-Wo, Dainee Nor Fardzila Ahmad Tugi, Maziah Mahmud, Nor Aza Hassan and Mohamad Asri Ramli***

Radiochemistry and Environment Group
Waste and Environmental Technology Division
Malaysian Nuclear Agency, 43000 KAJANG, MALAYSIA
*Corresponding author: yii@nm.gov.my

***ABSTRACT***

*Beverage consumption containing radionuclides may contribute to radiation dose and poses a higher cancer risk to human. Studies were conducted to determine the concentration of radionuclides present in the pre-mix instant beverage. Based on the consumption rate by Malaysian adults, the annual effective dose and the associated cancer risk were estimated. The activity concentration was found to range between 63 to 1360 Bq/kg for $^{40}K$. For other natural radionuclides of $^{226}Ra$, $^{228}Ra$, $^{232}Th$, and $^{238}U$, it ranged between 0.88 – 6.43 Bq/kg, 0.83 – 8.48 Bq/kg, 0.62 – 5.73 Bq/kg and 2.64 –21.49 Bq/kg, respectively, whilst the artificial radionuclides were less than 2 Bq/kg. Calculated annual effective doses due to the intake of radionuclides by ingestion were between 44.6 – 170.0 µSv/y, with the potential of cancer risk incurrence between 16 to 59 cases in every 100,000 people.*

**Keywords:** Radionuclides, pre-mix beverage, effective dose, cancer risk

## INTRODUCTION

Modernization and technological advancement had changed the living style of humans in modern days. Nowadays, multi-flavour beverages can be easily found in the market. Among those, pre-mix instant beverages are also available where people just have to add hot water to it and can enjoy a cup of hot beverage instantly. According to the survey conducted by Institute for Public Health, (IPH, 2014), Malaysian adults consumed on average 51.8 g (2-3 packages) of pre-mix beverages per day. For the black coffee package, averaged 3 packs per day of 13.5 g.

The potential of radionuclide contamination in the diet requires assessment to ensure food safety. Radionuclides can originate from various sources; by human activities ($^{134}Cs$, $^{137}Cs$), such as the release from nuclear weapons testing or accidents, or naturally occurring, such as primordial ($^{40}K$, $^{226}Ra$, $^{228}Ra$, $^{232}Th$, $^{238}U$) in the earth crust or through cosmogenic formation (UNSCEAR, 2000). These radionuclides can enter the human body either through inhalation of radon gas or ingestion of contaminated food (IAEA, 1989; UNSCEAR, 2000; Afshari et al., 2009; Alharshan et al., 2017; Jemii and Mazouz, 2020). Ingestion of radioactive contaminated foods contributes a large fraction of internal radiation exposure (Baeza et al., 2004; UNSCEAR, 2008; Afshari et al., 2009; Alamoudi, 2013; Godyn´ et al., 2014; Desideri et al., 2014; Uwatse et al., 2015; Sahar et al., 2016). Therefore, food radioactivity and its associated dose assessment are necessary for establishing rules and regulations related to radiation protection (Alharshan et al., 2017).

Depending on the radionuclide's chemical properties, they will act differently inside the human body. For instance, radiums, which behaves like calcium, will be absorbed into bone and teeth (VKM, 2017). Prolonged internal exposure of humans to high levels of radium may produce bone and sinus cancers. Whilst, uranium, and thorium can get accumulated in the bone up to an extent of 70%

(UNSCEAR, 2000). On the other hand, potassium-40 will behave the same as other potassium isotopes in the environment, being assimilated into the tissues of all plants and animals through normal biological processes and then distributed uniformly in the human body (Baeza et al., 2004). Caesium which is in the same chemical group as potassium will be expected to behave similarly (VKM, 2017).

Sahar et al. (2016) reported that the concentration of natural radioactivity in food is often in the range of 40 to 600 Bq/kg of food while the artificial level varies depending on the incident and the level of exposure. The concentrations of $^{226}$Ra, $^{228}$Ra, $^{232}$Th and $^{238}$U radioactivity in different foods varies from <0.0004 – 9.4 Bq/kg, 0.038 – 0.32 Bq/kg, 0.0002 – 0.33 Bq/kg and 0.0001 – 2.9 Bq/kg, respectively (UNSCEAR, 2000). Priharti and Samat (2017) reported that natural radionuclide activity concentration ($^{226}$Ra, $^{232}$Th dan $^{40}$K) in staple food, vegetables, fruits and dishes in the central area of Malaysia varies from 0.45 – 5.64 Bq/kg, 0.39 – 4.40 Bq/kg, 75.39 – 1072.59 Bq/kg, respectively.

The total annual effective dose from natural radionuclides present within our human body works out to be approximately 0.3 mSv annually (Rao, 2012). Priharti and Samat (2017) also reported that annual dose exposure due to food intake from natural radionuclides of $^{232}$Th and $^{238}$U series, and $^{40}$K is 0.12 mSv and 0.17 mSv, respectively. A typical annual effective dose ranges from the ingestion of foods ranging between 0.2 – 1 mSv (UNSCEAR 2008). International Commission on Radiological Protection (ICRP) recommended 1 mSv as the annual effective dose for a member of the public due to the operation of nuclear facilities and the applications of radiation and radionuclides. Dose from medical exposure and background exposure to naturally occurring radionuclides is not included in the dose limit for the members of the public (Rao, 2012).

Cancer and heritable effects are the most important health effects of ionizing radiation at relatively low doses and dose rates. Based on both animal studies and epidemiological research, the International Agency for Research on Cancer (IARC) has categorized all types of ionising radiation as carcinogenic for humans (IARC, 2012). There is no doubt that these health effects are indeed occurring (at least found in mice study, for heritable effects); but the magnitude of the risk at low doses and low dose rates is debatable. Cancer is well documented in the range of doses defined as moderate, 100 mSv – 1 Sv. This documentation is based on epidemiological cancer studies of cohorts irradiated in association with the use and testing of nuclear weapons, and from radiation accidents, workers exposed to radiation, and groups subject to medical exposures (UNSCEAR, 2013).

Potential cancer risk at very low doses, including those resulting from natural background radiation, is, in general, too low to be determined in observational (epidemiological) studies. However, experimental studies have shown that DNA damage can also be induced at very low doses. Depending on the type of cancer, the latency period can range from 2 to 30 years. Thyroid and bone cancer, and leukemia can appear within a few years of radiation exposure, whereas most types of cancer are not expressed until at least 10 years after exposure (VKM, 2017).The study aims to determine the concentration of some natural and artificial radionuclides in the pre-mix package beverage, estimate the annual effective dose and associated cancer risk that arise from the consumption of pre-mix beverages among Malaysian adults (> 17 y), based on Malaysian consumption study and the concentration of radionuclides found in the beverages.

## EXPERIMENTAL DETAILS

### Activity concentration of radionuclides

Activity concentration of natural ($^{40}$K, $^{226}$Ra, $^{228}$Ra, $^{232}$Th, $^{238}$U) and artificial ($^{134}$Cs, $^{137}$Cs) radionuclides reported in this article was based on measurement from a total of twenty-two different beverage samples using the same unit of HPGe gamma spectrometry for 15 hours each. The sample was prepared in a 350 ml cylindrical container, sealed with PVC tape and stored for a month to achieve secular equilibrium. Equipment set-up and radionuclides identification are the same as reported earlier in Yii (2019). The reference material IAEA-Soil-6 was used as quality control evaluation. If measurement values for the reference material were within the 95% confidence level (as stated in the certificate), the results of samples will be accepted. The minimum detectable activities (MDA) following the Currie Limit method set for $^{40}$K was 5 Bq/kg, for $^{226}$Ra, $^{228}$Ra, $^{232}$Th and $^{238}$U was 0.5 Bq/kg, and for $^{134}$Cs and $^{137}$Cs was 1.0 Bq/kg, respectively, after considering the sample size and counting time (Wan-Mahmood et al., 2016). However, some samples having lighter density will expected to give higher detection limit. Measured samples were 3-in-1coffee (including white coffee), chocolate drinks and black coffee available from local markets.

### Calculation of annual effective dose

The annual effective dose due to the intake of radionuclides in foods can be calculated using the Formula given by (Till and Moore, 1988; Alam et al.,1999; UNSCEAR, 2000) as follows:

$$\mathbf{A_D = A_C * C_F * A_I} \quad \ldots \text{Eq (1)}$$

Where:
$A_D$ is the annual effective dose (Sv/y) to an individual due to the ingestion of radionuclides,
$A_C$ is the activity concentration of radionuclides in the ingested beverages (Bq/kg),
$C_F$ is the dose conversion factor for ingested radionuclides (Sv/Bq) (ICRP, 1995), and
$A_I$ is the annual intake of pre-mix beverages (kg/y) for Malaysians (IPH, 2014).

The conversion factor 'CF' varies depending on both radionuclides and the age of the individual based on the publication by ICRP (ICRP, 1995; ICRP, 2012). For the dose calculation, the total dose was obtained by using the sum of contributions for the radionuclides in the samples with the recommended conversion factors given by ICRP (ICRP, 1995; ICRP, 2012) as in Table 1.

Table 1: Dose conversion factors for radionuclides ($^{40}$K, $^{226}$Ra, $^{228}$Ra, $^{232}$Th, $^{238}$U, $^{134}$Cs, $^{137}$Cs) in adults

| Radionuclides | Dose conversion factors (Sv/Bq ) |
|---|---|
| $^{40}$K | $6.2 \times 10^{-9}$ |
| $^{226}$Ra | $2.8 \times 10^{-7}$ |
| $^{228}$Ra | $6.9 \times 10^{-7}$ |
| $^{232}$Th | $2.3 \times 10^{-7}$ |
| $^{238}$U | $4.5 \times 10^{-8}$ |
| $^{134}$Cs | $1.9 \times 10^{-8}$ |
| $^{137}$Cs | $1.3 \times 10^{-8}$ |

Annual effective dose arises from food consumption strongly dependent on the amount of food consumed (Alzahrani, 2012; Kolapo, 2014). In this study, the amount of beverage powder consumed by adults in Malaysia was estimated to be 18.9 kg/y (for samples 1 – 15) based on a survey conducted by the Institute for Public Health of Malaysia (IPH) (IPH, 2014). Black coffee consumed was estimated to be three packs per day of 4.9 kg/y (for samples 16 – 22).

### Calculation of relative cancer risk

Since the results of radiation effects on cell cultures, animal studies, and human epidemiology studies may be interpreted differently, variations are found in the published relative risk values, but they are within a few percentage points of each other (Peck and Samei, 2017). According to Lin (2010), one Sievert carries a 5% excess death risk from cancer and this is extrapolated linearly for lower doses. In this article, the effective dose from consumption of each sample and the 5% chance of cancer risk was used for the calculation of cumulative dose and risk up to the age of 70 years for the public. The calculation was performed using an online calculation spreadsheet provided under the Wise Uranium project. The cancer risk for 1 mSv/y exposure is equivalent to 350 cases per 100,000 people (Wise, 2018).

## RESULTS AND DISCUSSION

### Activity concentration of radionuclides

The measured activity concentrations of $^{40}$K, $^{226}$Ra, $^{228}$Ra, $^{232}$Th, $^{238}$U, $^{134}$Cs, and $^{137}$Cs in the twenty-two beverage samples under the present study were summarized in Table 2. It can be noticed that $^{40}$K was detected in all samples and was one to three orders of magnitudes higher when compared to the other radionuclides in the sample. It varied between 63 – 1360 Bq/kg (mean 601 Bq/kg). Meanwhile, the activity concentration for other natural radionuclides of $^{226}$Ra, $^{228}$Ra, $^{232}$Th, and $^{238}$U, was ranged between 0.88 – 6.43 Bq/kg (mean 2.46 Bq/kg), 0.83 – 8.48 Bq/kg (mean 3.11 Bq/kg), 0.62 – 5.73 Bq/kg (mean 2.29 Bq/kg) and 2.64 – 21.49 Bq/kg (mean 7.62 Bq/kg), respectively.

Table 2 : Concentration of radionuclides ($^{40}$K, $^{226}$Ra, $^{228}$Ra, $^{232}$Th, $^{238}$U, $^{134}$Cs, $^{137}$Cs) in individual pre-mix beverage

| No | Type | Activity concentration (Bq/kg) | | | | | | |
|---|---|---|---|---|---|---|---|---|
| | | $^{40}$K | $^{226}$Ra | $^{228}$Ra | $^{232}$Th | $^{238}$U | $^{134}$Cs | $^{137}$Cs |
| 1 | 3 in 1 coffee | 384 ± 32 | <1.38 | <1.28 | <0.96 | 5.56 ± 0.57 | <1.00 | <1.00 |
| 2 | 3 in 1 coffee | 517 ± 43 | 3.35 ± 0.28 | 2.36 ± 0.21 | 1.71 ± 0.15 | 5.47 ± 0.42 | <1.00 | <1.00 |
| 3 | 3 in 1 coffee | 276 ± 23 | <1.00 | <0.93 | <0.70 | 2.75 ± 0.29 | <1.00 | <1.00 |
| 4 | 3 in 1 coffee | 263 ± 22 | 1.54 ± 0.13 | 2.82 ± 0.24 | 1.94 ± 0.17 | 3.61 ± 0.36 | <1.00 | <1.00 |
| 5 | 3 in 1 coffee | 258 ± 21 | 0.94 ± 0.08 | <0.84 | <0.63 | 3.96 ± 0.38 | <1.00 | <1.00 |
| 6 | 3 in 1 coffee | 275 ± 23 | <0.88 | <0.83 | <0.62 | 3.26 ± 0.30 | <1.00 | <1.00 |
| 7 | 3 in 1 coffee | 322 ± 27 | <0.99 | 1.50 ± 0.13 | 1.34 ± 0.11 | 5.31 ± 0.49 | <1.00 | <1.00 |
| 8 | 3 in 1 coffee | 292 ± 24 | 1.74 ± 0.15 | 2.35 ± 0.21 | 1.74 ± 0.15 | 4.51 ± 0.51 | <1.00 | <1.00 |
| 9 | 3 in 1 white coffee | 63 ± 5 | 4.30 ± 0.36 | 3.60 ± 0.31 | 2.67 ± 0.23 | 8.14 ± 0.90 | <1.00 | <1.00 |
| 10 | 3 in 1 white coffee | 392 ± 33 | <1.71 | 3.75 ± 0.32 | 2.82 ± 0.24 | 5.94 ± 0.71 | <1.00 | <1.00 |
| 11 | 3 in 1 Espresso | 463 ± 38 | 4.53 ± 0.37 | 5.10 ± 0.44 | 3.41 ± 0.29 | 11.31 ± 1.19 | <1.00 | <1.00 |
| 12 | Choc drink | 392 ± 32 | <0.93 | 1.54 ± 0.14 | 1.27 ± 0.11 | 2.64 ± 0.27 | <1.00 | <1.00 |
| 13 | Choc drink | 360 ± 30 | 1.10 ± 0.09 | 1.00 ± 0.08 | 0.96 ± 0.08 | 3.46 ± 0.38 | <1.00 | <1.00 |
| 14 | Choc drink | 376 ± 31 | <0.91 | 1.29 ± 0.12 | 1.08 ± 0.09 | 4.56 ± 0.46 | <1.00 | <1.00 |
| 15 | Choc drink | 386 ± 32 | 0.98 ± 0.08 | 2.67 ± 0.23 | 1.92 ± 0.16 | 4.91 ± 0.56 | <1.00 | <1.00 |

| | | | | | | | | |
|---|---|---|---|---|---|---|---|---|
| 16* | Black coffee | 1327 ± 108 | 3.72 ± 0.31 | 8.48 ± 0.73 | 5.73 ± 0.49 | 14.66 ± 1.42 | <1.00 | 1.46 ± 0.27 |
| 17* | Black coffee | 958 ± 79 | <2.08 | 3.18 ± 0.28 | 1.96 ± 0.18 | 9.50 ± 1.05 | <1.00 | <1.00 |
| 18* | Black coffee | 1360 ± 111 | 4.09 ± 0.34 | 7.51 ± 0.65 | 5.48 ± 0.47 | 15.71 ± 1.68 | <1.00 | 1.17 ± 0.22 |
| 19* | Black coffee | 1258 ± 102 | 2.87 ± 0.24 | 4.80 ± 0.41 | 3.41 ± 0.29 | 11.92 ± 1.09 | <1.00 | 1.04 ± 0.19 |
| 20* | Black coffee | 1345 ± 110 | 6.43 ± 0.53 | 3.19 ± 0.27 | 2.47 ± 0.21 | 21.49 ± 2.33 | <1.00 | 1.75 ± 0.32 |
| 21* | Black coffee | 895 ± 74 | <2.80 | <2.84 | <2.16 | <5.12 | <1.00 | <1.00 |
| 22* | Black coffee | 1053 ± 86 | 5.89 ± 0.48 | 6.67 ± 0.56 | 5.49 ± 0.45 | 13.91 ± 1.17 | <1.00 | <1.00 |
| | **Range** | 63 – 1360 | 0.88 – 6.43 | 0.83 – 8.48 | 0.62 – 5.73 | 2.64 – 21.49 | < 1.00 | 1.00 – 1.75 |

Remarks: Samples marked with '*' are sugar free black coffees where quantity consumed was different.

Most of these radioactivities values are significantly lower than the mean levels reported by UNSCEAR (2000) in soil (33 and 45 Bq/kg for $^{226}$Ra and $^{232}$Th, respectively). Meanwhile, the activity concentration for the artificial radionuclides of $^{134}$Cs and $^{137}$Cs was <1.00 Bq/kg and 1.00 – 1.75 Bq/kg (mean 1.06 Bq/kg), respectively. The obtained results are compared with the reported data in the literature as presented in Table 3. Generally, radioactivities found in the present study are higher than the values reported by Al-Alawy et al. (2020) but comparable to the study carried out by Kamal et al. (2015) and lower than those reported by Alharbi and Alamoudi (2017).

In this study, it was found that in most of the beverages, the concentration of $^{40}$K accounted for more than 95% of the total gamma activity. However, in sample no. 9, it was found that $^{40}$K only accounted for 75% of the total gamma activity. Radionuclides are believed to be transferred from the soil to plants, then to the final products (UNSCEAR, 2008; Al-Alawy et al., 2020).

Meanwhile, higher radioactivities were found in black coffee samples no. 16, 18, 19, and 20. These coffees are pre-mixed coffee with Ganoderma extract. Ganoderma, as a fungus is believed to absorb nutrients and minerals from its host and the environment. They accomplish this by growing through and within the substrate on which they are fed. Numerous hyphae network through the wood, cheese, soil, or flesh from which they are growing (UCMP, 2022).

Table 3: Comparison of the radionuclides activity concentrations (Bq/kg) of the present study with other literatures in coffee

| **Region** | **$^{40}$K** | **$^{226}$Ra** | **$^{228}$Ra** | **$^{232}$Th** | **$^{238}$U** | **$^{134}$Cs** | **$^{137}$Cs** | **Reference** |
|---|---|---|---|---|---|---|---|---|
| Malaysia | 63 – 1360 | 0.88 – 6.43 | 0.83 – 8.48 | 0.62 – 5.73 | 2.75 – 21.49 | < 1.00 | 1.00 – 1.75 | Present study |
| Malaysia | (429.4 ± 305.5) | (2.1 ± 0.7) | | (2.2 ± 0.3) | (1.8 ± 0.2) | | | Kamal et al. (2015) |
| Iraq | 93.8 – 183.2 | | | 0.36 – 3.21 | 1.63 – 8.34 | | 0.27 – 0.48 | Al-Alawy et al. (2020) |
| Arabian coffee | 840 – 1197 | 2.57 – 10.63 | | ND – 8.01 | ND – 135.11 | | ND | Alharbi and Alamoudi (2017) |
| Turkish coffee | 161 – 2411 | ND – 10.09 | | ND – 9.75 | ND – 57.16 | | ND | Alharbi and Alamoudi (2017) |

Remarks: ND – Non-Detectable; Value in bracket is average value.

**Annual effective dose**

The total annual effective dose (sum of total radioactivity dose) for adults who consumed the pre-mix beverages was presented in Table 4. The calculation was performed with Eq. 1 above by using the quantity of beverage powder consumed in a year (18.9 kg/y for samples 1 – 15, and 4.9 kg/y for

samples 16 – 22) multiplied by the sum of the total dose per year obtained for each radionuclide concentration (Table 2) and the dose conversion factor (Table 1). From the results presented in Table 4, we could find that the annual effective dose ranged between 44.6 – 170.0 μSv/y. All samples except samples no. 2, 10 and 11 are having an effective dose of less than 100 μSv/y. Therefore, consumption of these pre-mix beverages would be considered to present an insignificant health hazard to human.

As mentioned above, $^{40}$K accounted for most of the total gamma activity in the sample. Since potassium is an essential element for humans and it is absorbed mainly from the ingested food. There is no legislation governing $^{40}$K since it cannot be eliminated, and consumption of foods also does not significantly alter the potassium content, hence the potassium radioactivity inside the body (Stansfield, 2003; WHO, 2017). Under such consideration, the contribution of $^{40}$K to the total effective dose can then be ignored and subtracted. From the current study, $^{40}$K concentration in all samples, was found to contribute about 30 – 60% of the total dose except for sample no. 9, which is only having an 8% dose contribution from the $^{40}$K. Figure 1 presented the total dose with and without considering the contribution from $^{40}$K. After subtracting the contribution of $^{40}$K, most samples will have an effective dose of less than 100 μSv/y except sample no. 11. Overall, it appears that the estimated annual dose from the consumption of pre-mix beverages is below the reference value of 1.0 mSv as recommended by ICRP (ICRP, 1995).

Table 4: Estimated effective dose and excess lifetime cancer risk after consumption of various beverages

| **Sample No** | **Effective dose (μSv/y)** | **Excess lifetime cancer risk (case per 100,000)** |
|---|---|---|
| 1 | 78.6 | 28 @ (1:3635) |
| 2 | 121.9 | 43 @ (1:2344) |
| 3 | 55.9 | 20 @ (1:5111) |
| 4 | 87.9 | 31 @ (1:3250) |
| 5 | 52.9 | 19 @ (1:5401) |
| 6 | 53.7 | 19 @ (1:5321) |
| 7 | 73.4 | 26 @ (1:3893) |
| 8 | 86.2 | 30 @ (1:3315) |
| 9 | 96.3 | 34 @ (1:2967) |
| 10 | 121.9 | 43 @ (1:2344) |
| 11 | 170.0 | 59 @ (1:1681) |
| 12 | 81.3 | 28 @ (1:3514) |
| 13 | 68.8 | 24 @ (1:4153) |
| 14 | 75.0 | 26 @ (1:3810) |
| 15 | 98.5 | 34 @ (1:2901) |
| 16* | 84.5 | 30 @ (1:3381) |
| 17* | 47.5 | 17 @ (1:6015) |
| 18* | 82.7 | 29 @ (1:3455) |
| 19* | 65.4 | 23 @ (1:4369) |
| 20* | 68.6 | 24 @ (1:4165) |
| 21* | 44.6 | 16 @ (1:6406) |
| 22* | 72.5 | 25 @ (1:3941) |
| Range | 44.6 – 170.0 | 16 – 59 cases per 100,000 people |

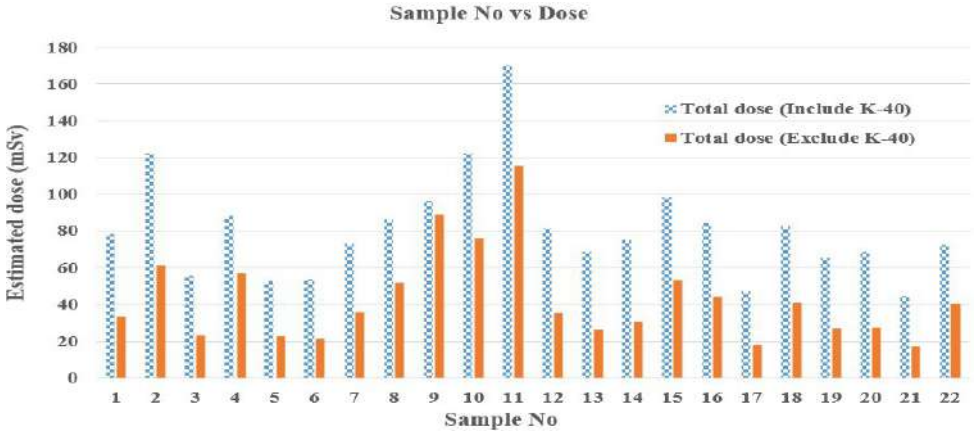


Figure 1: The estimated effective dose for individual samples, with and without the contribution from $^{40}K$.

**Excess lifetime cancer risk**

From the estimated effective dose value, the cumulative lifetime cancer risk was calculated and presented in Table 4. Sample no. 11 shows the highest effective dose of 170.0 µSv/y with the potential risk of cancer occurrence is 59 cases in every 100,000 people. Radiation hazards associated with drinking this particular beverage may face greater health risks as compared to the others. Meanwhile, estimated doses ranged between 44.6 – 121.9 µSv/y if consuming other samples, which corresponds to the cancer risk occurrence of 16 – 43 case per 100,000 people. This cancer risk probability is comparable to the 14.4 – 18.1 cases per 100,000 as reported by Moon et al. (2016) for a study conducted in Korea but is lower when compared to cancer risk as reported by Priharti and Samat (2016) for Malaysian adults due to the intake of vegetables (81.3 case per 100,000) and fruits (68.3 case per 100,000).

## CONCLUSIONS

In this study, the concentrations of some natural and artificial radionuclides in pre-mix beverages were measured. Based on the Malaysian adults' consumption rate of pre-mix beverages, the annual cumulative internal dose due to the beverage intake was calculated. In general, the largest contributor to the dose arising from the ingestion of beverages by people was due to the presence of natural radionuclides, particularly the $^{40}K$, which is also an essential constituent of human cellular tissue. The total annual effective dose in an adult due to the ingestion of all radionuclides was estimated along with the excess lifetime cancer risk. From the calculation, the estimated doses ranged between 44.6 to 170.0 µSv/y which corresponds to the probability of cancer risk between 16 – 59 cases per 100,000 people. The highest cancer risk concern arises from the consumption of sample no. 11 with 59 cases in every 100,000 people. When the accumulated dose is higher, so do the cancer risk. Overall, the dose received by the population is still below the 1 mSv/y recommended limit by WHO and ICRP for radiological safety. Cooperation with the local authorities can be helpful for this study to collect more varieties of pre-mix beverage samples that should be tested in future to ensure that they are safe for consumption by Malaysian.

**ACKNOWLEDGEMENTS**

The authors would like to express special appreciation to the Malaysian Nuclear Agency. This study is part of the project "Malaysia's Foods – The Radioactivity Concentrations, Annual Effective Dose and Cancer Risk, NM- R&D-20-38." The authors are also thankful to the staff in the group for their kind cooperation and support during the implementation of this study.

**REFERENCES**

Afshari, N.S., Abbasisiar, F., Abdolmaleki, P. and Nejad, M.G. (2009). Determination of $^{40}$K concentration in milk samples consumed in Tehran-Iran and estimation of its annual effective dose, Iran. *J. Radiat. Res.* 7:159–164.

Al-Alawy, I.T., Nasser, H.J. and Mzher, O.A. (2020). Natural Radionuclide Activity Concentrations and Radiological Hazard in Tea, Coffee, Wheat Fluor, and Powder Milk Consumed in Iraqi Markets, *AIP Conf. Proc.* 2213:020225.

Alam, M.N., Chowdhury, M.I., Kamal, M., Ghose, S., Islam, M.N. and Anwaruddin, M. (1999). Radiological assessment of drinking water of the Chittagong region of Bangladesh, *Radiat. Prot. Dosimetry* 82:207–214.

Alamoudi, Z.M. (2013). Assessment of Natural radionuclides in Powdered milk Consumed in Saudi Arabia and Estimates of the Corresponding annual Effective Dose, *J. Am. Sci.* 9:267–273.

Alharbi, W.R. and Alamoudi, Z.M. (2017). Radiological hazard of coffee to humans: a comparative study of Arabian and Turkish coffees, *Afr. J. Agric. Res.* 12(5):327–341.

Alharshan, G.A., Aloraini, D.A., Al-Ghamdi, H., Almuqrin, A.H., El-Azony, K.M. and Alsalamah, A.S. (2017). Measuring the Radioactivity Concentration of $^{40}$K and $^{137}$Cs and Calculating the Annual Internal Doses from Ingesting Liquid and Powdered Milk, *Radiochemistry* 59:98–103.

Alzahrani, J.H. (2012). Natural Radioactivity and Heavy Metals in Milk Consumed in Saudi Arabia and Population Dose Rate Estimates, *Life Sci.* 9:651–656.

Baeza, A., Corbacho, J.A. and Miro, C. (2004). Temporal evaluation of natural and man-made radioactivity levels in milk samples: dosimetry implications, *Bull. Environ. Contam. Toxicol*. 72:547–556.

Desideri, D., Meli, M.A., Roselli, C., Forini, N., Rongoni, A. and Feduzi, L. (2014). Natural radionuclides in Italian diet and their annual intake, *J. Radioanal. Nucl. Chem.* 299:1461–1467.

Godyn´, P., Dołhan´czuk-S´ro´dka, A., Ziembik, Z., Moliszewska, E. (2014). Estimation of the committed radiation dose resulting from gamma radionuclides ingested with food*, J. Radioanal. Nucl. Chem.* 299:1359–1364.

Institute for Public Health (2014). National Health and Morbidity Survey 2014: Malaysia Adult Nutrition Survey (MANS) T. Aris, A.A. Zainuddin, N.A. Ahmad and N. Yoep (eds.). Vol. III: Food Consumption Statistics of Malaysia, *Ministry of Health Malaysia*, Kuala Lumpur, 143.

IARC. (2012). Monographs on the Evaluation of Carcinogenic Risks to Humans Volume 100D, Radiation, *WHO*, Lyon, 363.

IAEA. (1989). Measurement of Radionuclides in Food and the Environment, Tech. Rep. Series No. 295, *IAEA*, Vienna, 169.

ICRP. (1995). Age - dependent Doses to Members of the Public from intake of Radionuclides - Part 5: Compilation of Ingestion and Inhalation Coefficients, ICRP Publication 72, Ann. ICRP 26 (1), *Pergamon*, Oxford.

ICRP. (2012). Compendium of Dose Coefficients based on ICRP Publication 60. ICRP Publication 119, Ann. ICRP 41(Suppl.) *Elsevier*, Essen.

Jemii, E. and Mazouz, M. (2020) Measurement of Radioactivity in Carbonated Soft Drinks and Annual Dose Assessment, *J. Environ. Prot. Sci.* 11:682–689.

Kamal, N.N.H.K., Khalid, N., Bahri, C.N.A.C.Z. and Majid, A.A. (2015). Determination of radionuclide activity and radiological impact from the intake of milk, wheat flour, tea and coffee, *Malaysian J. Anal. Sci.* 19(2):300–308. (In Malays).

Kolapo, A.A. (2014). Assessments of Natural Radioactivity and Heavy Metals in Commonly Consumed Milk in Oke-Ogun Area, Nigeria and Estimation of Health Risk Hazard to the Population, *J. Environment. Analytic. Toxicol.* 4:253–257.

Lin, E.C. (2010). Radiation Risk from Medical Imaging, *Mayo Clin. Proc*. 85(12):1142–1146.

Wan-Mahmood, Z., Yii, M.W., Khalid, M.A., Kontol, K.M., Ishak, A.K. and Yusof, M.A.W. (2017). Assessment of natural radioactivity level and radiological index in the vicinity of Lynas rare-earth processing plants, *ASEAN J. Sci. Technol. Dev.* 34:67–78.

Moon, E.K., Ha, W.H., Seo, S.W., Jin, Y.W., Jeong, K.H., Yoon, H.J., Kim, H.S., Hwang, M.S., Choi, H. and Lee, W.J. (2016). Estimates of Radiation Doses and Cancer Risk from Food Intake in Korea, *J. Korean Med. Sci.* 31:9– 12.

Peck, D.J. and Samei, E. (2017). How to Understand and Communicate Radiation Risk. Access online on 04th December 2018 at *The American College of Radiology*. Retrieved from https://www.imagewisely.org/Imaging-Modalities/Computed-Tomography/How-to-Understand-and-Communicate-Radiation-Risk.

Priharti, W. and Samat, S.B. (2016). Radiological risk assessment from the intake of vegetables and fruits in Malaysia, *Malays. J. Anal. Sci.* 20(6):1247–1253.

Priharti, W. and Samat, S.B. (2017). Evaluation of Natural Radionuclides $^{226}$Ra, $^{232}$Th and $^{40}$K Activity Concentration in Food at the Central Area of Malaysia, *Sains Malays.* 46:945–951. (In Malays).

Rao, D.D. (2012). Radioactivity in human body and its detection, *Radiat. Prot. Environ.* 35:57–58.

Sahar, A.A., Al-kafaje, M.S.M. and Al-Ani, R.R. (2016). Assessment of Natural radionuclides in Powdered milk Consumed in Iraq, *J. Nat. Sci. Res.* 6:112–115.

Stansfield, C.M. (2003) Legislation - Contaminants and Adulterants. In: Encyclopedia of Food Sciences and Nutrition, B. Caballero, P. Finglas and F. Toldra (eds). 2nd edn, *Academic Press,* London, 3507–3513.

Till, J.E. and Moore, R.E. (1988). A pathway analysis approach for determining acceptable levels of contamination of radionuclide in soil, *Health Phys.* 55:541–548.

UNSCEAR. (2000). United Nations Scientific Committee on the Effects of Atomic Radiation, Sources, Effects and Risks of Ionizing Radiation. *United Nations*, New York.

UNSCEAR. (2008). United Nations Scientific Committee on the Effects of Atomic Radiation, Sources, Effects and Risks of Ionizing Radiation. *United Nations*, New York.

UNSCEAR. (2013). Levels and effects of radiation exposure due to the nuclear accident after the 2011 great east-Japan earthquake and tsunami, Annex A Sources, effects and risks of ionizing radiation, Report to the General Assembly with Scientific Annexes. *United Nations*, New York.

University of California Museum of Paleontology (2022). Fungi: Life History and Ecology. Access online on 05th April 2022. Retrieved from https://ucmp.berkeley.edu/fungi/fungilh.html#:~:text=Fungi%20are%20 heterotrophic.,on%20which%20 they%20are%20feeding.

Uwatse, O.B., Olatunji, M.A., Khandaker, M.U., Amin, Y.M., Bradley, D.A., Alkhorayef, M. and Alzimami, K. (2015). Measurement of Natural and Artificial Radioactivity in Infant Powdered Milk and Estimation of the Corresponding Annual Effective Dose, *Environ. Eng. Sci*. 32:1–9.

VKM, Alexander, J., Brantsæter A.L., Brunborg, G., Fæste, C.K., Jaworska, A., Komperød, M., Lillegaard, I.T.L., Rosseland, C., Skuterud, L., Andersen, L.F., Elvevoll, E.O., Hjeltnes, B., Hofshagen, M., Krogdahl, Å., Källqvist, T., Opsahl-Sorteberg, H.G., Rafoss, T., Skaar, I., Skåre, J.U., Steffensen, I-L., Vandvik, V., Wasteson, Y. and Hemre, G-I. (2017). Risk assessment of radioactivity in food. Opinion of the Scientific Steering Committee of the Norwegian Scientific Committee for Food Safety (2017). VKM report 2017:25, *VKM*, Oslo, 150.

Wise Uranium project (2022). Radiation Risk to Dose Converter. Access online on 05th April 2022. Retrieved from http://www.wise-uranium.org/rdcri.html.

WHO. (2017). Guidelines for Drinking -water Quality, 4th edn. (Incorporating the first addendum), *WHO*, Interligar, 631.

Yii, M.W. (2019). Measurement of activity concentrations in powdered milk and estimation of the corresponding annual effective dose, *J. Radioanal. Nucl. Chem*. 320 (1):193–199.

e-Jurnal Sains Nuklear Malaysia, 2023, Vol. 35 (No.1): 22 – 28
*eISSN: 2232-0946*

# DOSE MAPPING USING THERMOLUMINENSCENE DOSIMETER (TLD) AND GEOGRAPHICAL INFORMATION SYSTEM (GIS) TOOL FOR LONG TERM STORAGE FACILITY (LTSF), BUKIT KLEDANG, PERAK, MALAYSIA

***Nur Khairunisa Zahidi[1], Faizal Azrin Abdul Razalim[1], Yii Mei Wo[2], Nazran Harun[2], Raymond Yapp Tze Loong[1], Noor Ezati Shuib[1], Ahmad Bazlie Abdul Kadir[1], Hassan Sham[1], Mohd Taufik Dollah[1], Rafizi Salehudin[2], Nurul Hani Farhana Mohamad Haider[1], Ahmad Hasnulhadi Che Kamaruddin[2], Azuhar Ripin[1], Abdul Rahmad Khalid[3], Muhammad Amirul Md Noor[3] and Nur Ain Abd Razak[3]***

[1]Radiation Safety and Health Division,
Malaysian Nuclear Agency, Bangi, 43000 Kajang, Selangor, Malaysia
[2]Waste Technology and Environmental Division,
Malaysian Nuclear Agency, Bangi, 43000 Kajang, Selangor, Malaysia
[3]Menteri Besar Incorporated, Perbadanan Menteri Besar Perak,
30020, Ipoh Perak, Malaysia
Correspondence author: khairunisa@nm.gov.my

***ABSTRACT***

*Dose mapping is one of the methods used to identify the dose distribution in any radiation facility. This study aims to visualise dose distribution at Long Term Storage Facility (LTSF), Bukit Kledang using thermoluminenscene dosimeter (TLD) by Geographical Information System (GIS). A total of 50 point were identified at LTSF for dose mapping using passive measurement, thermoluminescence dosimeter (TLD). TLD chips undergo anneal process before using, installed at dedicated location, exposed for one month and analysed using TLD reader at Secondary Standard Dosimetry Laboratory (SSDL), Malaysian Nuclear Agency. The obtained results showed, the average cumulative dose per month and annual dose ranged from 0.04 – 0.16 and 0.08 – 0.38 respectively. The results showed that there were no significant increase as compared to previous continuing environmental programme (EMP) in 2017 and the annual dose is also below the stipulated limit for public by Atomic Energy Licensing Board (AELB).*

**Keywords**: Dose mapping, passive measurement, radiation, *Long Term Storage Facility (LTSF), thermoluminescence dosimeter (TLD), Geographical Information System (GIS)*

## INTRODUCTION

Nuclear radiation can be found anywhere and human has always been exposed internally (inhalation, ingestion, skin absorption, open wound) and externally (irradiation from gamma, x-rays) to radiation from natural background and man-made. Environmental surveillance is an important component of the verification system to verify that the controls on the releases of radioactive substances to the environment are functioning under normal working conditions (IAEA, 1982). The environmental surveillance can be done by numerous methodologies and one of the methodologies discussed in this paper is by creating a dose mapping using passive measurement, TLD and GIS tools at LTSF, Bukit Kledang Perak. The repository facility is upgraded from LTSF upon completion of decontamination and decommissioning (D&D) process (AELB, 2016). The previous site license holder of the repository facility is Asian Rare Earth (ARE) Sdn Bhd. ARE is a joint venture between Malaysians and Japanese, which was incorporated in Ipoh on November 23,1979 and began operating in May

1982, its function being to extract rare earths from monazite sand, a residue of tin mining (Wagner et.al., 1989). Monozite sand contains rare earth and the radioactive element thorium. Prior to be collected for further processing, piles of monazite are found throughout the environments of Ipoh in amang factories. Amang is the residue of mixed minerals that remains in sand after the extraction of tin. After extraction rare earth completed, the concentration is twice original content, 12%. The final residue is treated as radioactive waste and stored in controlled area known as LTSF. The surrounding community believes that the study area is hazardous and provides additional external radiation. The main objective of this paper is to establish the dose mapping for LTSF, Bukit Kledang for better understanding of dose distribution in mentioned area.

## MATERIALS AND METHODS

### *Sampling area*

This study has been carried out at the LTSF, Bukit Kledang, Perak which is located at Mukim Blanja and ~15km driving from Ipoh town. The repository in Mukim Belanja are from ARE plant and LTSF decommissioning projects. After the completion of three-year surveillance period by ARE contractor, the responsibility to manage the repository site has been transferred to the Perak State Government (PSG) through MB Inc. Menteri Besar Incorporated (MB Inc.) Perak State.

### *Sampling and sample preparation*

A total 50 points were identified at on-site LTSF and 3 points off-site LTSF and act as a control for this study. Dosimeter box were placed at 1-metre-high at specified location. Each thermoluminescence dosimeter (TLD) undergo annealing process using anneal oven and were placed in dosimeter box for one (1) month. The TLD chips were analysed using TLD reader at Secondary Standard Dosimetry Laboratory (SSDL), Malaysian Nuclear Agency. The sampling was carried out four (4) times in a year. The sampling locations are shown as in Figure 1.


Figure 1: Sampling location at LTSF Bukit Kledang, Perak.

***Visualize dose mapping***

The average cumulative dose for each point were visualised by colour using GIS tools. The Inverse Distance Weighted (IDW) technique is used to interpolate dose at LTSF, Bukit Kledang Perak. IDW estimates unknown values with specifying search distance, closet point, power setting and barriers (GISGeography, 2022). The dose distribution is categorized into six (6) group with different colour. The visualize dose mapping using IDW was shown as in Figure 2.

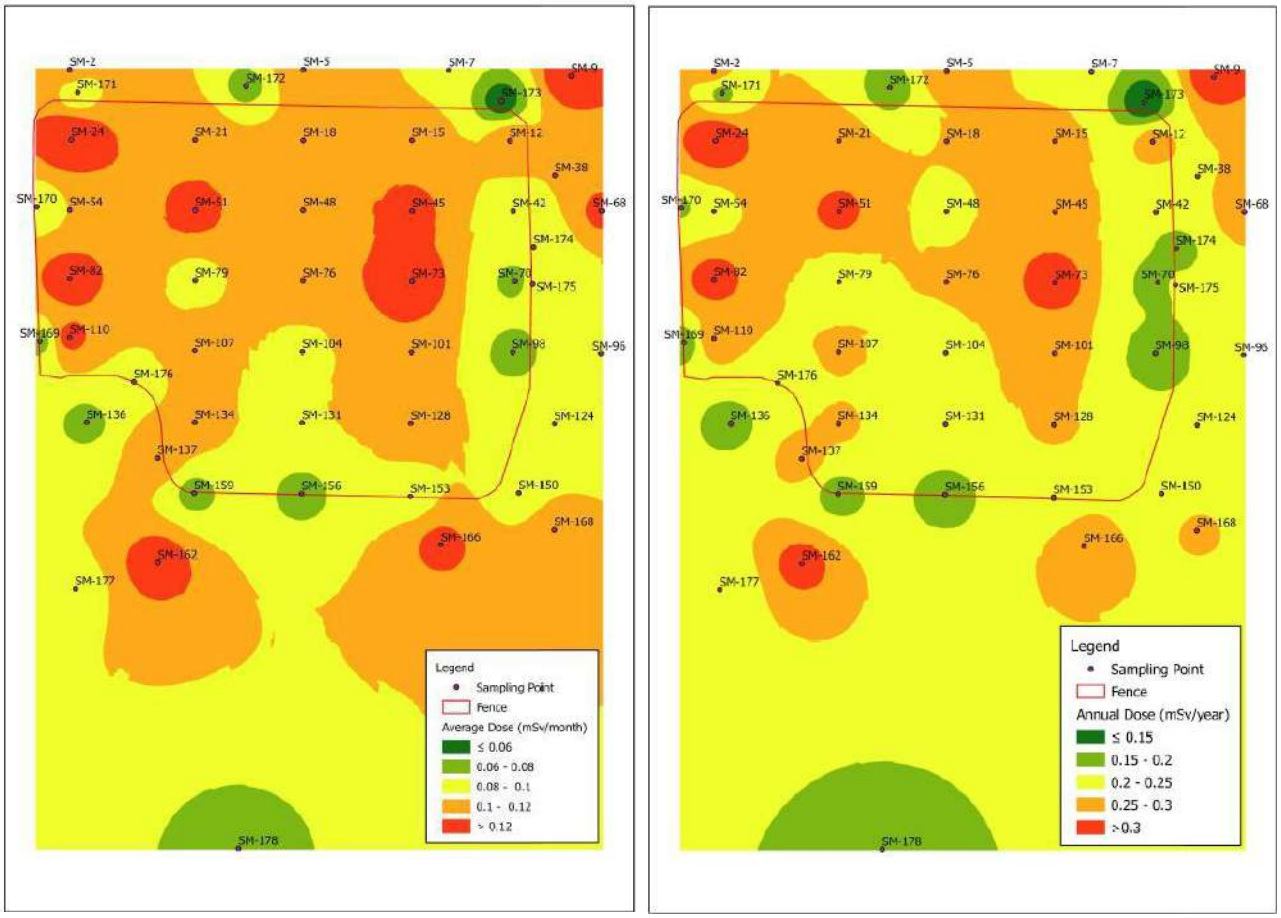


Figure 2: Visualise dose mapping (mSv/month and mSv/year) at LTSF Bukit Kledang, Perak using GIS tools.

***Annual Dose Calculation***

The annual dose is calculated using the following equation:

Annual effective dose (mSv) = $D \times 12 \times 0.2$ …… Eq (1)

where,
*D*: Average cumulative dose in mSv/month,
12: month in a year
0.2: external occupancy factor

**RESULTS AND DISCUSSION**

Table 1.0 shows the average results of measurement of 50 sampling points at sampling area. The minimum and maximum average dose per month and per year is 0.04 and 0.16, respectively. The data shown is compared with the previous monitoring using the same passive measurement. In the previous environmental program of continuing EMP for LTSF Bukit Kledang Perak in 2017, the average dose per month ranged between 0.18 – 0.82 at on-site and off-site monitoring station (MB Inc. Perbadanan Menteri Besar Perak, 2019) thus the data shows no remarkable increase of average dose per month at LTSF Bukit Kledang, Perak. Based on Figure 3.0, the maximum annual dose and the average annual dose is 0.38 and 0.24 ± 0.06 mSv, respectively. The value shown is below the dose limit for public member, 1 mSv/year as stipulated by AELB (AELB, 2010). There is no similar research related to

this study in other country. However, there is one study in German regarding the radiation dose level at fence with additional cask in the repository facility since 1997 until 2011 and the maximum annual dose found to be 0.22 mSv (Oelschlager. L. et al., 2013). The results from this study are similar as in Germany repository facility study where the annual dose at fence of LTSF Bukit Kledang is ranged between 0.16 t0 0.22 mSv annually.

Table 1: The results of average dose monitoring at LTSF, Bukit Kledang, Perak.

| Sampling Point | GPS Coordinates | | Average Dose (mSv/month) | Annual Dose (mSv/year) |
|---|---|---|---|---|
| | Latitude (DMS) | Longitude (DMS) | | |
| SM-2 | 4°33'14.7" | 101°00'46.8" | 0.12 ± 0.03 | 0.28 |
| SM-5 | 4°33'14.7" | 101°00'50.4" | 0.12 ± 0.04 | 0.29 |
| SM-7 | 4°33'14.7" | 101°00'54.0" | 0.09 ± 0.06 | 0.22 |
| SM-9 | 4°33'14.5" | 101°00'54.0" | 0.15 ± 0.06 | 0.36 |
| SM-12 | 4°33'13.4" | 101°00'54.0" | 0.12 ± 0.02 | 0.28 |
| SM-15 | 4°33'13.4" | 101°00'54.0" | 0.12 ± 0.04 | 0.28 |
| SM-18 | 4°33'13.4" | 101°00'50.4" | 0.11 ± 0.07 | 0.25 |
| SM-21 | 4°33'13.4" | 101°00'46.8" | 0.12 ± 0.04 | 0.28 |
| SM-24 | 4°33'13.4" | 101°00'46.8" | **0.16 ± 0.06*** | **0.38*** |
| SM-38 | 4°33’12.7” | 101°00’54.0” | 0.10 ± 0.04 | 0.25 |
| SM-42 | 4°33’12.1” | 101°00’54.0” | 0.09 ± 0.08 | 0.21 |
| SM-45 | 4°33’12.1” | 101°00’54.0” | 0.13 ± 0.04 | 0.30 |
| SM-48 | 4°33’12.1” | 101°00’50.4” | 0.10 ± 0.07 | 0.23 |
| SM-51 | 4°33’12.1” | 101°00’46.8” | 0.13 ± 0.07 | 0.32 |
| SM-54 | 4°33’12.1” | 101°00’46.8” | 0.13 ± 0.04 | 0.23 |
| SM-68 | 4°33’12.1” | 101°00’54.0 | 0.13± 0.04 | 0.30 |
| SM-70 | 4°33’10.8” | 101°00’54.0” | 0.07 ± 0.08 | 0.17 |
| SM-73 | 4°33’10.8” | 101°00’54.0” | 0.15 ± 0.03 | 0.35 |
| SM-76 | 4°33’10.8” | 101°00’50.4” | 0.11 ± 0.06 | 0.25 |
| SM-79 | 4°33’10.8” | 101°00’46.8” | 0.09 ± 0.05 | 0.21 |
| SM-82 | 4°33’10.8” | 101°00’46.8” | 0.14 ± 0.04 | 0.34 |
| SM-96 | 4°33’09.4” | 101°00’54.0” | 0.10 ± 0.05 | 0.23 |
| SM-98 | 4°33’09.5” | 101°00’54.0” | 0.07 ± 0.05 | 0.17 |
| SM-101 | 4°33’09.5” | 101°00’54.0” | 0.12 ± 0.02 | 0.28 |
| SM-104 | 4°33’09.5” | 101°00’50.4” | 0.09 ± 0.06 | 0.22 |
| SM-107 | 4°33’09.5” | 101°00’46.8” | 0.11 ± 0.04 | 0.26 |
| SM-110 | 4°33’09.7” | 101°00’46.8” | 0.13 ± 0.04 | 0.30 |
| SM-124 | 4°33’08.1” | 101°00’54.0” | 0.09 ± 0.04 | 0.20 |
| SM-128 | 4°33’08.1” | 101°00’54.0” | 0.11 ± 0.02 | 0.26 |
| SM-131 | 4°33’08.1” | 101°00’50.4” | 0.10 ± 0.01 | 0.25 |
| SM-134 | 4°33’08.1” | 101°00’46.8” | 0.11 ± 0.03 | 0.26 |
| SM-136 | 4°33’08.1” | 101°00’46.8” | 0.07 ± 0.05 | 0.17 |
| SM-137 | 4°33’07.5” | 101°00’46.8” | 0.12 ± 0.06 | 0.28 |
| SM-150 | 4°33’06.9” | 101°00’54.0” | 0.09 ± 0.03 | 0.20 |
| SM-153 | 4°33’06.8” | 101°00’54.0” | 0.09 ± 0.04 | 0.20 |
| SM-156 | 4°33’06.8” | 101°00’50.4” | 0.07 ± 0.05 | 0.17 |
| SM-159 | 4°33’06.8” | 101°00’46.8” | 0.07 ± 0.05 | 0.17 |
| SM-162 | 4°33’05.5” | 101°00’46.8” | 0.14 ± 0.03 | 0.33 |
| SM-166 | 4°33’05.9” | 101°00’54.0” | 0.13 ± 0.04 | 0.30 |
| SM-168 | 4°33’06.2” | 101°00’54.0” | 0.11 ± 0.04 | 0.26 |

| | | | | |
|---|---|---|---|---|
| SM-169 | 4°33’09.6” | 101°00’46.8” | 0.07 ± 0.05 | 0.16 |
| SM-170 | 4°33’12.1” | 101°00’46.8” | 0.08 ± 0.06 | 0.19 |
| SM-171 | 4°33’14.2” | 101°00’46.8” | 0.08 ± 0.04 | 0.18 |
| SM-172 | 4°33’14.4” | 101°00’50.4” | 0.07 ± 0.05 | 0.16 |
| SM-173 | 4°33’14.1” | 101°00’54.0” | **0.04 ± 0.03*** | **0.08*** |
| SM-174 | 4°33'11.4" | 101°00'54.0" | 0.08 ± 0.02 | 0.18 |
| SM-175 | 4°33'10.7" | 101°00'54.0" | 0.09 ± 0.05 | 0.21 |
| SM-176 | 4°33'08.9" | 101°00'46.8" | 0.09 ± 0.07 | 0.22 |
| SM-177 | 4°33'05.0" | 101°00'46.8" | 0.09 ± 0.04 | 0.20 |
| SM-178 | 4°33'00.3" | 101°00'50.4" | 0.07 ± 0.05 | 0.16 |

***** The bold characters represent the minimum and maximum values.

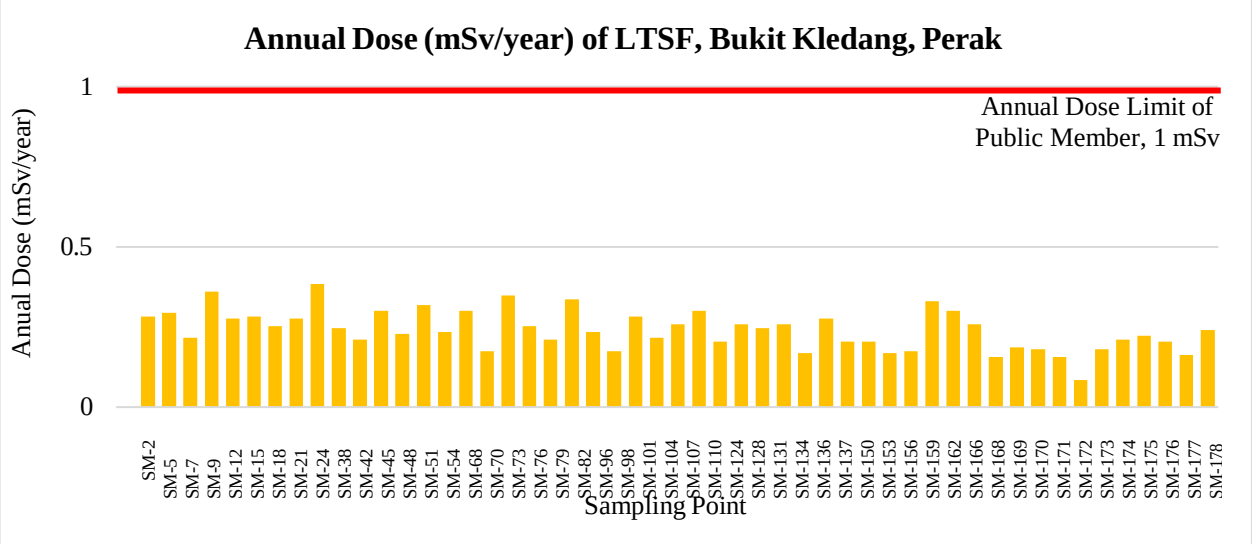


Figure 3: Annual dose (mSv/year) at LTSF Bukit Kledang, Perak and dose limit for public member.

## CONCLUSIONS

The measurement of 50 points at on-site LTSF using TLD were analysed by monthly basis in each sampling. The maximum annual dose and the average annual dose is 0.38 and 0.24 ± 0.06 mSv, respectively. The value shown is far compared to the dose limit for public member, 1 mSv/year as stipulated by AELB (AELB, 2010).

## REFERENCES

AELB. (2010). *Basic Safety Radiation Protection Regulations.* Atomic Energy Licensing Act 1984.

AELB. (2016). Tapak Repositori Jangka Panjang di Malaysia. Lembaga Perlesenan Tenaga Atom, Bangi.

GISGeography. (2022). *Inverse Distance Weighting (IDW) Interpolation.* https://gisgeography.com/inverse-distance-weighting-idw-interpolation/

IAEA, International Atomic Energy Agency. (1982). *Nuclear Power, The Environment and Man.*

MB Inc. Perbadanan Menteri Besar Perak. (2019). Historical Summary of Previous Analytical Result for Environmental Monitoring Program at Repository, Mukim Belanja Perak.

Oelschlager. L, Heck. M & Graf. W. (2013). GNS Experience on The Long-Term Storage at Dry Interim Storage Facilities Especially In Ahaus And Gorleben. Safety of Long-term Interim Storage Facilities. *Workshop Proceedings Munich.* Germany.

Wagner, Henry N, Ketchum & Linda. E. (1989). *Living with Radiation.* London: The John Hopkns University Press Ltd.

e-Jurnal Sains Nuklear Malaysia, 2023, Vol. 35 (No.1): 29 – 36
*eISSN: 2232-0946*

# ROBUSTNESS OF POLONIUM-210 TEST METHOD IN TERMS OF PHYSICAL AND CHEMICAL ASPECTS

***Nurrul Assyikeen Md. Jaffary*, Muhammad Hafiz Kamarozaman, Jalal Sharib@Sarip, Chriscius Anthonius, Mohd Tarmizi Ishak, Zulkifli Daud and Nurul Zakila Azlan***

Radiochemistry and Environemntal Laboratory,
Waste and Environmental Technology Division,
Malaysian Nuclear Agency, Bangi, 43000 KAJANG, MALAYSIA
*Corresponding author: assyikeen@nm.gov.my

## *ABSTRACT*

*Accurate measurement of $^{210}$Po in environmental samples is very important because $^{210}$Po is a major contributor to the natural radiation dose received by all living organisms. This study is carried out since no comprehensive work validates the $^{210}$Po in-house test method in Radiochemistry and Environmental Group, Malaysian Nuclear Agency. This paper defines the procedure used to determine $^{210}$Po in sediment samples, which involved acid digestion followed by auto-plating for counting using an alpha spectrometry system. Validation in terms of robustness including physical and chemical aspects was done. The physical parameter involves different counting geometry, plating time, and counting time intervals, while chemical aspects include iron content in the sample. This study found that this method is robust.*

**Keywords/Kata kunci:** Polonium-210, alpha spectrometry, method validation, robustness
*Polonium-210, spektrometri alfa, pengesahan kaedah, keteguhan*

## INTRODUCTION

Polonium-210 ($^{210}$Po) is a radioactive isotope discovered in July 1898 by Maria Sklodowska-Curie. Polonium-210 is a naturally occurring alpha emitter and exists in the environment due to $^{210}$Pb decay within the $^{238}$U decay chain. Being part of the $^{238}$U decay series, $^{210}$Po is ever-present in our environment. Two key processes lead to its spread in the environment: 1) the disintegration of $^{226}$Ra- in seawater and 2) the release of $^{222}$Ra from the earth's crust, which disperses radioisotopes through numerous environmental compartments (Matthews et al. 2007). The release of $^{210}$Po into aquifers and ultimately food chains is also caused by industrial operations such uranium mining (Carvalho 2016; Martin & Ryan 2004), phosphate industries, and oil-fired power plants (Boryło et al. 2013; Vaasma et al. 2017). Due to its widespread distribution and potential for human radiation exposure through ingestion and inhalation, $^{210}$Po is one of the most hazardous naturally occurring radionuclides and one of the most significant environmental radionuclides.

The Radiochemistry and Environmental Group is developing an in-house method for detecting $^{210}$Po in soil/sediment samples for testing services as part of the operations to support the Malaysian Nuclear Agency services. In order to measure alpha-emitter radioactivity in the environment using the alpha spectrometry system, reliable and accurate radiochemical separation and detection procedures are crucial.

Method validation verifies how a particular test's analytical process was carried out. The goal of this project is to expand the application of ISO 17025: 2017 to Radiochemistry and Laboratory (RAS) in response to the requirement for method validation in accordance with ISO clauses (7.2.2.1 and

7.2.2.4). A laboratory shall validate non-standard methods, laboratory-developed methods, and standard methods used outside of their intended scope, according to clause 7.2.2.1. While in accordance with clause 7.2.2.4, the laboratory must keep the following validation records: documentation of the validation procedure's use, a list of the prerequisites, an assessment of the method's performance characteristics, the results obtained, and a declaration of the procedure's validity, including a description of its suitability for the intended use. In this work, the robustness of the test technique was evaluated during method validation.

The term "robustness" refers to a measurement of an analytical method's sensitivity in the presence of small variations in the method's experimental conditions. The geometry of the counting disc (square and round form), differences in Fe content that may affect the sufficiency of HAC, contact time during polonium plating on the silver disc, and counting time interval all contributed to the robustness of the procedure. The reporting data was used to assess the robustness of the method.

## MATERIAL AND METHODS

Each radionuclide that emits alpha has a distinctive energy that can be used for their identification. The majority of the radionuclides for alpha particles have a small range of energy, often between 10 and 20 keV, which is close to the resolution of the silicon detector. As a result, chemical separation of the $^{210}$Po radionuclide is required before analysis.

The following steps make up the radiochemical process for $^{210}$Po determination: sample decomposition, preparing alpha sources, and measurement using alpha spectrometry. A soil/sediment sample of around 0.5g is digested using hot acid digestion. The samples are then evaporated with strong HCl, and over a period of four hours at a temperature not more than 90°C, polonium spontaneously deposits on a silver disc. A typical technique for $^{210}$Po determination involves auto-plating $^{210}$Po on a silver disc to prepare an alpha source. However, the radiochemical approach and sample preparation methods employed in the current process has no standard procedure. Therefore, there is always have chances for this procedure to be enhanced or optimised, especially with regard to sample preparation. Specific methodologies for polonium's radiochemical composition has reported previously (Nurrul et al. 2021).

Alpha spectrometry system is used to measure the activity concentrations of alpha emitter radionuclides, including $^{210}$Po. For energy and efficiency calibration, a multinuclide point source ($^{238}$U, $^{234}$U, $^{239}$Pu, $^{241}$Am) was used, and the samples were counted under the same measuring conditions as calibrated alpha spectrometry system. Known that the sample geometry and the distance between the counting source and the detector can affect the detection efficiency. Alpha Vision was used to analyse each spectrum. For $^{210}$Po determination, the measurement time was 24hrs and counting shelf was the closest to the detector (Shelf no. 1).

Certified reference materials from the International Atomic Energy Agency (IAEA) with a variety of compositions, such CRM IAEA-384 (Povinec et al. 2007), IAEA-385 (IAEA 2008), IAEA-410, and IAEA-412 with a known amount of $^{210}$Po, were used to complete this study. In this investigation, a $^{209}$Po NIST traceable radiotracer with an accessible radioactivity value was used for the recovery check.

## RESULTS AND DISCUSSION

### *Square vs. round shape silver disk geometry*

In order to validate the method of determining polonium, the radioactivity data obtained through alternative counting source geometries (square vs. round shape) were compared in terms of robustness. Before plating, the 99% pure silver disc had been cut into square and round shapes and cleaned with silver polish to remove any oxides or other impurities from its surface.

As demonstrated in Table 1, both data utilising square and round shape geometry for the counting disc were recorded within certified range activity concentration (Bq/kg) with a high recovery value (almost 90%).

Table 1: Set of CRM data using different geometry of the silver disk

| Sample Number | Po-210 activity (Bq/kg) | Recovery (%) | Silver disk geometry |
|---|---|---|---|
| 1. | 28.00 | 98.56 | Round Shape |
| 2. | 28.81 | 96.95 | Round Shape |
| 3. | 27.81 | 94.25 | Round Shape |
| 4. | 27.36 | 91.80 | Round Shape |
| 5. | 30.1 | 91.8 | Square Shape |
| 6. | 30.8 | 104.7 | Square Shape |
| 7. | 29.3 | 88.9 | Square Shape |
| 8. | 28.3 | 90.4 | Square Shape |

T-test has been used to analyse the method's robustness when using different geometries of the counting source (square vs. round shape). Both square shape geometry and round shape geometry were comparable by > 95% confidence level according to T-test calculations in Table 2.

Table 2: T-test calculation

| Statistical analysis | Round shape geometry | Square shape geometry |
|---|---|---|
| Mean | 27.9963 | 29.6367 |
| Standard Deviation | 0.5237 | 0.9107 |
| Varian | 0.2742 | 0.8294 |
| Number of replicates | 4 | 4 |
| T-value | 3.123024135 | |
| Degree of Freedom | 6 | |
| Critical Value based on T distribution table | 2.45 | |
| 95% confidence level | <0.05 | |
| T-test | 0.445 | |

***Variations in Fe content that may affect the adequacy of hydroxylamine hydrochloride, HAC***

For the conversion of $Fe^{3+}$ to $Fe^{2+}$, hydroxylamine hydrochloride (HAC) is added to the plating media as a reducing agent. Environmental samples are known to contain interference ions of manganese (Mn), iron (Fe), selenium (Se), chromium (Cr), or Tellurium (Te) that disrupt the deposition of polonium. Hydroxylamine hydrochloride (HAC) were added to eliminate $Fe^{3+}$ that will interfere the deposition of $Po^{2+}$ onto silver disc by reduction reaction to $Fe^{2+}$.

The amount of iron (Fe) in the CRM was measured using neutron activation analysis (NAA). The stated amounts of Fe in various CRM were used to demonstrate that just 1 g Hydroxylamine hydrochloride (HAC) used in the developed procedure is required to convert $Fe^{3+}$ ions to $Fe^{2+}$. Additionally, by converting $Mn^{4+}$ to $Mn^{3+}$, potassium permanganate (KMnO4) can be used as a colour indicator to determine how much hydroxylamine hydrochloride is required.

***Fe analysis using Neutron Activation Analysis (NAA)***

Using the idea that an element in the sample emits gamma rays after being bombarded and activated by neutrons at a rate that is directly proportional to its concentration, neutron activation analysis (NAA) was used to determine the amount of Fe in Certified Reference Materials (CRM), IAEA-384, IAEA-385, IAEA-410, and IAEA-412. Samples were placed in a rotating rack within the TRIGA MARK reactor, where Fe identify from 2 energy peaks, which are 1099 keV and 1292 keV using gamma spectrometry. The Fe element content for each CRM is shown in Table 3.

According to Table 4, the computed u-score which is smaller than the suggested value, 1.64 between the experimental value and the certified value of the reference materials IAEA-384, IAEA-385, IAEA-410, and IAEA-412 is recorded as 0.31, 0.03, 0.23, and 0.24, respectively. It can be seen from this that the stated outcome is consistent with what was anticipated (IAEA 2002; Manickam et al. 2010). Based on radioactivity data, the study demonstrated that 1g of HAC supplied during the plating method was sufficient and reliable for reducing $Fe^{3+}$ to $Fe^{2+}$ in all sediment samples. Applying the desired amount of HAC resulting successfully deposited of the $Po^{2+}$ ion on the silver disc (Szarlowicz 2019).

Table 3: Fe content (ppm) in various types of CRM

| **CRM** | **FE concentration (ppm)** | | |
|---|---|---|---|
| | 1099 keV | 1292keV | AVERAGE |
| IAEA-384 | 98.99 | 89.85 | 94.42 |
| IAEA-385 | 30630.65 | 30599.4 | 30615.03 |
| IAEA-410 | 6512.68 | 6462.33 | 6487.51 |
| IAEA-412 | 39211.15 | 39314.12 | 39262.64 |

Table 4: Po-210 measurement data and u-score using certified material IAEA-384, IAEA-385, IAEA-410 and IAEA-412

| Certified material | Exp No. | Experimental radioactivity ($Bqkg^{-1}$) | U-score |
|---|---|---|---|
| IAEA-384 | 1 | 12.24±4.80 | 0.31 |
| | 2 | 12.16±3.90 | |
| | 3 | 12.22±3.88 | |
| | AVERAGE | 12.21±4.17 | |
| IAEA-385 | 1 | 26.02±5.29 | 0.03 |
| | 2 | 29.5±4.7 | |
| | 3 | 28.06±4.99 | |
| | AVERAGE | 27.86±4.99 | |
| IAEA-410 | 1 | 222.64±23.64 | 0.23 |
| | 2 | 208.44±20.72 | |
| | 3 | 216.59±22.32 | |
| | AVERAGE | 215.89±22.23 | |
| IAEA-412 | 1 | 86.82±13.40 | 0.24 |
| | 2 | 86.19±12.95 | |
| | 3 | 86.21±11.85 | |
| | AVERAGE | 86.41±12.73 | |

***Plating time***

The deposition of polonium was carried out on a silver disc (99% purity) with a diameter 25mm. The silver disc was placed in a holder and immersed in solution for different times. In this experiment, the solution was stirred during the plating time. Based on Table 5, which examined the impact of contact time during Polonium auto-plating, it was determined that a plating period of 4 hours was the ideal amount of time.

Table 5: Radioactivity and FWHM of CRM IAEA-385 measured with different plating time

| Contact time | Average $^{210}$Po activity (Bq/kg),N=3 | Recovery (%) | Average $^{209}$Po FWHM | Average $^{210}$Po FWHM |
|---|---|---|---|---|
| 2hrs | 24.12 | 69.72 | 44.72 | 42.82 |
| 4hrs | 27.64 | 90.87 | 33.44 | 32.05 |
| 8hrs | 23.02 | 92.87 | 32.54 | 34.46 |
| 16hrs | 33.26 | 45.00 | 65.60 | 64.74 |

According to this study, 4-hour deposition durations result in high quality measurement sources, which yield thin, uniform alpha sources with excellent peak resolution (30 keV) (Figure 1) and $^{210}$Po sample radioactivity readings within the certified value of 26 to 30 Bq/kg. $^{210}$Po is challenging to fit into the certified value after an 8-hour plating process. It is thought that iron has impeded the deposition of polonium. It is well known that some interferences, including ions of Mn, Fe, Se, Cr, or Te, can be found in environmental samples and prevent the polonium from depositing. Due to its high abundance on Earth in terms of mass, iron is the metal that produces the most interference during

the analysis of sediment samples (Szarlowicz 2019). It's also possible that the longer hours spent plating in the acid solution caused the silver disc to start to degrade. Figure 2 illustrates the thick alpha sources, which exhibited the worst peak in resolution at 16 hours of deposition.

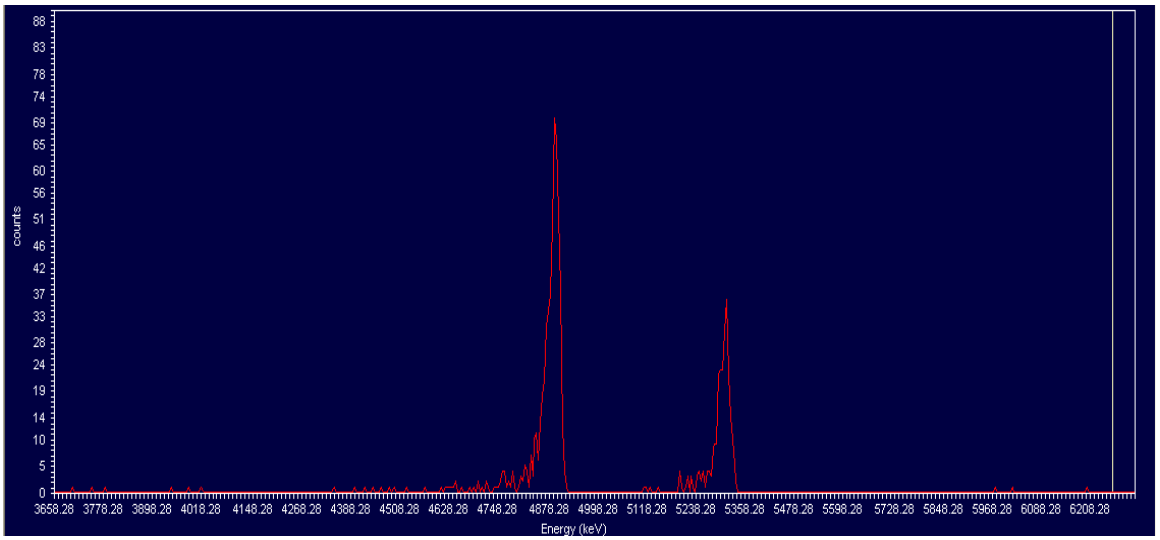


Figure 1: Spectrum with high peak resolution (30 keV)

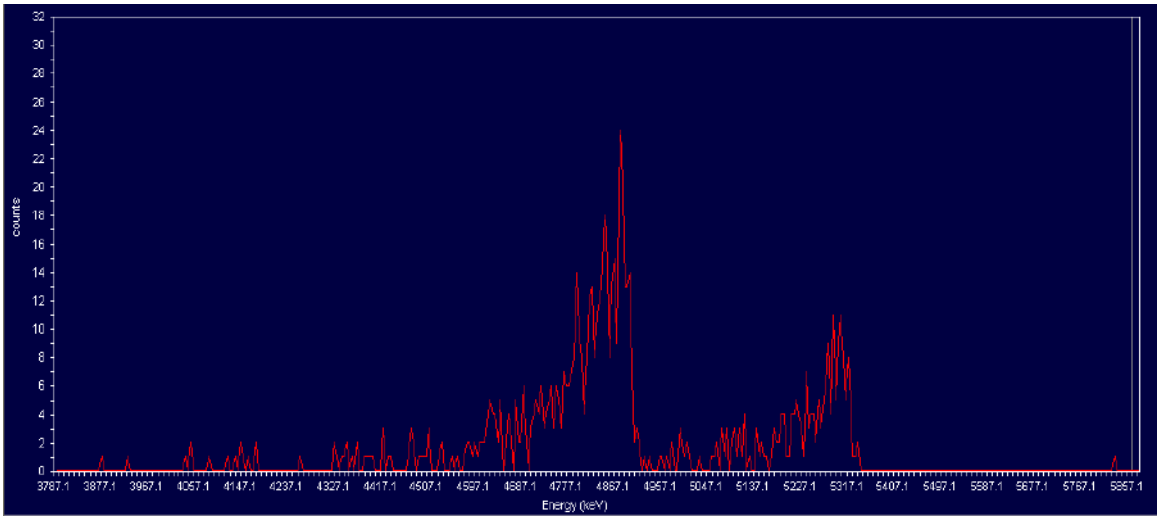


Figure 2: Spectrum with worse peak resolution (60 keV)

**Counting time interval**

The activity of CRM IAEA-385 is determined by study at various counting time intervals. Using the same sample preparation source, samples were recounting at day 1$^{st}$, 9$^{th}$, and 21$^{st}$ and 60$^{th}$ after the separation date. Table 6 displays the measured activity. The method is confirmed to be reliable for measurement time intervals up to 21 days by the U-score analysis, which revealed that the radioactivity measured has no significant difference at different counting time intervals.

Table 6: Radioactivity of CRM IAEA-385 measured at day 1, 9 and 21.

| Sample code | Counting date (counting date interval) | | | | | | | |
|---|---|---|---|---|---|---|---|---|
| | 16/6/2022 (Day 1st) | | 24/6/2022 (Day 9th) | | 6/7/2022 (day 21st) | | 15/8/2022(day 60th) | |
| | **Act** | **Unc** | **Act** | **Act** | **Unc** | **Act** | **Act** | **Unc** |
| I1 | 28.52 | 6.05 | 27.14 | 22.01 | 6.05 | 27.14 | 22.01 | 5.20 |
| I2 | 27.65 | 4.87 | 25.84 | 25.60 | 4.87 | 25.84 | 25.60 | 4.87 |
| I3 | 27.90 | 4.92 | 24.67 | 26.19 | 4.92 | 24.67 | 26.19 | 4.88 |
| I4 | 27.64 | 5.00 | 28.47 | 30.51 | 5.00 | 28.47 | 30.51 | 5.79 |
| I5 | 27.38 | 4.55 | 28.41 | 27.48 | 4.55 | 28.41 | 27.48 | 4.96 |
| I8 | 27.50 | 4.57 | 28.15 | 32.41 | 4.57 | 28.15 | 32.41 | 5.56 |
| AVERAGE | 27.77 | 4.99 | 27.11 | 27.37 | 4.99 | 27.11 | 27.37 | 5.21 |
| U-Score | 0.04 | | 0.17 | 0.11 | | 0.17 | 0.11 | |

## CONCLUSION

The technique employed to detect the activity $^{210}$Po in the environmental samples was determined to be robust. It is discovered that a minimum counting period of 24 hours is adequate to allow the alpha spectrometry to identify $^{210}$Po quantitatively. This measuring methodology is reliable in terms of physical and chemical parameters, according to the method validation; 1) Data employing geometric counting discs of square and round shapes recorded the activity concentration (Bq/kg) within the accepted range value, 2) For all sediment samples, 1g of HAC applied during the auto-plating method was sufficient and reliable to convert $Fe^{3+}$ to $Fe^{2+}$, with resulting $Po^{2+}$ ion successfully deposited on the silver disc, 3) The optimal plating time for alpha polonium is 4 hours, and during this procedure, thin, uniform alpha sources with excellent peak resolution (30 keV) are created, 4) The radioactivity measured has not significantly different at various counting time intervals up to 60$^{th}$ days. In conclusion, this analytical method has shown its robustness in quantifying $^{210}$Po in the samples.

## REFERENCES

Boryło, A., Olszewski, G. & Skwarzec, B. (2013). A study on lead (210Pb) and polonium (210Po) contamination from phosphogypsum in the environment of Wiślinka (northern Poland). *Environmental Sciences: Processes and Impacts 15*(8): 1622–1628.

Carvalho, F.P. (2016). Preliminary assessment of uranium mining legacy and environmental radioactivity levels in Sabugal region , Portugal 399–408.

IAEA. (2002). Advances in destructive and non-destructive analysis for environmental monitoring and nuclear forensics. *Advances in Destructive and Non-Destructive Analysis for Environmental Monitoring and Nuclear Forensics*. Karlsruhe.

IAEA. (2008). Reference Sheet for Certified Reference Material IAEA-385 Radionuclides In Irish Sea Sediment. Vienna.

Manickam, E., Sdraulig, S. & O'Brien, R. (2010). An improved and rapid radiochemical method for the determination of polonium-210 in urine. *Australian Journal of Chemistry 63*(1): 38–46.

Martin, P. & Ryan, B. (2004). Natural-Series Radionuclides in Traditional Aboriginal Foods in Tropical Northern Australia : A Review 77–95.

Matthews, K.M., Kim, C. & Martin, P. (2007). Determination of Po in environmental materials : A review of analytical methodology *65*: 267–279.

Nurrul, N.A., Azlan, N.Z., Sharib Sarip, J., Ishak, M.T., Daud, Z. & Adziz, M.I.A. (2021). 210Po determination in urine samples among radiation workers by alpha spectrum analysis. *Malaysian Journal of Analytical Sciences 25*(3): 498–507.

Povinec, P.P., Pham, M.K., Sanchez-Cabeza, J.A., Barci-Funel, G., Bojanowski, R., Boshkova, T., Burnett, W.C., Carvalho, F., Chapeyron, B., Cunha, I.L., Dahlgaard, H., Galabov, N., Fifield, L.K., Gastaud, J., Geering, J.J., Gomez, I.F., Green, N., Hamilton, T., Ibanez, F.L., Ibn Majah, M., John, M., Kanisch, G., Kenna, T.C., Kloster, M., Korun, M., Liong Wee Kwong, L., La Rosa, J., Lee, S.H., Levy-Palomo, I., Malatova, M., Maruo, Y., Mitchell, P., Murciano, I. V., Nelson, R., Nouredine, A., Oh, J.S., Oregioni, B., Le Petit, G., Pettersson, H.B.L., Reineking, A., Smedley, P.A., Suckow, A., Van Der Struijs, T.D.B., Voors, P.I., Yoshimizu, K. & Wyse, E. (2007). Reference material for radionuclides in sediment IAEA-384 (Fangataufa Lagoon sediment). *Journal of Radioanalytical and Nuclear Chemistry 273*(2): 383–393.

Szarlowicz, K. (2019). Optimization of the radiochemical procedure of 210Po determination in small amounts of sediment samples. *International Journal of Environmental Science and Technology 16*(10): 5735–5740. https://doi.org/10.1007/s13762-018-2156-2.

Vaasma, T., Loosaar, J., Gyakwaa, F., Kiisk, M., Özden, B. & Tkaczyk, A.H. (2017). Pb-210 and Po-210 atmospheric releases via fly ash from oil shale-fired power plants. *Environmental Pollution 222*: 210–218.

e-Jurnal Sains Nuklear Malaysia, 2023, Vol. 35 (No.1): 37 – 48
*eISSN: 2232-0946*

# POTENTIAL USE OF FALLOUT RADIONUCLIDES ($^{137}$Cs AND $^{210}$Pb$_{ex}$) IN ASSESSING SOIL EROSION RATES WITHIN THE LANGAT WATERSHED

***Noor Fadzilah Yusof[*], Tukimat Lihan[2], Wan Mohd Razi Idris[2], Mohd. Abdul Wahab Yusof[1], Norfaizal Mohamed@Muhammad[1], Nooradilah Abdullah[1], Dainee Nor Fardzila Ahmad Tugi[1] and Muhammad Izzat Muammar Ramli[1]***

[1]Malaysian Nuclear Agency, 43000 Kajang, Bangi, Selangor
[2]Department of Earth Sciences and Environment, Faculty of Science and Technology, Universiti Kebangsaan Malaysia, UKM Bangi, Selangor
Corresponding author: fadzilah@nm.gov.my

## *ABSTRACT*

*Soil erosion is a severe environmental problem arising due to human intervention such as deforestation, urbanization, rapid land use change and overgrazing. Langat watershed is highly risk in erosion potential as it is exposed to land clearing activities due to population growth. The objective of this study is to assess the potential use of $^{137}$Cs and excess $^{210}$Pb in soil erosion assessment within the Langat watershed. A total of 15 individual sectioned soil cores were collected along the upstream to the downstream of Langat watershed. The net erosion rate based on $^{137}$Cs measurement ranged between -8 to -66 t ha$^{-1}$ yr$^{-1}$ with an average of -33 t ha$^{-1}$ yr$^{-1}$, whereas, based on $^{210}$Pb$_{ex}$, the net erosion rate ranged between -5 to -50 t ha$^{-1}$ yr$^{-1}$ with an average of -28 t ha$^{-1}$ yr$^{-1}$. The sediment delivery ratio estimated by both radionuclides were above 90% indicating that most of the sediment transported out of the watershed. Fallout radionuclides (FRN) method is proven to be a significant alternative to overcome constraints and limitations encountered in conventional approach. Thus, FRN method appeared to be an essential and effective alternative in soil erosion assessment.*

**Keywords:** *$^{137}$Cs, $^{210}$Pb$_{ex}$, fallout radionuclide, Langat, soil redistribution*

## INTRODUCTION

Over recent years, there has been a growing concern over water-induced soil erosion and its associated environmental impacts. There is an increased demand to obtain reliable information on soil erosion rates and sediment deposition. Nevertheless, such information is difficult to acquire when using conventional techniques due to validation, accuracy, time-consuming and cost concerns (FAO, 2019a, 2019b). Thus, the potential for using fallout radionuclides have been explored widely in various region and scale (Chaboche et al., 2021; Moustakim et al., 2019; Porto et al., 2018).

Fallout radionuclides, namely, caesium-137 ($^{137}$Cs) is a man-made radionuclide (half-life = 30.2 ± 0.2 years) and lead-210 ($^{210}$Pb) (half-life = 22.20 ± 0.22 years) is a naturally occurring radionuclide, are widely used as environmental tracers to study soil redistribution (He and Walling, 1996; Walling, 1999). Soil redistribution consist of soil erosion, transportation and sediment deposition imposed a serious environmental problem globally. $^{137}$Cs is originated from nuclear power plant, weapon test or nuclear power plant accident such as Chernobyl in Russia and Fukushima in Japan (Panin et al., 2001; Tagami et al., 2019).

The application of $^{210}$Pb is still limited and needs more investigation and validation, even though it has been used extensively in sediment dating. Lead-210 is often used as a complementary radionuclide besides $^{137}$Cs due to the low concentration of $^{137}$Cs. $^{210}$Pb is a natural product of the decay series of uranium-238 ($^{238}$U). It is derived from radon gas decay, known as the daughter of $^{226}$Ra (half-life = 1600 ± 7 years). The diffusion of radon gas from soil, which produces $^{210}$Pb into the atmosphere and, subsequently, its fallout provides a continuous input of radionuclides to the soil surface and sediment. The fallout radionuclide is identified as "unsupported" or "excess" $^{210}$Pb. Due to its natural existence, $^{210}$Pb is often measured as a complimentary radionuclide to $^{137}$Cs in measuring soil erosion. Both radionuclides ($^{137}$Cs and $^{210}Pb_{ex}$) reach the soil surface as fallout and are rapidly absorbed by soil particles. As they clamped onto the soil surface, they acted as a tracer when soil redistribution was controlled by deposition, erosion and transportation processes (Zheng et al., 2007). $^{137}$Cs and $^{210}Pb_{ex}$ will provide information on medium-term (40 years) and long-term (100 years) erosion rates and patterns, respectively.

The objective of this paper is to assess the potential use of fallout radionuclides in assessing soil erosion rates within the Langat watershed. Rapid changes in land use activities in the Langat watershed vicinity would induce significant soil redistribution. Therefore, an erosion study was needed to explore the rates and patterns of soil erosion within a larger watershed based on a tropical climate. The findings of this study will provide an understanding of the erosion system and scientific basis to implement an effective countermeasure for the increasing erosion potential.

## MATERIALS AND METHODS

### Study Area

This study was conducted at the Langat watershed with a catchment area of 2287 km$^2$ (Figure 1). Langat River originated from Mount Nuang, Titiwangsa Range with a total length of 141 km (LUAS, 2011, 2015) and flows through three states namely Selangor, the Federal Territory of Putrajaya and Negeri Sembilan, towards the Straits of Malacca near Banting town, Kuala Langat. The Langat watershed has a tropical climate with mean annual temperature varies from 23°C to 31°C (based on years 1979-2014). Maximum rainfall normally occurs in November and minimum rainfall occurs in February with an annual precipitation at 2061 mm (DID, 2010).

The main tributaries include Semenyih River, Beranang River and Labu River with two important dams, namely, Langat dam and Semenyih dam. The Langat watershed is regarded as one of the most critical water catchment areas providing domestic and industrial water to the population within the Langat River.

In this study, the sampling area was divided into fifteen stations along the Langat watershed as shown in Figure 1 and the description of each sampling station is given in Table 1. Sampling activities included a field survey (coordinate and land use) were conducted from February to July 2019 (upstream, middle stream and downstream).

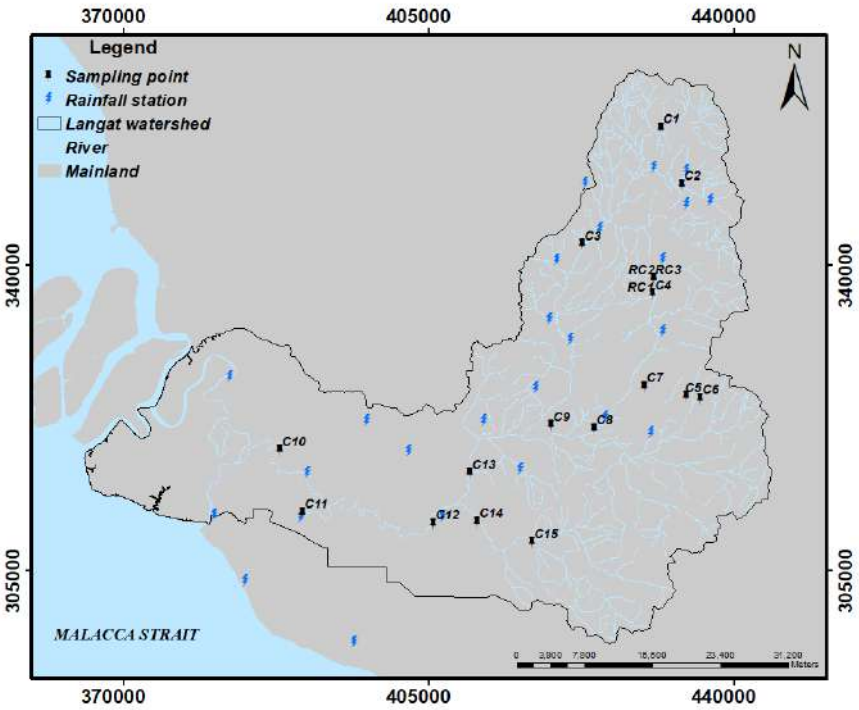


Figure 1: Sampling location along the Langat watershed

Table 1: Area description of sampling station

| Stations | Area description |
|---|---|
| Reference point (RC1, RC2 and RC3) | Forestry area near Forest Reserve Ulu Langat, Forest Reserve Gunung Nuang and Forest Reserve Sungai Tekala |
| C1 | Forest area near Pangsun River |
| C2 | Fruit farm near Lui River |
| C3 | Forest area |
| C4 | Palm oil plantation near main road |
| C5 | Rubber plantation near Broga road |
| C6 | Cleared land near hill side |
| C7 | Grassland near residential area |
| C8 | Rubber plantation near Rinching |
| C9 | Palm oil plantation near main road |
| C10 | Palm oil plantation near Langat River |
| C11 | Bushes near Langat Riverbank |
| C12 | Palm oil plantation near paper factory |
| C13 | Bushes near Langat Riverbank |
| C14 | Sandy soil near Hartalega factory |
| C15 | Palm oil plantation between Batang Nilai River and Labu River |

**Sampling Strategy**

Soil erosion rates were estimated using $^{137}C$ and $^{210}Pb_{ex}$ are based on the comparison between individual and reference inventory obtained from a representative local fallout (Mabit et al., 2008). In this study, a relatively undisturbed, flat, stable site, and at the highest altitude is considered to minimize soil erosion (Khodadadi et al., 2021). Three stations were considered as reference points namely, Forest Reserve Ulu Langat, Forest Reserve Gunung Nuang and Forest Reserve Sungai Tekala (Table 1). The reference site and individual points should receive the same amount of precipitation and have similar geomorphological parameters (Nouira et al., 2003).

At each station, a stainless-steel soil corer with 40 cm long and 10.5 cm diameter was used to collect segmented core at 2 cm increments. The maximum depth is limited to 30 cm depth due to stony soil at certain sampling points. The location of the study area which included latitude, longitude and elevation were determined by a Global Positioning System (GPS).

A total of 15 individual soil cores were collected within the Langat watershed following the same procedure as the reference point. The individual cores were collected based on different types of land use. There were two core samples collected from secondary forest, five from palm oil plantation, two from rubber plantation, three from bushes/riverbank, one each from fruit farm, cleared land and grassland, respectively.

**Sample Preparation and Analyses**

Soil samples were oven dried at 60ºC, disaggregated, and passed through a 2 mm sieve. Particle size analysis was carried out by using a particle size analyser (Model: Microtrac-X100 from USA). Besides, organic matter and soil texture were estimated using standard soil analysis method (Miyazawa et al., 2000). After sample pre-preparation, a readily weighted sample was packed into a 6 ml cylindrical container or in 30 ml plastic container and sealed for at least 21 days (International Atomic Energy Agency, 2014) to establish the secular equilibrium between $^{226}Ra$ and $^{222}Rn$ (half-life = 3.8235 ± 0.0003 days).

Measurement of $^{137}Cs$ and unsupported $^{210}Pb$ activities were undertaken simultaneously by high-purity germanium (HPGe) gamma spectrometry system (Model: Canberra from USA). The sample was counted for over 50 000s with an analytical precision at ± 10% at the 95% level of confidence. The detector is a closed end coaxial well-detector operated on 2000 HV bias supply. The p-type detector with the FWHM resolution of 0.82 keV at 122 keV gamma line of $^{57}Co$ and 1.85 keV at 1.3 MeV gamma line of $^{60}Co$, with the relative efficiency of 25% (Yii and Wan Mahmood, 2020). The activity of $^{137}Cs$ in the soil sample was obtained from the count rate at 662 keV peak energy. The unsupported $^{210}Pb$ activity concentration in the sample was calculated from difference between the total $^{210}Pb$ (46.5 keV peak energy) and the $^{226}Ra$ (measured via its daughter $^{214}Bi$, 609.3 keV peak energy) (Montes et al., 2019; Rabesiranana et al., 2016). Activity concentration for each radionuclide was estimated using the equation below:

$$A = \frac{\left[\left(\frac{C_1}{T}\right) - \left(\frac{B}{T_b}\right)\right]}{E.w.\gamma} \qquad \text{Eq..(1)}$$

Where, A is the radionuclide activity concentration (Bq $kg^{-1}$), $C_1$ is the sample peak area (count), T is the sample counting time (s), B is the peak area for sample background (count), $T_b$ is the

background counting time (s), E is the efficiency of the equipment (%), w is the sample weight (g) and γ is the emission probability (%).

Gamma spectrometry detector was calibrated using standard multi-nuclide standard source purchased from Isotope Products Laboratories, USA (Yii and Wan Mahmood, 2020). The minimum detectable activity (MDA) was estimated to be 5 Bq $kg^{-1}$ for total $^{210}Pb$, 1 Bq $kg^{-1}$ for $^{137}Cs$ and 1 Bq $kg^{-1}$ for $^{226}Ra$.

**Estimation of Erosion Rates**

Soil erosion rate was estimated based on the comparison between inventory at a specific point to the reference point. The radionuclide inventory was estimated using the equation below:

$$I_a = \sum A_i \rho_i H_i \qquad \text{Eq...(2)}$$

Where, $I_a$ is the radionuclide inventory, $A_i$ is the sample activity of the $i^{th}$ sample at depth increment (Bq $kg^{-1}$), $\rho_i$ is the bulk density of $i^{th}$ sample (kg $m^{-3}$) and $H_i$ is the depth of the $i^{th}$ sample at depth increment (m). The radionuclide inventory was denoted by unit Bq $m^{-2}$.

The conversion model developed by Walling et al. (2001) was applied to estimate soil erosion rates for the sampling sites. Difference conversion models were used for $^{137}Cs$ and $^{210}Pb_{ex}$ measurement which are proportional model and mass balance model 2 (MBM2), respectively. A software package based on an Excel Add-in is available to convert the radionuclide inventory to soil redistribution rates (International Atomic Energy Agency, 2014).

Based on the study by Porto et al. (2014), the $^{137}Cs$ fallout input is assumed to be completely mixed within the cultivated layer and the soil reduction is directly proportionate to the decline of $^{137}Cs$ in the soil profile. The average annual soil loss rate, Y (t $ha^{-1}$ $yr^{-1}$) can be given as (International Atomic Energy Agency, 2014) :

$$Y = 10\ \frac{BdX}{100TP} \qquad \text{Eq....(3)}$$

Where, X is the percentage decline in total $^{137}Cs$ inventory (given as $A_{ref} - A/A_{ref}$ x 100), d is the ploughing depth (m), T is the time elapsed since the initiation of $^{137}Cs$ accumulation (year) which is assumed at 1963, B is the bulk density of the soil (kg $m^{-3}$), P is the particle size correction factor, $A_{ref}$ is the local $^{137}Cs$ reference inventory (Bq $m^{-2}$), and A is the total measured inventory at the individual sampling point (Bq $m^{-2}$).

As for $^{210}Pb_{ex}$, the MBM2 can be expressed as Walling et al. (2001):

$$\frac{d(A)}{dt} = (1-\Gamma)I(t) - (\lambda + (\frac{PR}{m}))A(t) \qquad \text{Eq….(4)}$$

Where, A(t) is the $^{210}Pb_{ex}$ inventories (Bq $m^{-2}$); R is the soil erosion rate (kg $m^{-2}$ year); t is the time since the onset of $^{210}Pb_{ex}$ fallout (year); I(t) is the annual deposition flux at the time t (Bq $m^{-2}$ year); m is the cumulative mass depth representing the average plough depth (kg $m^{-2}$); λ is the decay constant for $^{210}Pb_{ex}$ ($year^{-1}$); P is the particle size factor; Γ is the proportion of the freshly deposited $^{210}Pb_{ex}$ removed by erosion before mixing into the plough layer; Γ is expressed as $\Gamma = p\ \gamma\ (1-e^{-R/H})$ where γ is the proportion of the annual $^{210}Pb_{ex}$ input susceptible to removal by erosion, and H is the relaxation

mass depth of the initial distribution of fallout $^{210}Pb_{ex}$ in the soil profile (Rabesiranana et al., 2016; Walling et al., 2001). The soil erosion rates based on $^{137}Cs$ and $^{210}Pb_{ex}$ measurement were spatially mapped using the spatial analyst tool in ArcGIS ver. 10.3.

## RESULTS AND DISCUSSION

The mean inventories of $^{137}Cs$ and $^{210}Pb_{ex}$ for three segmented soil cores from the reference site were estimated. The mean reference inventories for $^{137}Cs$ and $^{210}Pb_{ex}$ were estimated at 160 ± 5 Bq $m^{-2}$ and 2040 ± 5 Bq $m^{-2}$, respectively. The mean reference inventory for $^{137}Cs$ is similar to the inventory estimated by Gharibreza et al. (2013a), however, it is five times lower than study by Zainudin and Wan Ruslan (2012). This is proven that the spatial variability in fallout deposition occurred in some areas (Yang et al., 2011).

Unlike $^{137}Cs$, limited reference inventories or fallout flux of $^{210}Pb_{ex}$ have been reported in Malaysia. However, it has been documented that $^{210}Pb_{ex}$ was successfully estimated in Lake Bera, Malaysia (Gharibreza et al., 2013b), Zambia (Walling et al., 2003) and Spain (Gaspar et al., 2017). The global annual deposition for $^{210}Pb_{ex}$ reference inventory was reported in the range of 766 to 12, 233 Bq $m^{-2}$. The mean reference inventory (2040 ± 5 Bq $m^{-2}$) reported in this study is in the range of global deposition.

The individual soil cores were divided into fifteen corers numbered from C1 to C15 according to their location from upstream to downstream of the Langat watershed. The concentrations of $^{137}Cs$ and $^{210}Pb_{ex}$ in cultivated soils were relatively uniform throughout the soil profile. These individual soil cores had experienced net erosion due to rapid land use change since 1970s (Rapport et al., 2002).

The mean of inventories estimated from fifteen individual points for both radionuclides were lower than the reference inventory, thus, it is observed that erosion has occurred at the study area (Khodadadi et al., 2021). The mean of inventories for $^{137}Cs$ measured for 15 individual cores collected ranged between 43 ± 6 Bq $m^{-2}$ to 139 ± 19 Bq $m^{-2}$ with an average of 88 ± 13 Bq $m^{-2}$. On the other hand, the mean inventories for $^{210}Pb_{ex}$ ranged between 429 ± 13 Bq $m^{-2}$ to 2312 ± 26 Bq $m^{-2}$ with an average of 1080 ± 21 Bq $m^{-2}$.

The net erosion rates calculated using Eq. (3) ranged from -8 to -66 t $ha^{-1}$ $yr^{-1}$ with an average of -33 t $ha^{-1}$ $yr^{-1}$ based on $^{137}Cs$ measurement. The average sediment delivery ratio based on $^{137}Cs$ measurement is 95%. Moreover, based on $^{210}Pb_{ex}$ measurement, the net erosion rates calculated using Eq. (4) was ranged from -5 to -50 t $ha^{-1}$ $yr^{-1}$ with an average of -28 t $ha^{-1}$ $yr^{-1}$. The average sediment delivery ratio estimated based on $^{210}Pb_{ex}$ is 90%. A negative signed indicated the soil loss at the Langat watershed.

The spatial distribution of $^{137}Cs$ inventories in the Langat watershed was highly variable (Figure 2). In general, the distribution of $^{137}Cs$ inventories presented a contrast between the upstream to the downstream of the watershed. The highest $^{137}Cs$ inventories were found at the Labu sub-basin and some of area at the Banting town. In contrast, lower $^{137}Cs$ inventory was recorded on the middle stream near Semenyih, Buah and Dengkil sub-basin. Subsequently, the spatial distribution of soil erosion rates contrasts with the distribution pattern of the $^{137}Cs$ inventories. It was noted that, the highest erosion rate was found in the middle stream near Semenyih, Buah and Dengkil sub-basin, whereas the lowest erosion rates occurred near Labu sub-basin towards Banting town (Figure 3).

Based on $^{210}Pb_{ex}$ measurement, the highest inventory was found at the northern part of the Langat watershed. The northern part of Langat watershed was surrounded by the steep slope and mountainous area. The dense forest on the steep slope protects the soil surface from soil erosion, thus, the higher inventory of $^{210}Pb_{ex}$ were found (Gaspar et al., 2013). The lowest inventories were noted from the middle stream towards the downstream to the Malacca Strait (Figure 4). Similar to the $^{137}Cs$ measurement, the spatial distribution of soil erosion rates was slightly different than the inventories. The highest erosion rate occurred from the middle stream towards the Malacca Strait. On the other hand, the lowest erosion risk is located to the north of the Langat watershed (Figure 5).

The spatial distribution for $^{210}Pb_{ex}$ inventories has a different pattern than $^{137}Cs$ inventories in the Langat watershed. $^{210}Pb_{ex}$ is more sensitive to recent changes in soil erosion rates compared to $^{137}Cs$ measurements due to its constant fallout inputs and the shorter half-life of $^{210}Pb$ (Porto et al., 2016; Walling et al., 2003).

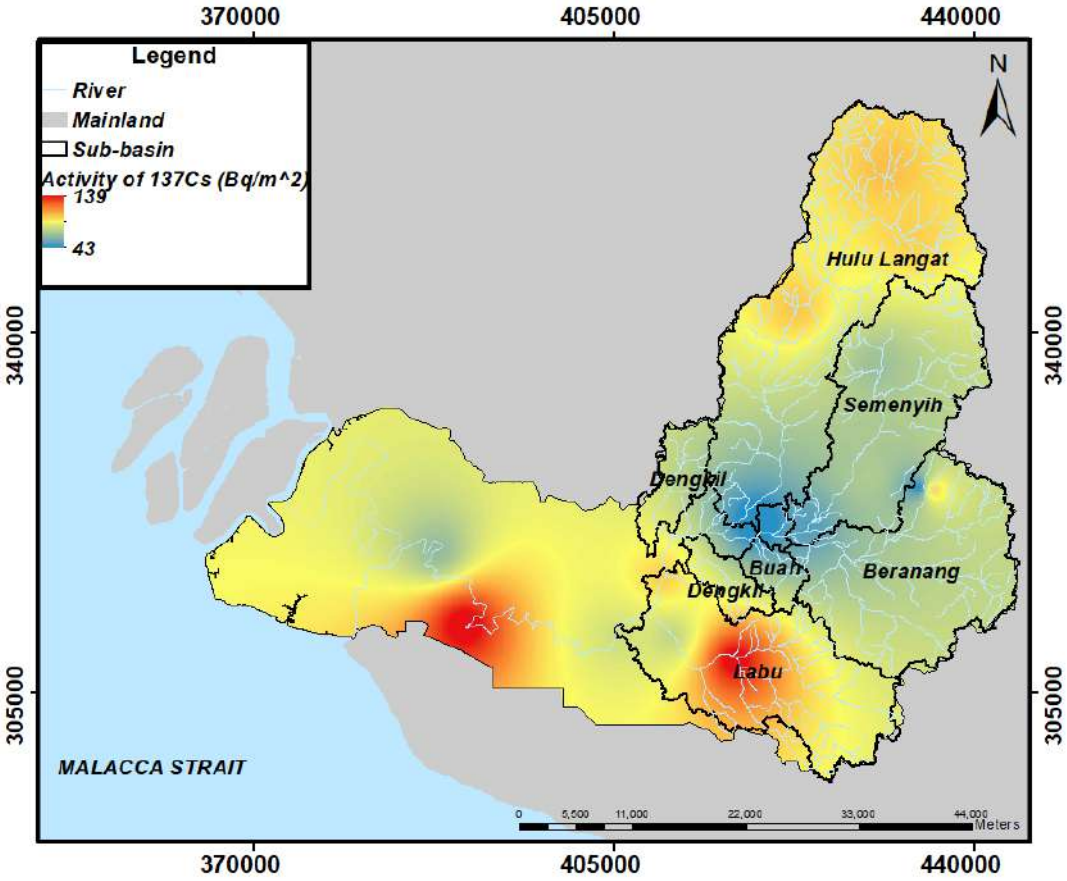


Figure 2: Spatial distribution of $^{137}Cs$ inventories in Langat watershed

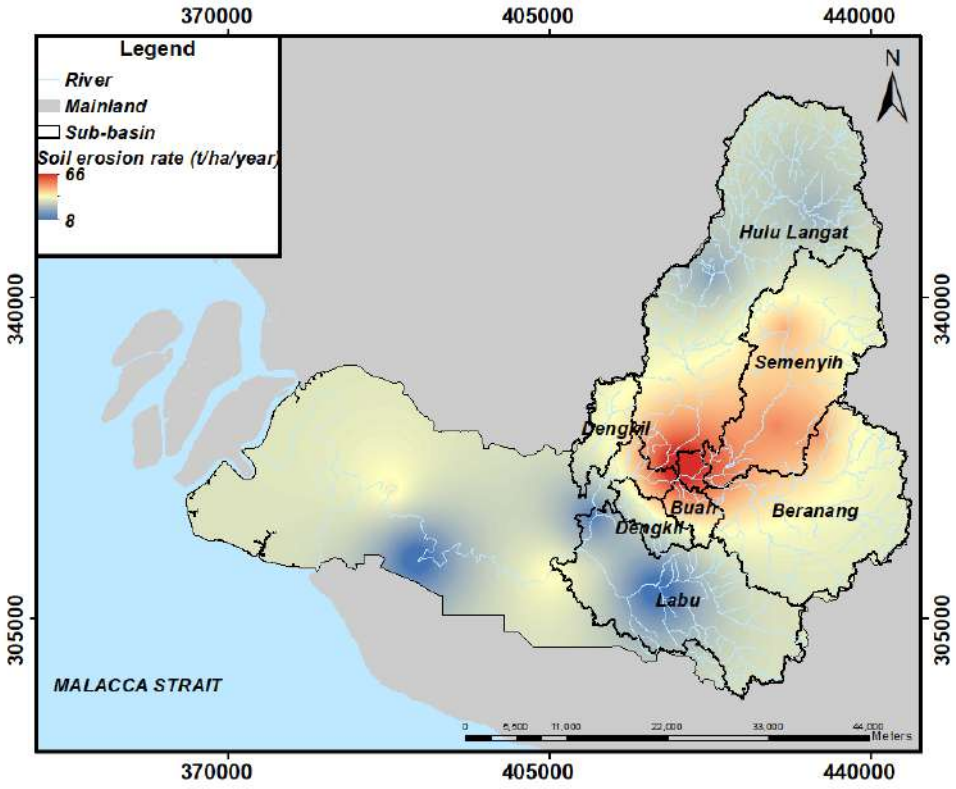


Figure 3: Spatial distribution of estimated net erosion rates by $^{137}Cs$

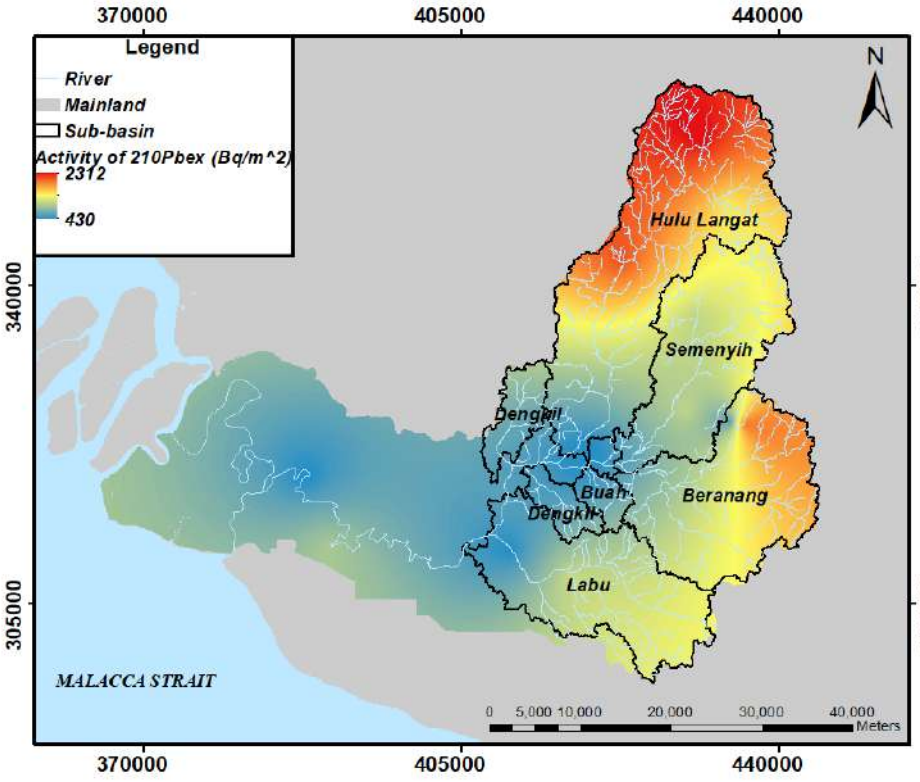


Figure 4: Spatial distribution of $^{210}Pb_{ex}$ inventories in Langat watershed

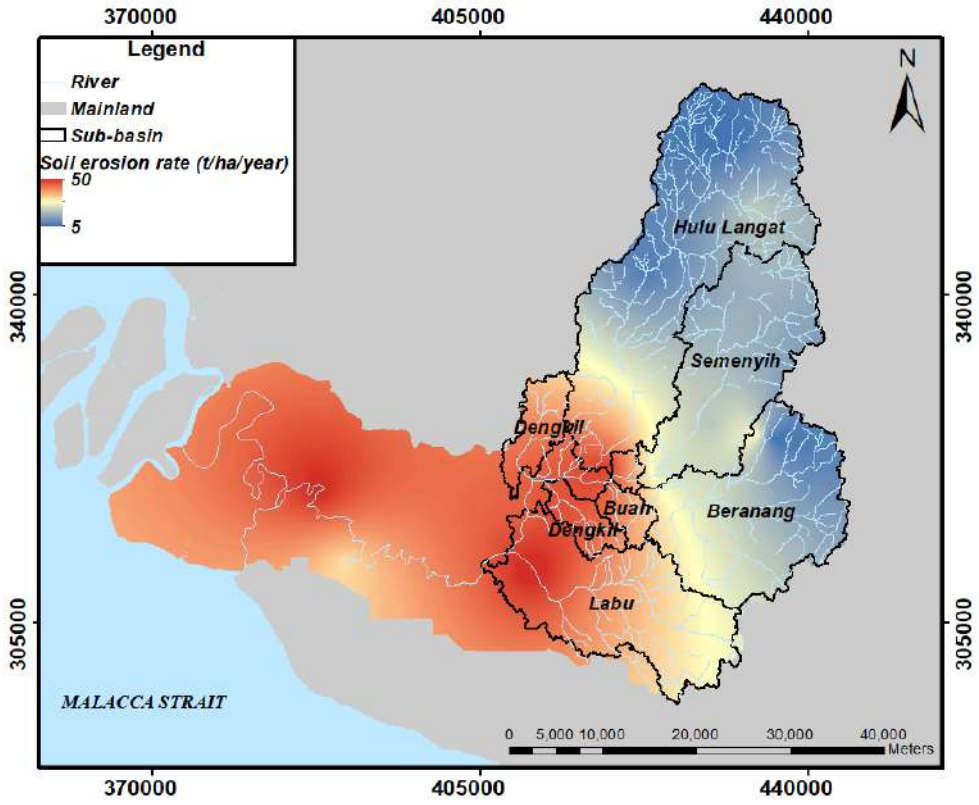


Figure 5: Spatial distribution of estimated net erosion rates by $^{210}Pb_{ex}$

## CONCLUSION

The spatial distribution of fallout radionuclides inventories ($^{137}Cs$ and $^{210}Pb_{ex}$) provided the basis for estimating soil erosion rates at the Langat watershed. This contribution proved the potential use of fallout radionuclides to quantify the medium- and long-term soil erosion rates and provides quantitative information on the relationship between erosion and inventory.

Based on the result obtained, it is proven that the radionuclide inventories are inversely proportional to the soil erosion rate. This study also illustrates the importance of establishing reference inventory within the local catchment. Individual inventory was relatively lower compared to the reference inventory, indicating erosion occurred at the specific point.

The combination of fallout radionuclides measurements with GIS software highlighted the soil redistribution processes occurring on the different geomorphic components identified within the Langat watershed. This potential combination encouraged the ability to upscale this study to a large watershed and help to strategies for a cost-effective method of assessing soil redistribution with limited sampling points.

**ACKNOWLEDGEMENT**

The authors would like to thank the Universiti Kebangsaan Malaysia and Malaysian Nuclear Agency for its facilities and support for this project. Also, a special gratitude to Universiti Kebangsaan Malaysia for providing financial support through Research University Grant (GUP-2019-043).

**REFERENCES**

Chaboche, P.-A., Saby, N. P. A., Laceby, J. P., Minella, J. P. G., Tiecher, T., Ramon, R., Tassano, M., Cabral, P., Cabrera, M., da Silva, Y. J. A. B., Lefevre, I., and Evrard, O. (2021). Mapping the spatial distribution of global $^{137}$Cs fallout in soils of South America as a baseline for Earth Science studies, *Earth-Science Reviews.* 214: 103542.

Department of Irrigation and Drainage (DID). (2010). *Guideline for Erosion and Sediment Control in Malaysia*. Kuala Lumpur: Ministry of Natural Resources and Environment, Department of Irrigation and Drainage Malaysia.

FAO. (2019a). Outcome Document of the Global Symposium on Soil Erosion.

FAO. (2019b). Soil Erosion: The Greatest Challenge to Sustainable Soil Management.

Gaspar, L., Navas, A., Machín, J., and Walling, D. E. (2013). Using $^{210}Pb_{ex}$ measurements to quantify soil redistribution along two complex toposequences in mediterranean agroecosystems, Northern Spain, *Soil and Tillage Research.* 130: 81-90.

Gaspar, L., Webster, R., and Navas, A. (2017). Fate of $^{210}Pb_{ex}$ fallout in soil under forest and scrub of the central Spanish Pre-Pyrenees, *European Journal of Soil Science.* 68: 259-269.

Gharibreza, M., John Kuna, R., Ismail, Y., Zainudin, O., Wan Zakaria, W. M. T., and Mohammad Aqeel, A. (2013a). Land use changes and soil redistribution estimation using $^{137}$Cs in the tropical Bera Lake catchment, Malaysia, *Soil and Tillage Research.* 131: 1-10.

Gharibreza, M., John Kuna, R., Ismail, Y., Zainudin, O., Wan Zakaria, W. M. T., and Mohammad Aqeel, A. (2013b). Sedimentation rates in Bera Lake (Peninsular Malaysia) using $^{210}$Pb and $^{137}$Cs radioisotopes, *Geosciences Journal.* 17: 211-220.

He, Q., and Walling, D. E. (1996). Interpreting particle size effects in the adsorption of $^{137}$Cs and unsupported $^{210}$Pb by mineral soils and sediments, *Journal of Environmental Radioactivity.* 30: 117-137.

International Atomic Energy Agency. (2014). Guidelines for using fallout radionuclides to assess erosion and effectiveness of soil conservation strategies (ISBN 978-92-0-105414-2).

Khodadadi, M., Alewell, C., Mirzaei, M., Ehssan-Malahat, E., Asadzadeh, F., Strauss, P., and Meusburger, K. (2021). Deforestation effects on soil erosion rates and soil physicochemical properties in Iran: a case study of using fallout radionuclides in a Chernobyl contaminated area, *Soil Discussions [preprint]*. 2.

LUAS. (2011). *State of the River Report 2011: Sungai Langat*.

LUAS. (2015). *State of the River Report 2015: Sungai Langat*.

Mabit, L., Benmansour, M., and Walling, D. E. (2008). Comparative advantages and limitations of the fallout radionuclides $^{137}Cs$, $^{210}Pb_{ex}$ and $^{7}Be$ for assessing soil erosion and sedimentation, *Journal of Environmental Radioactivity.* 99: 1799 -1807.

Miyazawa, M., Pavan, M. A., de, O., Ionashiro, M., and Silva, A. K. (2000). Gravimetric determination of soil organic matter, *Brazilian Archives of Biology and Technology*. 43: 475-478.

Montes, M. L., Rizzoto, M. G., Ayub, J. J., Torres Astorga, R., and Taylor, M. A. (2019). An alternative methodology to determine $^{210}Pb$ activity soil profiles, *Journal of Environmental Radioactivity*. 208-209: 105998.

Moustakim, M., Benmansour, M., Zouagui, A., Nouira, A., Benkdad, A., and Damnati, B. (2019). Use of caesium-137 re-sampling and excess lead-210 techniques to assess changes in soil redistribution rates within an agricultural field in Nakhla watershed, *Journal of African Earth Sciences.* 156: 158-167.

Nouira, A., Sayouty, E. H., and Benmansour, M. (2003). Use of $^{137}Cs$ technique for soil erosion study in the agricultural region of Casablanca in Morocco, *Journal of Environmental Radioactivity.* 68: 11-26.

Panin, A. V., Walling, D. E., and Golosov, V. N. (2001). The role of soil erosion and fluvial processes in the post-fallout redistribution of Chernobyl-derived caesium-137: a case study of the Lapki catchment, Central Russia, *Geomorphology.* 40: 185-204.

Porto, P., Walling, D. E., and Callegari, G. (2018). Using repeated $^{137}Cs$ and $^{210}Pb_{ex}$ measurements to establish sediment budgets for different time windows and explore the effect of connectivity on soil erosion rates in a small experimental catchment in Southern Italy, *Land Degradation & Development.* 29: 1819-1832.

Porto, P., Walling, D. E., and Capra, A. (2014). Using $^{137}Cs$ and $^{210}Pb_{ex}$ measurements and conventional surveys to investigate the relative contributions of interrill/rill and gully erosion to soil loss from a small cultivated catchment in Sicily, *Soil and Tillage Research.* 135: 18-27.

Porto, P., Walling, D. E., Cogliandro, V., and Callegari, G. (2016). Exploring the potential for using $^{210}Pb_{ex}$ measurements within a re-sampling approach to document recent changes in soil redistribution rates within a small catchment in Southern Italy, *Journal of Environmental Radioactivity*. 164: 158-168.

Rabesiranana, N., Rasolonirina, M., Solonjara, A. F., Ravoson, H. N., Raoelina, A., and Mabit, L. (2016). Assessment of soil redistribution rates by $^{137}Cs$ and $^{210}Pb_{ex}$ in a typical Malagasy agricultural field, *Journal of Environmental Radioactivity.* 152: 112-118.

Rapport, D. J., Lasley, B. L., Rolston, D. E., Nielsen, N. O., Qualset, C. O., and Damania, A. B. (2002). Managing for Healthy Ecosystems. CRC Press, Florida, USA

Tagami, K., Tsukada, H., and Uchida, S. (2019). Quantifying spatial distribution of $^{137}$Cs in reference site soil in Asia, *CATENA.* 180: 341-345.

Walling, D. E. (1999). Linking land use, erosion and sediment yields in river basins, *Hydrobiologia.* 410: 223-240.

Walling, D. E., Collins, A. L., and Sichingabula, H. M. (2003). Using unsupported lead-210 measurements to investigate soil erosion and sediment delivery in a small Zambian catchment, *Geomorphology.* 52: 193-213.

Walling, D. E., Zhang, Y., and He, Q. (2001). Models for Converting Measurements of Environmental Radionuclide Inventories ($^{137}$Cs, Excess $^{210}$Pb, and $^{7}$Be) to Estimates of Soil Erosion and Deposition Rates (Including Software for Model Implementation).

Yang, Y.-H., Yan, B.-X., and Zhu, H. (2011). Estimating soil erosion in northeast China using $^{137}$Cs and $^{210}Pb_{ex}$, *Pedosphere.* 21: 706-711.

Yii, M. W., and Wan Mahmood, Z. U. y. (2020). Estimation of sediment accumulation rate at different season in Juru River and Perai River (Perai Industrial Area, Penang, Malaysia), *Jurnal Sains Nuklear Malaysia.* 32: 8-22.

Zainudin, O., and Wan Ruslan, I. (2012). Using environmental radionuclide, $^{137}$Cs to investigate soil re–distribution in an agricultural plot in Kalumpang, Selangor, Malaysia, *Kajian Malaysia.* 30: 45-70.

Zheng, J.-J., He, X.-B., Walling, D. E., Zhang, X.-B., Flanagan, D., and Qi, Y.-Q. (2007). Assessing soil erosion rates on manually-tilled hillslopes in the Sichuan Hilly basin using $^{137}$Cs and $^{210}Pb_{ex}$ measurements, *Pedosphere.* 17: 273-283.

e-Jurnal Sains Nuklear Malaysia, 2023, Vol. 35 (No.1) : 49 – 66
*eISSN: 2232-0946*

# PENILAIAN PRESTASI R&D TEKNOLOGI NUKLEAR: KAJIAN KES AGENSI NUKLEAR MALAYSIA

***Fairuz Suzana Mohd Chachuli, Mohd Azmi Sidid Omar, Azlinda Binti Aziz, Abdul Quddoos Abu Bakar and Faridah Mohd Idris***

Planning & International Relations Division,
Malaysian Nuclear Agency, 43000 Kajang, Selangor
Corresponding author: fairuz@nm.gov.my

## *ABSTRACT*

*Nuclear technology has started in Malaysia since the establishment of the Malaysian Nuclear Agency (Nuclear Malaysia) in 1972. The agency was established to promote the peaceful application of nuclear science and technology for national development. Nuklear Malaysia also plays important role in providing research, development, commercialisation, and innovation (RDCI) in line with national interests, including industry, medicine and healthcare, food and agriculture, natural resources, energy, and nuclear safety and security. This paper aims to examine the performance and the growth of nuclear technology R&D in Nuklear Malaysia from 2011-2021 using the data envelopment analysis (DEA) and Malmquist index (MI) analysis. The study uses two inputs, namely RDC & Development budget (RM Million) and Operating budget (RM Million), and three outputs, namely revenue (RM Million), no. of R&D products and no. of publications. The result shows that the performance of nuclear technology R&D in Nuklear Malaysia is 96.70 per cent from 2011-2021. The study shows that nuclear R&D growth decreased by 8.3 per cent for the entire study period. The technological changes decreased at 8.3 per cent, while the efficiency changes remain. The study also found that nuclear technology R&D growth index in Nuklear Malaysia is mainly affected by technological changes due to policy changes compare to the resources provided since efficiency changes remain. The findings of the study help management and officials of Nuklear Malaysia to realign the institution's direction to ensure the nuclear technology RDCI contribute to the socio-economic development of the country.*

**Keywords**: *efficiency, growth, nuclear technology, performance, R&D*

## INTRODUCTION

Agensi Nuklear Malaysia (Nuklear Malaysia) marks its 50$^{th}$ years of anniversary in the year 2022 and highlights its important role as a premier research and development (R&D) organisation in nuclear science and technology in the country. Nuklear Malaysia also continues to play an active role and contributes to the implementation and realisation of national science and technology (S&T) policies to ensure it remains a relevant public research institute for the country (Nuklear Malaysia, 2022). After the 50$^{th}$ year of establishment, Nuklear Malaysia is mature and capable to face challenges and manage changes efficiently. Nuklear Malaysia has an emphasis on building the human capital potential and ensuring that all activities fit the mainstream S&T and national interest.

In realising the potential of S&T as an agent for new economic development for the nation, particularly in facing the global competitive market, Nuklear Malaysia has focused its R&D activities on six priority areas, namely advanced material, advanced manufacturing, biotechnology, ICT, advanced alternative energy, and nanotechnology (Nuklear Malaysia, 2013). With its multidisciplinary features, nuclear technology could offer a technical solution to arising technical

problems. The R&D projects are market-driven to produce beneficial products to generate economic returns through downstream activities. Efforts have been made to ensure that research products can be commercialised through technology transfer and licensing. Continuous research efforts and knowledge expansion in nuclear science and technology are necessary to further technological innovation, which in turn brings about new benefits for country.

After the 50$^{th}$ year of establishment, it is a crucial time to evaluate the performance of nuclear technology R&D activities in Nuklear Malaysia which are mainly funded by the Government. Most research organizations, including Nuklear Malaysia are faced with increasing demands on their existing resources and there is a constant need to improve resource allocation and utilization. As the R&D process utilizes scarce resources, it becomes crucial to assess its efficiency. The assessment of R&D efficiency has the dual advantage of identifying the better performers for benchmarking and it also throws light on ways to improve efficiency by highlighting areas of weakness. The efficiency of the R&D process can be the ratio of the R&D outputs and inputs. The major inputs to the R&D process are expenditure on R&D and human resources. The outputs are patents and publications since both patents and publications are used extensively in measuring R&D efficiency and innovation.

This paper measures the relative efficiency of the nuclear technology R&D activities and the R&D growth of nuclear science and technology in Nuklear Malaysia from 2011-2021 using Data Envelopment Analysis (DEA) and Malmquist Index (MI) analysis. In this study, Nuklear Malaysia is selected as a case study since its role as a leading R&D organization in the field of nuclear science and technology in Malaysia. This paper would significantly contribute to future strategic decision-making on the success of R&D of nuclear science and technology activities in Nuklear Malaysia. The rest of the paper is organized as follows. The second section presents a review of the existing literature on R&D performance and growth. The third section describes the methodology followed in the current work. The results and discussions are presented in the fourth section. Section five summarizes the study and provides a conclusion.

**Literature review**

Some researchers have conducted studies on evaluating R&D performance to see institutional efficiency. An effective R&D operation is a major source of competitive advantage in today's rapidly globalizing economy. Thus, the evaluation of R&D performance has been the important problem for both academic interest and practical needs (I.J. Asmara et al., 2019). It is difficult to measure the R&D efficiency due to the complicated characteristics of these activities and DEA method is a widely used as a nonparametric approach to measure the R&D efficiency (O. Belgin, 2019). R&D efficiency attracts the attention of the researchers, and many papers can be encountered on the R&D efficiency of firms, institutions, academic research, countries, or regions.

Zhang et al. (2003) investigated the impact of ownership on the R&D efficiency of Chinese firms using the stochastic frontier estimation. They found that foreign firms have higher R&D and productive efficiency than domestic collective-owned enterprises and joint stock companies. The higher R&D efficiency of foreign firms appears to be due to a higher R&D intensity, which in turn leads to higher productivity. Lu (2009) investigated the R&D efficiency and marketability of Taiwan's IC-design firms using DEA. They found that it is not desirable that firms often ignore marketability in the R&D process. Chuang et al. (2011) measured the R&D efficiency of the Taiwanese semiconductor industry's new product development. They found that 58% of the IC semiconductor industry is efficient in new product development.

Bae and Chang (2012) analysed the impact of open and closed innovation on the performance of Korean firms. They found that both efficiency and effectiveness were statistically higher among open

innovation firms than among their closed counterparts. It may thus be concluded that the acquisition of outside technology or knowledge has a positive impact on firm performance. Hung and Shiu (2014) evaluated the R&D efficiency of projects using three-stage DEA and Tobit regressions. They found that technology type and accumulative experience enabled R&D projects to be advantageously implemented in the human resource department, whereas group diversity was disadvantageous and created superfluous repetition in human resources. Chun et al. (2015) examined the efficiency of R&D processes of Korean manufacturing firms using two-stage DEA. They found that R&D efficiency is different by firm size and industry type. Jang (2016) measured the cumulative change in R&D efficiency of globally leading R&D companies in the technology industry using the DEA and Malmquist Index. Results indicated that the overall R&D efficiency of these globally leading R&D companies declined slightly during the period 2007–2013.

Khoshnevis and Teirlinck (2017) analysed the efficiency of R&D active firms using DEA models. They found that firms in specialized supplier industries tend to outperform, while firms in science-based industries are found to underperform. Qin and Du (2018) measured the R&D performance of universities in China's provinces using a network data envelopment analysis. They found that universities' R&D activities are considered efficient and effective only in a small number of provinces, while in most provinces, these activities can generally be considered less efficient and effective. Xiong et al. (2018) evaluated the R&D efficiency of Chinese research institutes using DEA. They found that the institutes experienced significant improvements in system efficiency, mainly due to the improvements in transfer efficiency. Fairuz et al. (2021) explored the performance of R&D activities in five renewable energy resources in Malaysia from 2012 to 2017 using DEA. They found that mini hydro is the most efficient renewable energy source in Malaysia, whereas wind is the most inefficient one from the perspective of R&D activities.

The current study uses two variables, namely RDC & Development budget (RM Million) and operating budget (RM Million) as input for R&D activities, whilst revenue (RM Million), number of R&D products and number of publications are identified as an output for R&D activities. The DEA model and the Malmquist productivity index analysis are used in this study to assess the R&D performance of nuclear technology in Nuklear Malaysia, as well as to evaluate the impact of the policy interventions, toward nuclear technology R&D in Nuklear Malaysia from 2011 to 2021 using these variables. The policy interventions related to nuclear technology R&D activities considered in this study are Malaysian Nuclear Agency Strategic Plan 2012-2020: Strategy and Action Plan, Dasar Sains, Teknologi dan Inovasi Negara (DSTIN) 2013 – 2020, 10$^{th}$ Malaysia Plan 2010-2015 (10$^{th}$ MP) and 11$^{th}$ Malaysia Plan 2016-2020 (11$^{th}$ MP).

## METHODOLOGY

### *DEA*

DEA is a widely used tool by academics and practitioners to assess the performance of firms. DEA is a comparison approach based on linear mathematical programming, in which units use multiple inputs to produce multiple outputs, resulting in a single measure of overall performance (F.S. Mohd Chachuli et al., 2020). Every DMU in DEA compares their efficiency to its peers by considering a variety of input and output criteria (H. Zhou et al., 2018). The DEA method is based on the mathematical

technique to make the most efficient use of resources to meet a decision-making objective. According to Charnes, Cooper, and Rhodes (1978), the weighted total of output to the weighted sum of input for each DMU evaluation cannot exceed 1 (A. Charnes et al., 1978). The Charnes–Cooper– Rhodes (CCR) model and the Banker–Charnes–Cooper (BCC) model are two types of DEA models often used to estimate the degree of inefficiency in the input-output ratio, particularly to prioritise the ranking of each DMU. The BCC model's capacity to comprehend varied returns to scale (VRS) distinguishes it from the CCR model (R.D. Banker et al., 1984). Efficiency is measured on a scale of 0 to 1, where a value of 1 indicates the unit is relatively efficient, and a value less than 1 indicates the unit is inefficient. The efficiency score of a unit will vary according to the factors and DMUs included in the analysis.

For static analysis, this study employs the BCC-DEA model with the VRS assumption. The MI analysis is utilised for dynamic analysis to evaluate the impact of strategic papers on nuclear technology R&D activities in Nuklear Malaysia. The CCR-DEA output-oriented model is presented in Eq. (1) (R.D. Banker et al., 1984).

$Min\ \Phi$

Subject to

$$\sum_{j=1}^{n} z_i x_{ij} + s^- = x_0, (i = 1, \ldots, m)$$

$$\sum_{j=1}^{n} z_j y_{rj} - s^+ = \theta_0 y_0, (r = 1, \ldots, s)$$

$$z_0 \geq 0, j = 1, \ldots, n$$

For VRS, add $\sum^{n}{}_{j=1}\, z_j = 1,$ Eq...(1)

where $n$ is the number of DMUs. $m$ is the input and $s$ is the output for each $DMU_j$ ($j$ = 1,2, …, $n$). $x_{ij}$ (i = 1,2, …,$n$) is the $i$th input of $DMU_j$, and $y_{rj}$ is the $r$th output of $DMU_j$. Slack variables, $s_i^-$ and $s_j^+$, measure the excess of inputs and outputs. The efficiency value is denoted by $\theta_0$, which is in the range of (0,1].

***Malmquist productivity index***

The Malmquist productivity index analysis is employed in this study to assess productivity changes in nuclear technology R&D activity (N.K. Avkiran, 2006; C. Woo, 2015). The index is usually applied to the measurement of productivity change over time and can be multiplicatively decomposed into an efficiency change index and a technological change index. The Malmquist productivity index was generalised by Färe and Grosskopf based on the geometric mean of two indices (R Fare, 1994). This index examines the change in productivity between periods $t$ and $t$+1 (D.W. Caves, 1982). In addition, this index compares the ratios of two distance functions to determine their productivity (A.N. Menegaki, 2013).

Eq. (2) expresses the Malmquist productivity change which has two parts: technical efficiency change (EFFCH) and technological change (TECHCH), as follows [33]:

$$M_t^{t+1} = \left[\frac{D_0^t(x_0^{t+1},y_0^{t=1})}{D_0^t(x_0^t,y_0^t)}\frac{D_0^{t+1}(x_0^{t+1},y_0^{t+1})}{D_0^{t+1}(x_0^t,y_0^t)}\right]^{1/2}, \quad \text{Eq...(2)}$$

$$EFFCH = \frac{D_0^t(x_0^{t+1},y_0^{t+1})}{D_0^t(x_0^t,y_0^t)}, \quad \text{Eq...(3)}$$

$$TECHCH = \left[\frac{D_0^t(x_0^{t+1},y_0^{t+1})}{D_0^{t+1}(x_0^{t+1},y_0^{t+1})}\frac{D_0^t(x_0^t,y_0^t)}{D_0^{t+1}(x_0^t,y_0^t)}\right]^{1/2}, \quad \text{Eq...(4)}$$

where $M_t^{t+1}$ is the index between periods *t* and *t*+1; $D_0^t(x_0^t, y_0^t)$ and $D_0^{t+1}(x_0^t, y_0^t)$ are the distance functions between *t* and *t*+1 for inputs and outputs, respectively.

In Eq. (2), efficiency increases if $M_t^{t+1}$>1, remains constant if $M_t^{t+1}$=1 and decreases if $M_t^{t+1}$<1.

In Eq. (3), the EC component calculates the catch-up impact of whether a specific DMU is closer or further away from the production frontier in periods *t* and *t*+1. The frontier shift effect or TC quantifies the technological progress or regress of DMUs between *t* and *t+1*.

The Malmquist productivity index is a dynamic analysis tool designed to compensate for the inadequacies of DEA. DEA can only examine a static scenario during a specified period. Without assuming a preset production index, the Malmquist productivity index assesses the ratio of input to output, allowing for a dynamic assessment of efficiency changes. The Malmquist productivity index is computed by multiplying EFFCH and TECHCH. EFFCH represents the difference in the object of study's proximity to the production frontier from one period to the next, whereas TECHCH depicts how technological change affects efficiency through time. When EFFCH and TECHCH ideas are applied to government policy, EFFCH indicates how efficiently resources are used to achieve a policy's goal. TECHCH, on the other hand, shows changes beyond the policy control such as the introduction of a new programme or operational policy. It should be noted that, EFFCH values bigger than 1 represents an increase in performance, and EFFCH values less than 1 represents a decrease in performance. Also, the TECHCH values bigger than 1 indicate the progress of the technology, and the values less than 1 indicate the regress of the technology.

***Research design***

Figure 1 depicts the conceptual framework in this study. Throughout the policy implementation in Nuklear Malaysia, three inputs and two outputs are selected to analyse the R&D performance of nuclear technology in Nuklear Malaysia from 2011 to 2021. DEA model is used to assess the efficiency of nuclear technology R&D, whilst the Malmquist Index analysis is used to assess the R&D growth over the years and evaluate the impact of the policy intervention towards nuclear technology R&D activities in Nuklear Malaysia such as Malaysian Nuclear Agency Strategic Plan 2012-2020: Strategy and Action Plan, Dasar Sains, Teknologi dan Inovasi Negara (DSTIN) 2013 – 2020, 10$^{th}$ Malaysia Plan 2010-2015 (10$^{th}$ MP) and 11$^{th}$ Malaysia Plan 2016-2020 (11$^{th}$ MP).

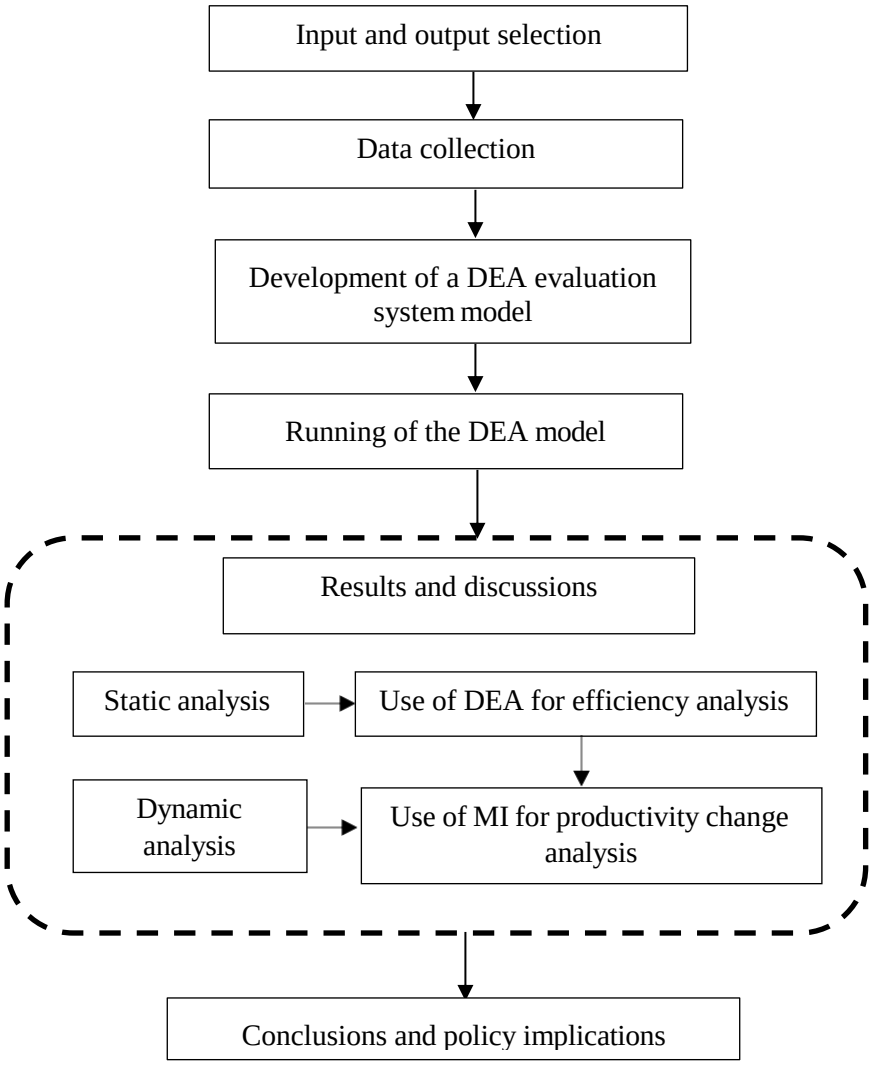


Figure 1: Proposed DEA research framework

***Data collection***

Table 1 shows the inputs and outputs data used collected in this study. In this study, the annual RDC & Development budget (RM Million) and Operating budget (RM Million) are selected as input from the Annual Report of the Malaysian Nuclear Agency from the year 2011-2021. Nuklear Malaysia received a total amount of RM 329.56 million for RDC & Development budget, while RM 864.13 million for the operating budget during this period. The total government funding received for Nuklear Malaysia amounted to RM1193.69 million for 11 years. Revenue (RM Million), no. of R&D products and no. of publications are selected as an output in the study. Income generation through commercialisation activities in Nuklear Malaysia recorded a total of RM125.63 million from 2011-2021. The average total budget ratio between the funding received by Nuklear Malaysia to revenue generated through commercialisation activities in Nuklear Malaysia is around 10.52% from the period 2011-2021. It is noticed that the revenue generation for Nuklear Malaysia decreased in the year 2020 and 2021 during the Covid-19 pandemic season last two years. The number of R&D products produced by Nuklear Malaysia shows an increasing trend over the years. From 2011-2021, the total R&D products produced from Nuklear Malaysia is 722 units including products, patents, procedures, and protocols. Another R&D output used in this study is the number of publications published by researchers of Nuclear Malaysia. Total publications published by Nuclear Malaysia is 5,993 units from 2011-2021, although, in the middle of the study period, the publishing trend shows a decreasing value in 2016 and 2017.

Table 1: Input and output data

| Year | RDC & Development budget (RM Million) | Operating budget (RM Million) | Revenue (RM Million) | No. of R&D products | No. of publications | Budget Ratio |
|---|---|---|---|---|---|---|
| 2011 | 10.20 | 66.21 | 15.78 | 53 | 568 | 20.65% |
| 2012 | 18.43 | 70.67 | 14.61 | 68 | 302 | 16.40% |
| 2013 | 25.42 | 72.90 | 12.45 | 49 | 683 | 12.66% |
| 2014 | 41.81 | 75.89 | 13.24 | 45 | 702 | 11.25% |
| 2015 | 34.07 | 76.77 | 11.41 | 71 | 625 | 10.29% |
| 2016 | 48.29 | 80.15 | 12.62 | 70 | 386 | 9.82% |
| 2017 | 44.50 | 81.50 | 10.38 | 45 | 434 | 8.24% |
| 2018 | 34.12 | 81.93 | 12.06 | 58 | 590 | 10.39% |
| 2019 | 20.87 | 84.79 | 10.43 | 76 | 653 | 9.87% |
| 2020 | 14.08 | 85.90 | 8.11 | 72 | 511 | 8.11% |
| 2021 | 37.75 | 87.40 | 4.54 | 115 | 539 | 3.63% |
| **Total** | **329.56** | **864.13** | **125.63** | **722** | **5993** | **10.52%** |

Table 2 shows the descriptive statistic of input and output data used in this study. The average amount of RDC & Developing a budget is RM29.96 million, with the highest amount being RM48.29 million received in 2016. The trend for operating budget is increasing every year to cover the daily expenses of the organization as well as to pay salaries for the staff. Nuklear Malaysia received the highest Operating budget at RM87.40 million in 2021, with the average amount being RM78.56 million during the study period. The highest revenue generated through commercialisation activities in Nuklear Malaysia is RM15.78 million in 2011, whilst the lowest revenue generated is RM4.54 million in 2021. Nuklear Malaysia produced an amount of 66 R&D products every year with the highest R&D products produced being 115 units in 2021. The highest number of publications published by Nuklear Malaysia is 702 units in 2014, whilst the lowest is at 302 in 2012.

Table 2: Descriptive statistics of input and output data

| | **RDC & Development budget (RM Million)** | **Operating budget (RM Million)** | **Revenue (RM Million)** | **No. of R&D products** | **No. of publications** |
|---|---|---|---|---|---|
| Mean | 29.96 | 78.56 | 11.42 | 66 | 545 |
| St. Deviation | 12.89 | 6.71 | 3.09 | 20 | 127.34 |
| Minimum | 10.20 | 66.22 | 4.54 | 45 | 302 |
| Maximum | 48.29 | 87.40 | 15.78 | 115 | 702 |

## RESULT AND DISCUSSION

### Performance evaluation of nuclear technology R&D activities

Fig. 2 depicts the comparison between the budget received by Nuklear Malaysia and the revenue generated through the commercialisation activities carried out in Nuklear Malaysia from 2011-2021. The operating budget, which covers the salary of staff and daily operations, and maintenance costs is increasing every year since 2011. The increasing operating budgets are mostly due to increasing salary of staff annually including when the staff got promoted in their grade position although the number of staff remain the same. The trend of RDC and development budget which is mainly distributed through the 5-year Malaysia Plan (MP) covers $10^{th}$ MP for 2011-2015 and $11^{th}$ MP for 2016-2020 was not consistent during the study period. It seems that the RDC and development budget is high in the year 2014 during the $10^{th}$ MP and the year 2016 during the $11^{th}$ MP. Both years remark a high RDC and development budget received by Nuklear Malaysia when the Thorium Flagship project entitled Development of Innovative Nuclear Reactor Technology – With the Spin-Off Based on Thorium (FP0214D052 DSTIN) was implemented from 2014 to 2018. The flagship project was implemented under the Dasar Sains, Teknologi Dan Inovasi Negara (DSTIN) 2013 – 2020 due the recommendation from the Jawatankuasa Kajian Penggunaan Torium Sebagai Bahan Asas Dalam Proses Penjanaan Tenaga Nuklear in 2013. However, the revenue generated from the commercialisation activities in Nuklear Malaysia recorded a decreasing trend over the years up to 28.76% compared to 2011 and 2021, especially during the Covid-19 pandemic phase. In addition, the decreasing trend in the revenue generated is observed due to the current efforts made by Nuklear Malaysia that have been made to ensure that research products and activities should be commercialised through technology transfer and licensing to their industrial partners.

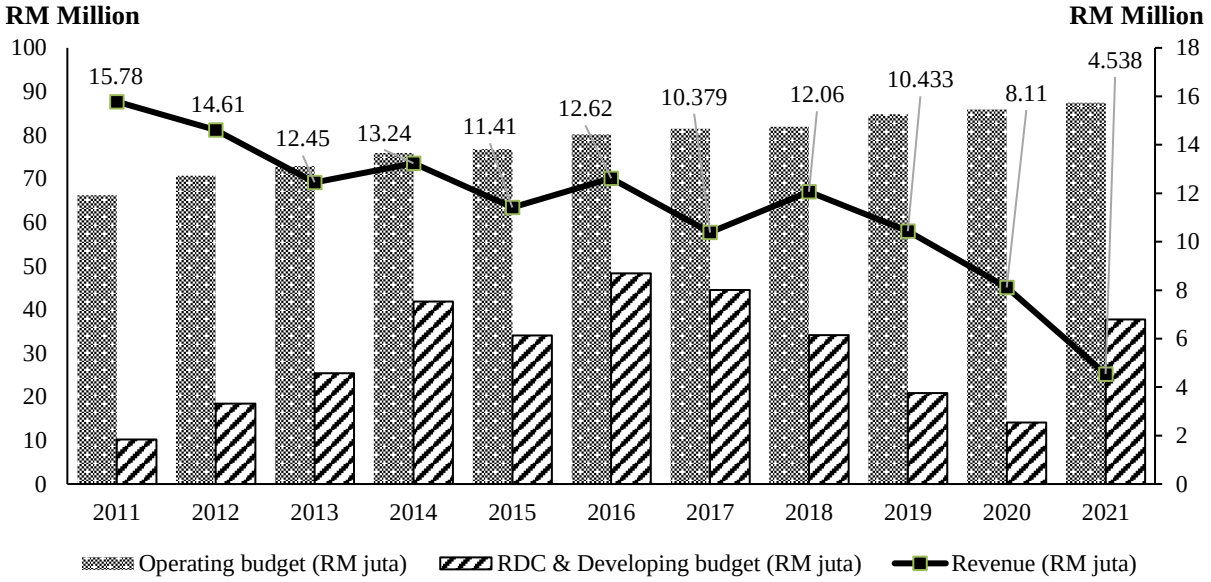


Figure 2: The budget received and revenue generated from 2011-2021

Fig.3 shows the trend of R&D outputs produced by Nuclear Malaysia from 2011-2020. The R&D outputs include innovation awards at national and international levels, number of Intellectual Property Rights (IPR) generated from MOSTI grants or other grants, number of publications, number of products, number of processes and procedures developed and number of potential products for commercialisation generated from Nuklear Malaysia. The total number of R&D products produced by Nuklear Malaysia is 722 units while the number of publications published is 5,993 units from 2011-2020. Although the total publications showed a decreasing trend from 2014 to 2016, the publications activities among Nuklear Malaysia's staff are increased over the years since then. However, the total R&D products including innovation awards, IPR, products, processes, procedures, and potential products for commercialisation show an increasing trend from 2011-2020. This is showing that Nuklear Malaysia's staff are actively conducting R&D activities related to nuclear science and technology concerning the budget received for Nuklear Malaysia either from the annual operating budget or RDC & development budget.

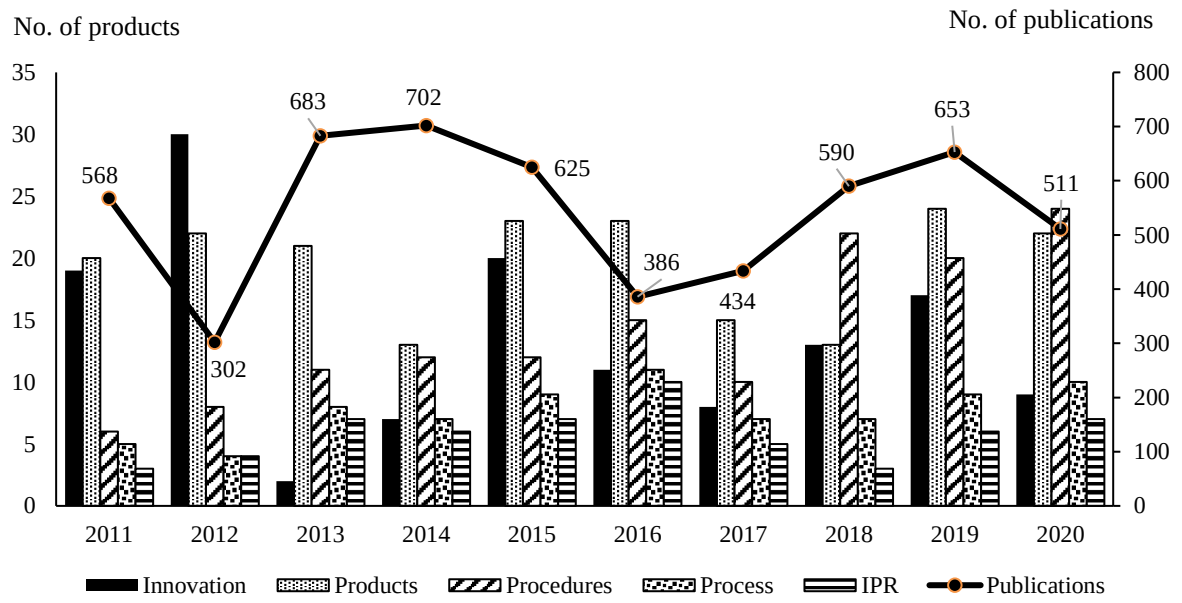


Figure 3: R&D outputs produced by the Malaysian Nuclear Agency from 2011-2020

The summary of efficiency scores using the DEA output-oriented model is shown in Table 3. The output-oriented model is selected in this study to make an inefficient unit to be efficient through the proportional increase of its outputs, while the proportions of the input remain. In this study, the Variable Returns to Scale (VRS) is selected to estimate efficiencies whether an increase or decrease in input or outputs does not result in a proportional change in the outputs or inputs respectively. In most cases, the VRS model is selected by researchers to reflect the real-world issues compared to the CRS model. Table 3 shows that the performance of nuclear technology R&D activities in Nuklear Malaysia is 96.70 per cent from 2011-2021. However, a decreasing trend in the R&D activities in Nuklear Malaysia is highlighted from 2016-2018 due to the decreasing number of R&D outputs produced during this period, especially total publications.

Table 3: Summary of efficiency scores using DEA output-oriented model

| Year | VRS technical efficiency scores |
|---|---|
| 2011 | 1.000 |
| 2012 | 1.000 |
| 2013 | 1.000 |
| 2014 | 1.000 |
| 2015 | 1.000 |
| 2016 | 0.961 |
| 2017 | 0.739 |
| 2018 | 0.935 |
| 2019 | 1.000 |
| 2020 | 1.000 |
| 2021 | 1.000 |
| **Average** | **0.967** |

**Nuclear technology R&D growth**

Table 4 shows the summary of Malmquist Index analysis during the study period. EFFCH indicates how efficiently resources are used to achieve a specific's goal, whilst TECHCH shows changes beyond the policy control such as the introduction of a new programme or operational policy. The average of EFFCH index remains unchanged during the study period, this means that Nuklear Malaysia efficiently used all resources provided to implement the nuclear technology R&D activities from 2011-2021. However, the average of TECHCH index achieved at 0.917, which means that the technological changes index has decreased at 8.3%. During the study period, the total factor productivity change (TFPCH) for nuclear technology R&D activities in Nuklear Malaysia is 0.917. This is means that the growth of nuclear technology R&D activities in Nuklear Malaysia is decreasing up to 8.3% during 2011-2021. Along the study period, Nuklear Malaysia has efficiently used all resources provided to implement the nuclear technology R&D activities from 2011-2021, however the implementation of the strategic documents as well as the operational policy such as DSTIN and 5-years Malaysia Plan give an impact to the nuclear technology R&D activities to Nuklear Malaysia.

Table 4: Malmquist Index Summary

| Period | EFFCH | TECHCH | PECH | SECH | TFPCH |
|---|---|---|---|---|---|
| 2011-2012 | 1.000 | 0.595 | 1.000 | 1.000 | 0.595 |
| 2012-2013 | 1.000 | 1.070 | 1.000 | 1.000 | 1.070 |
| 2013-2014 | 1.000 | 0.755 | 1.000 | 1.000 | 0.755 |
| 2014-2015 | 1.000 | 1.284 | 1.000 | 1.000 | 1.284 |
| 2015-2016 | 1.000 | 0.679 | 1.000 | 1.000 | 0.679 |
| 2016-2017 | 1.000 | 0.878 | 1.000 | 1.000 | 0.878 |
| 2017-2018 | 1.000 | 1.432 | 1.000 | 1.000 | 1.432 |
| 2018-2019 | 1.000 | 1.338 | 1.000 | 1.000 | 1.338 |
| 2019-2020 | 1.000 | 1.038 | 1.000 | 1.000 | 1.038 |
| 2020-2021 | 1.000 | 0.572 | 1.000 | 1.000 | 0.572 |
| **Average** | **1.000** | **0.917** | **1.000** | **1.000** | **0.917** |

The trends of efficiency changes (EFFCH) index and technological changes (TECHCH) index of nuclear technology R&D is shown in Fig. 4. EFFCH index remains unchanged during the study period with value of 1.000. However, TECHCH index shows different patterns during the study period. TECHCH index decreased in 2011-2012,2013-2014, 2016-2017 and 2020-2021 at value of 0.595, 0.755, 0.878 and 0.572 respectively. The low TECHCH index recorded during the transition period of new policy or strategic plan implementation especially during the 10$^{th}$ MP (2011-2012), DSTIN (2013-2014), 11$^{th}$ MP (2016-2017) and 12$^{th}$ MP (2020-2021). The decreasing value can be translated to the ability of Nuklear Malaysia in adapting the transition process of the new policy or programmes implementation. After the first year of implementation of new policy or strategic plan, TECHCH index increased up to shows an increasing value 2012-2013 (7.0%), 2014-2015 (28.4%), 2017-2018 (43.2%). During the implementation of 12$^{th}$ MP 2016-2020, the average TECHCH index is increased up to 5.16%, compared to implementation of 11$^{th}$ MP period which decreased at 12.34%.

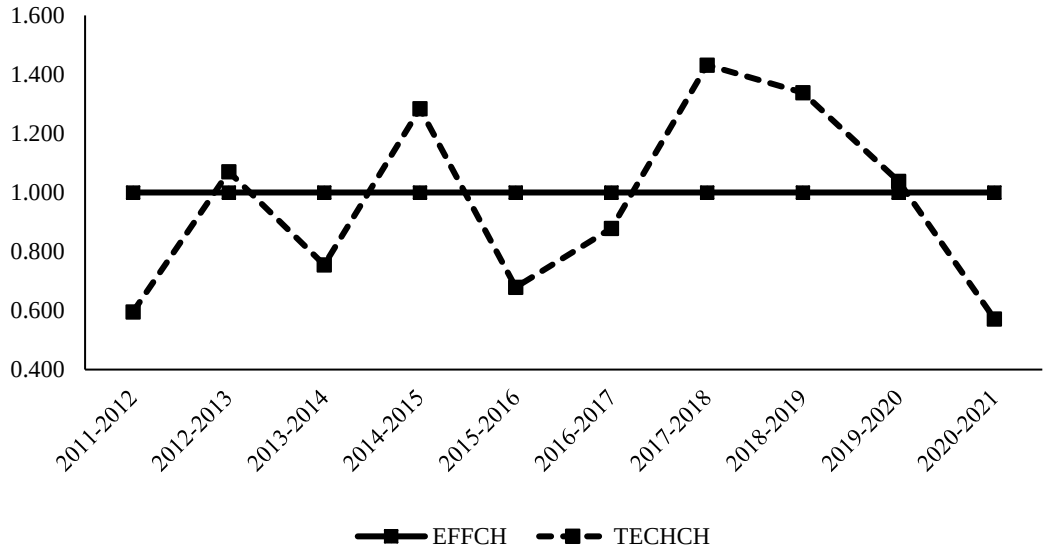


Figure 4: Efficiency changes and technological changes of nuclear technology R&D

Fig.5 shows the total factor productivity changes (TFPCH) index of Malmquist Index of nuclear technology R&D in Nuklear Malaysia from 2011-2021. The nuclear technology R&D growth index in Nuklear Malaysia is mainly affected by technological changes due to policy changes compare to the resources provided since efficiency changes remains the same. The nuclear technology R&D growth index shows different patterns during the study period. The nuclear technology R&D growth index decreased in 2011-2012,2013-2014, 2016-2017 and 2020-2021 at value of 0.595, 0.755, 0.878 and 0.572 respectively. The low nuclear technology R&D growth index recorded during the transition period of new policy or strategic plan implementation especially during the 10$^{th}$ MP (2011-2012), DSTIN (2013-2014), 11$^{th}$ MP (2016-2017) and 12$^{th}$ MP (2020-2021). The decreasing value can be translated to the ability of Nuklear Malaysia in adapting the transition process of the new policy or programmes implementation. After the first year of implementation of new policy or strategic plan, the nuclear technology R&D growth index increased up to shows an increasing value of 2012- 2013 (7.0%), 2014-2015 (28.4%), 2017-2018 (43.2%). It can be concluded that the nuclear technology R&D growth index is increased up to 5.16% during the implementation of 12$^{th}$ MP 2016-2020 compared to implementation of 11$^{th}$ MP 2011-2015 which decreased at 12.34%.

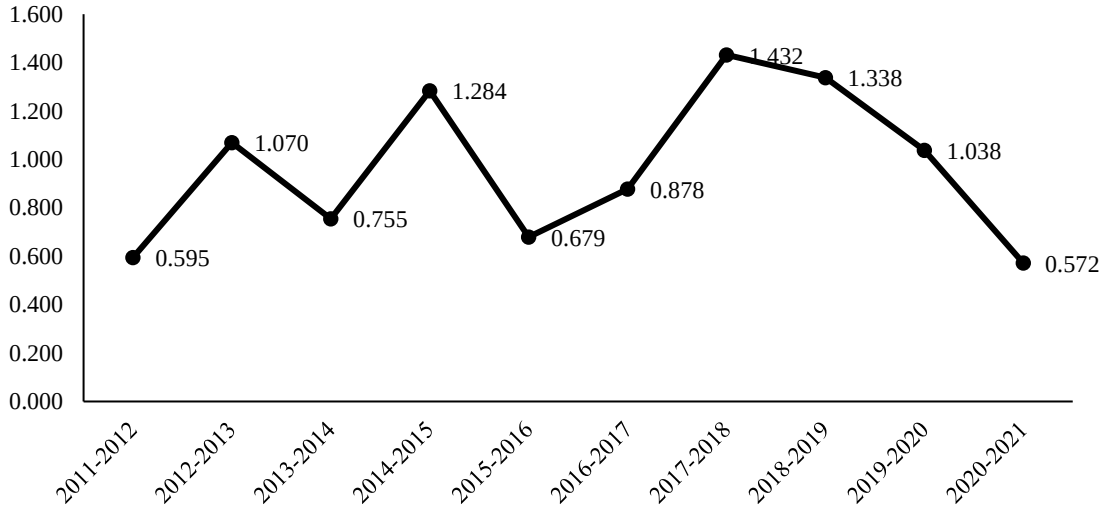


Figure 5: Total factor productivity changes (TFPCH) index of nuclear technology R&D

## DISCUSSIONS

The future economic progress for any country will be driven by the innovation and application of new technologies. The importance of R&D lies there, as it is one category of spending that develops and drives these new technologies. R&D plays an important role in enhancing the capability of research institutes because R&D activities stimulate innovative methods of production, reduce costs and improve product quality. The importance of R&D has become more evident everyday among the factors that directly related to the good economic performance of the emerging countries of 21$^{st}$ centuries. This is necessary because of continuous technology change and development as well as other competitors and the changing preferences of customers everyday which is not possible without an R&D program. Based on the finding from this study, a few recommendations are proposed to ensure the nuclear technology R&D activities in Nuklear Malaysia remains relevance to the national socio- economic development.

Innovation as an output from the R&D activities is a key driver of both economic growth and enhancing the social well-being of a country. Therefore, policies or strategic plan that promote innovation should be top priority for Nuklear Malaysia at any developmental stage. Ministry of Science, Technology and Innovation (MOSTI) can inspire innovation by creating a basic policy for nuclear technology research and development (R&D) to ensure Nuklear Malaysia able to provide appropriate returns to innovative investments. Continued development of emerging technologies, such as internet of things (IoT), artificial intelligence (AI), machine learning (ML), blockchain, cybersecurity and cloud computing, is paving the way for this ongoing R&D investment, as savvy businesses recognize the advantages early adopters have over their competition. Both the stakes and potential gains from investing in new technologies are continuing to increase rapidly alongside the pace of development, driving investment and research in the various sector, while the new technologies will themselves offer new opportunities for innovation.

Nuclear and isotopic techniques can be used as one of the solutions to tackle new global challenges, such as climate change, addressing the growing nutritional and medical demands of an increasing global population and supporting the expansion of industrialization for development. Therefore, the IAEA's platform for scientific collaboration, research and development and training should be grabbed as an opportunity for advancing the nuclear science and technology development to contribute to human wellbeing and sustainable development in Malaysia, particularly in the development areas, including food and agriculture, environmental protection, water management, industrial development, and human health. In addition, technology transfer is a critical ingredient for growth and facilitating it will require addressing the issues such as providing information and capacity building. This is critical for many developing countries, such Malaysia with weak human capital, because if there are lack of engineers and scientists to identify where and how a technology can be applied, there won't be an idea transfer, even if the business environment is in reasonable shape. Therefore, IAEA could assist Nuklear Malaysia in building connections with institutions outside the countries can ease the flow of information and increase countries' awareness of existing technologies.

Technology foresight and road mapping can be used as important tools and method to help keep nuclear science and technology at the forefront of national development, as well as advancing toward a sustainable future. Along with the ongoing innovations and advances in technology, nuclear science and technology continues to contribute to the wellbeing of humankind in the future. The complementary production factors such as qualified personnel, necessary machinery, financing, or managerial capabilities is critical to the complementary production factors necessary for innovation. These factors are also important in identifying and implementing new technologies or undertaking R&D in nuclear technology. In addition, developing countries such as Malaysia, may not have capability of carrying out an R&D project or the human capital to undertake the R&D-focused initiatives, specific policies need to focus on these areas first. Managerial upgrading programmes, which are when an outside expert analyses a company's performance and suggests an improvement plan have been proven to have a large impact on productivity and innovation.

## CONCLUSIONS

This paper has examined the performance and the growth of nuclear technology R&D in Nuklear Malaysia from 2011-2021 using the DEA and MI analysis. The result shows that the performance of nuclear technology R&D in Nuklear Malaysia is 96.70 per cent from 2011-2021. The study shows that nuclear R&D growth decreased by 8.3 per cent for the entire study period. The technological changes decreased at 8.3 per cent, while the efficiency changes remain. The study also found that nuclear technology R&D growth index in Nuklear Malaysia is mainly affected by technological changes due to policy changes compare to the resources provided since efficiency changes remain. The findings of the study help management and officials of Nuklear Malaysia to align the R&D institution's direction to ensure the nuclear technology R&D contribute to the socio-economic development of the country.

## ACKNOWLEDGEMENTS

The authors appreciate the support of the Planning and International Relations Division, Malaysian Nuclear Malaysia in this work.

**REFERENCES**

Agensi Nuklear Malaysia, (2021). Wawasan Nuklear Malaysia. Kajang, Selangor.

Ahn, H., Afsharian, M., Emrouznejad, A., Banker, R., (2018). Recent developments on the use of DEA in the public sector. Socioecon. Plann. Sci. 61, 1–3. https://doi.org/10.1016/j.seps.2017.06.001

Avkiran, N.K., (2006). Productivity Analysis in the Service Sector with Data Envelopment Analysis, Third Edit. ed. The University of Queensland, Australia.

Bae, Y., Chang, H., (2012). Efficiency and effectiveness between open and closed innovation: Empirical evidence in South Korean manufacturers. Technol. Anal. Strateg. Manag. 24, 967–980. https://doi.org/10.1080/09537325.2012.724164

Banker, R.D., Charnes, A., Cooper, W.W., (1984). Some Models for Estimating Technical and Scale Inefficiencies in Data Envelopment Analysis. Manage. Sci. 30, 1078–1092. https://doi.org/10.1287/mnsc.30.9.1078

Belgin, O., (2019). Analysing R&D efficiency of Turkish regions using data envelopment analysis. Technol. Anal. Strateg. Manag. 31, 1341–1352. https://doi.org/10.1080/09537325.2019.1613521

Carrillo, M., (2019). Measuring and ranking R&D performance at the country level. Econ. Sociol. 12, 100–114. https://doi.org/10.14254/2071-789X.2019/12-1/5

Caves, D.W., Christensen, L.R., Diewert, W.E., (1982). The Economic Theory of Index Numbers and the Measurement of Input, Output, and Productivity. Econometrica 50, 1393. https://doi.org/10.2307/1913388

Chachuli, F.S.M., Mat, S., Ludin, N.A., Zaharim, A., (2020). Analisis Kecekapan Aktiviti Penyelidikan dan Pembangunan (R&D) dalam Sektor Tenaga Boleh Diperbaharui di Malaysia. J. Kejuruter. 32, 121–130.

Charnes, A., Cooper, W.W., (1962). Programming with linear fractional functionals. Nav. Res. Logist. 9. https://doi.org/10.1002/nav.10100

Charnes, A., Cooper, W.W., Rhodes, E., (1978). Measuring the efficiency of decision making units. Eur. J. Oper. Res. 2, 429–444. https://doi.org/10.1016/0377-2217(78)90138-8

Chuang, L.M., Liu, C.C., Chao, S.T., (2011). Data envelopment analysis in measuring R&D ef?ciency of semiconductor industry's new product development in Taiwan. Actual Probl. Econ. 123, 418–429.

Chun, D., Chung, Y., Bang, S., (2015). Impact of firm size and industry type on R&D efficiency throughout innovation and commercialisation stages: evidence from Korean manufacturing firms. Technol. Anal. Strateg. Manag. 27, 895–909. https://doi.org/10.1080/09537325.2015.1024645

Cooper, W.W., Seiford, L.M., Tone, K., (1999). Data envelopment analysis: A comprehensive text with models, applications, references and DEA-solver software. Kluwer Academic Publishers.

Costa-Campi, M.T., Duch-Brown, N., García-Quevedo, J., (2014). R&D drivers and obstacles to innovation in the energy industry. Energy Econ. 46, 20–30. https://doi.org/10.1016/j.eneco.2014.09.003

deLlano-Paz, F., Calvo-Silvosa, A., Antelo, S.I., Soares, I., (2017). Energy planning and modern portfolio theory: A review. Renew. Sustain. Energy Rev. 77, 636–651. https://doi.org/10.1016/j.rser.2017.04.045

EPU, (2016). Rancangan Malaysia Kesebelas; Kertas Strategi 17: Penggunaan Tenaga yang Mampan bagi Menyokong Pertumbuhan. Putrajaya, Malaysia.

EPU, (2010). Rancangan Malaysia Ke Sepuluh 2011-2015. Putrajaya, Malaysia.

Fare, R., Grosskopf, S., Norris, M., Zhongyang Zhang, (1994). Productivity growth, technical progress, and efficiency change in industrialized countries. Am. Econ. Rev. 84, 66–83. https://doi.org/10.2307/2117971

Hung, C.L., Shiu, P.J., (2014). Evaluating project performance by removing external effects: Implications to the efficiency of research and development resource allocation. Res. Eval. 23, 366–380. https://doi.org/10.1093/reseval/rvu022

IAEA, (2018). Nuclear science & technology: addressing current and emerging development challenges.

J. Asmara, I., Achelia, E., G. Simamora, N., Sartono, B., (2019). Measuring R&D Performance Using Data Envelopment Analysis (DEA): Case Indonesia. Int. J. Soc. Sci. Humanit. 9, 91–96. https://doi.org/10.18178/ijssh.2019.v9.997

Jang, H., Lee, S., Suh, E., (2016). A comparative analysis of the change in R&D efficiency: a case of R&D leaders in the technology industry. Technol. Anal. Strateg. Manag. 28, 886–900. https://doi.org/10.1080/09537325.2016.1180354

Khoshnevis, P., Teirlinck, P., (2018). Performance evaluation of R&D active firms. Socioecon. Plann. Sci. 61, 16–28. https://doi.org/10.1016/j.seps.2017.01.005

Li, H., Chen, C., Cook, W.D., Zhang, J., Zhu, J., (2018). Two-stage network DEA: Who is the leader? Omega (United Kingdom) 74, 15–19. https://doi.org/10.1016/j.omega.2016.12.009

Liu, J.S., Lu, L.Y.Y., Lu, W.M., (2016). Research fronts in data envelopment analysis. Omega 58, 33–45. https://doi.org/10.1016/j.omega.2015.04.004

Liu, J.S., Lu, L.Y.Y., Lu, W.M., Lin, B.J.Y., (2013). A survey of DEA applications. Omega 41, 893–902. https://doi.org/10.1016/j.omega.2012.11.004

Lopez-Peña, A., (2014). Evaluation and design of sustainable energy policies: an application to the case of Spain.

Lu, W., (2009). The evolution of R&D efficiency and marketability: Evidence from Taiwan's IC-design Industry. Asian J. Technol. Innov. 17, 1–26. https://doi.org/10.1080/19761597.2009.9668671

Martin, B.R., (1996). Technology foresight: Capturing the benefits from science-related technologies. Res. Eval. 6, 158–168. https://doi.org/10.1093/rev/6.2.158

MEA, (2018). Mid-term Review of the Eleventh Malaysia Plan 2016-2020. Putrajaya, Malaysia.

Menegaki, A.N., (2013). Growth and renewable energy in Europe: Benchmarking with data envelopment analysis. Renew. Energy 60, 363–369. https://doi.org/10.1016/j.renene.2013.05.042

Mohd Chachuli, F.S., Ahmad Ludin, N., Md Jedi, M.A., Hamid, N.H., (2021a). Transition of renewable energy policies in Malaysia : Benchmarking with data envelopment analysis. Renew. Sustain. Energy Rev. 150, 111456. https://doi.org/10.1016/j.rser.2021.111456

Mohd Chachuli, F.S., Mat, S., Ahmad, N., (2021b). Performance evaluation of renewable energy R&D activities in Malaysia. Renew. Energy 163, 544–560. https://doi.org/10.1016/j.renene.2020.08.160

MOSTI, (2021). National science, technology and innovation policy 2021-2030. Putrajaya, Malaysia.

MOSTI, (2013). Dasar Sains, Teknologi dan Inovasi Negara (DSTIN) 2013-2020.

Nuklear Malaysia, (2022). Sejarah Nuklear Malaysia [WWW Document]. URL https://www.nuclearmalaysia.gov.my/sejarah.php (accessed 8.23.22).

Nuklear Malaysia, (2013). Malaysian Nuclear Agency: Strategic Plan 2012-2020.

Qin, X., Du, D., (2018). Measuring universities' R&D performance in China's provinces: a multistage efficiency and effectiveness perspective. Technol. Anal. Strateg. Manag. 30, 1392–1408. https://doi.org/10.1080/09537325.2018.1473849

Schoemaker, P.J.H., Mavaddat, V.M., (2000). Scenario planning for disruptive technologies. Whart. Manag. Emerg. Technol. 206–241.

Shakouri, H.G., Nabaee, M., Aliakbarisani, S., (2014). A quantitative discussion on the assessment of power supply technologies: DEA (data envelopment analysis) and SAW (simple additive weighting) as complementary methods for the "Grammar." Energy 64, 640–647. https://doi.org/10.1016/j.energy.2013.10.022

Shevchenko, Y., Pomogaev, V., Stukach, V., Nikulin, D., (2017). Designing and implementing future scenarios: Foresight methodology, economics, technologies, society and ecology. MPRA.

Xiong, X., Yang, G.L., Guan, Z.C., (2018). Assessing R&D efficiency using a two-stage dynamic DEA model: A case study of research institutes in the Chinese Academy of Sciences. J. Informetr. 12, 784–805. https://doi.org/10.1016/j.joi.2018.07.003

Yu, F., Guo, Y., Le-Nguyen, K., Barnes, S.J., Zhang, W., 2016. The impact of government subsidies and enterprises' R&D investment: A panel data study from renewable energy in China. Energy Policy 89, 106–113. https://doi.org/10.1016/j.enpol.2015.11.009

Zhang, A., Zhang, Y., Zhao, R., (2003). A study of the R&D efficiency and productivity of Chinese firms. J. Comp. Econ. 31, 444–464. https://doi.org/10.1016/S0147-5967(03)00055-6

Zhou, H., Yang, Y., Chen, Y., Zhu, J., (2018). Data envelopment analysis application in sustainability: The origins, development and future directions. Eur. J. Oper. Res. 264, 1–16. https://doi.org/10.1016/j.ejor.2017.06.023

e-Jurnal Sains Nuklear Malaysia, 2023, Vol. 35 (No.1): 67 – 76
*eISSN: 2232-0946*

# EFFECTS OF NCO/OH RATIO ON THE PROPERTIES OF RADIATION CURABLE WATERBORNE POLYURETHANE ACRYLATE

***Khairul Azhar Abdul Halim[1*], Anas Aiman Malek Faisal[2], Rosley Che Ismail[1], Abdul Muizz Mohd Sani[1], Nurul Huda Mudri[1]and Naurah Mat Isa[1]***

[1]Radiation Processing Technology Division, Malaysian Nuclear Agency,
Ministry of Science & Technology, Bangi, 43000 Kajang, Selangor, Malaysia
[2]Faculty of Science & Technology, Universiti Sains Islam Malaysia,
Bandar Baru Nilai, 71800, Negeri Sembilan, Malaysia
*Correspondence author: azharhalim@nm.gov.my

## *ABSTRACT*

*A series of radiation-curable waterborne polyurethane dispersion was synthesized with two different NCO/OH ratios of 1.5 and 2.0. The polyurethane prepolymer was synthesized by reacting polypropylene glycol (MW=2000) with isophorone diisocyanate to produce -NCO end-capped polyurethane prepolymer. The prepolymer chain was then terminated with hydroxyethyl acrylate and dispersed with deionized water to produce waterborne polyurethane acrylate (WPUA) dispersion. The WPUA dispersions were mixed with two types of photoinitiators, Irgacure 500 and Darocur 1173, and cured under a medium pressure mercury ultraviolet lamp with a wavelength of 365 nm to produce PUA films. The effects of NCO/OH ratios and different types of photoinitiators on the properties of WPUA dispersion and PUA film were studied. Both dispersions with NCO/OH ratios of 1.5 and 2.0 exhibited similar properties, with a pH value of approximately 7 and good dispersion stability. The zeta potential was measured at -60.9 for the NCO/OH ratio of 1.5 and -48.78 for the NCO/OH ratio of 2.0. The viscosity of the dispersions increased as the NCO/OH ratio increased. Regarding the curing speed of the WPUA dispersions, it was observed that Irgacure 500 performed better than Darocur 1173 for low film thicknesses of 50 µm at 5 passes. However, as the thickness of the PUA film increased to 100 µm, the curing speed became similar for all dispersions, requiring 9 passes, irrespective of the NCO/OH ratio or type of photoinitiator. The hardness of the PUA films was evaluated using a pendulum hardness test. It was found that the type of photoinitiator did not have an impact on the film hardness. However, the NCO/OH ratio influenced the hardness, with higher ratios resulting in increased hardness. These findings contribute to the understanding of the properties and performance of radiation curable waterborne polyurethane dispersions and provide valuable insights for their potential applications.*

***Keywords:*** *Radiation curable, Prepolymer, Dispersion, Polyurethane Acrylate*

## INTRODUCTION

Waterborne polyurethane has attracted a lot of interest lately and is widely used as coatings because of its nontoxic and environmentally friendly appeal. Coatings are essential in many different industries because they provide protection and aesthetic improvement to a variety of substrates. Conventional polyurethane (PU) coatings frequently use organic solvents to improve their ability to adhere to various surfaces. These solvents, however, usually contain hazardous air pollutants and volatile organic compounds (VOC) that are dangerous towards the environment and health (Jiménez-López, A. M., 2022). In addition, most organic solvents are toxic and carcinogenic in nature. In response to the increased emphasis on environmental awareness, many countries have started to issue various regulations and laws related to the production of coatings. Due to this, waterborne coatings

have gained rapid development in coatings, adhesives, and textile industry (Honarkar H., 2018; Zhou X., 2015; Santamaria-Echart, 2021; Kang, S.Y., 2018). Because of their low toxicity, decreased emissions of hazardous compounds, and enhanced eco-friendliness, waterborne PUs represent a promising alternative. However, a major drawback of water-based PUs is that they take longer to cure at room temperature than solvent-based PUs.

To address this challenge, radiation curing technology offers a viable solution. By incorporating radiation curable property into the formulation of water-based coatings, instant drying can be achieved, providing both environmental and energy-friendly benefits. Radiation curing offers a rapid and efficient curing process that minimizes the need for extended drying times, allowing for enhanced productivity and reduced energy consumption (Zareanshahraki, F., 2020). Waterborne PU coatings derived from radiation induced polymerization are becoming progressively more attractive due to increasing environmental demands and owing to their good physicochemical, rheological and optical properties (Agnol, L. D., 2021).

Although radiation curable waterborne PUs have drawn more interest, there is not much work on the factors that influence the properties of radiation curable waterborne PU. Waterborne polyurethane acrylate dispersion (WPUA) was synthesized from the flexible polyol as the soft segment while diisocyanates and hydroxyl acrylate act as the hard segment. Apart from adjusting the NCO/OH ratio, the performance of PUA can be altered by changing the structure of polyol, diisocyanates and hydroxyl acrylate used in the formulation [8], the performance of PUA can be tailored to meet specific requirements. This paper aims to investigate the effects of isocyanate to hydroxyl (NCO/OH) ratios of WPUA dispersion and PUA films. Furthermore, this paper also evaluates the effects of different types of photoinitiators on the properties of polyurethane acrylate (PUA) films.

## METHODOLOGY

### Materials

Polypropylene glycol (PPG; MW = 2000), dimethylol propionic acid (DMPA), N-methyl-2-pyrrolidone (NMP), hydroxyethyl acrylate (HEA) and deionized water were procured from Acros Organics (Belgium). Tin-II-2-ethylhexanoate and isophorone diisocyanate (IPDI; 98%) were procured from Sigma Aldrich (Germany). Triethylamine (TEA), hydrochloric acid, di-n-butylamine, toluene and bromophenol blue indicator were procured from Fisher Scientific (USA). Isopropyl alcohol was procured from Systerm (Malaysia). Irgacure 500 and Darocur 1173 were procured from Ciba Specialty Chemicals (Switzerland).

### Synthesis of Waterborne Polyurethane Acrylate

The molar ratio between the isocyanate (NCO) group from IPDI and the hydroxyl (OH) groups from PPG polyol and DMPA was calculated to reach the NCO: OH molar ratio of 1.5 and 2.0. Initially, to produce polyurethane acrylate (PUA) prepolymer, PPG and DMPA were added and allowed to mix with NMP as co-solvent in a 3-neck flask equipped with a heating mantle, overhead mechanical stirrer, and thermometer as in Figure 1. The reaction temperature was maintained constant under 80°C and stirrer continuously until all the chemicals were homogenous. Then, IPDI was added drop wise using a dropping funnel for 30 minutes followed by addition of catalyst. The reaction is monitored hourly with titration (ASTM D2572) until NCO content reaches theoretical value. Next, HEA was dropped gradually and allowed to react at 60°C until all remaining NCO had been fully consumed. The carboxylic acid group of the DMPA was then neutralized with TEA for 30 minutes. Finally, the

PUA prepolymer was then dispersed in deionized water. The dispersion was prepared at 40% solid content, the volume of deionized water was calculated and added into the reactor flask over the course of 30 minutes with vigorous stirring.

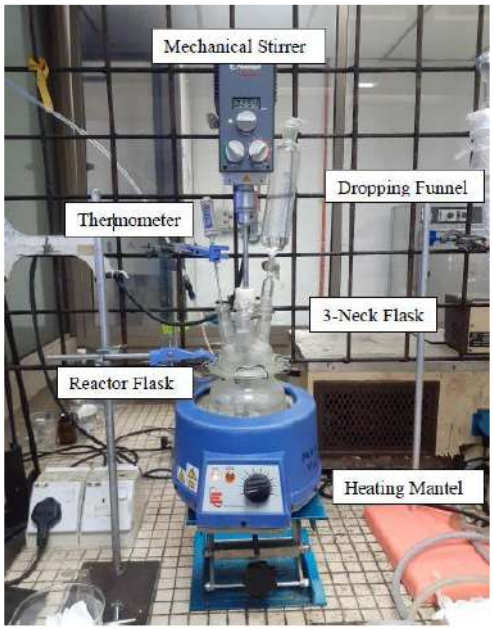


Figure 1: WPUA synthesis setup

**Characterisation of WPUA Dispersion**

***i. Viscosity***

The viscosity of both WPUAs were measured with rotational viscometer (DV2T Touch Screen, AMETEK Brookfield, USA) at ambient temperature, for 60 seconds at different speed of 1, 10 and 50 rpm with a Spindle-51.

***ii. pH***

The pH was measured using pH meter (PB-10, Sartorius, German) by dipping the probe into the sample at room temperature. After each usage, the probe was rinsed with distilled water to clean the probe.

***iii. Isocyanate Standard Test Method (ASTM D2572)***

Along the synthesis step, the amount of NCO content remaining in the mixture was monitored with dibutylamine back titration method (ASTM D2572) (Figure 2) to calculate the amounts of HEA needed to end-cap the remaining NCO group. The standard test method for calculating the content of NCO groups in urethane prepolymers was done by reacting the remaining NCO in the prepolymer with excess dibutylamine in toluene.

The NCO content was calculated as below:

$$NCO\ content\ (\%) = \frac{[(B\ -\ V)\ x\ N\ x\ 0.0420]}{W}\ x\ 100$$

Eq…(1)

Where:
B = Volume of titration of blank, mL
V = Volume of titration with sample, mL
N = Normality of HCl
0.0420 = milliequivalent weight of NCO group
W = Weight of sample, g

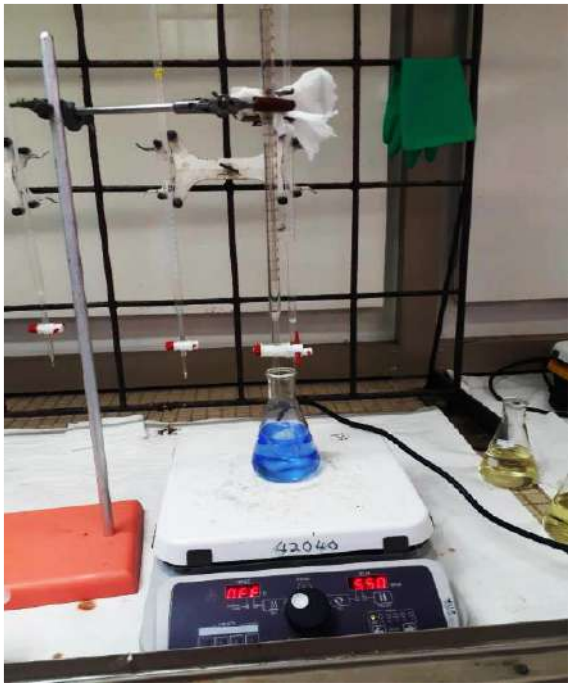


Figure 2: ASTM D2572 titration set up

***iv. Zeta Potential***

The WPUA 1.5 and WPUA 2.0 dispersion was diluted with deionized water to a solid content of 1 wt%. Then, a single drop of the mixture was further diluted with distilled water in the equipment's sample cell–electrode assembly and measured by zeta potential analyser (ZetaPlus, Brookhaven, USA).

***v. Solid Content***

The solid content of WPUAs were calculated by weighing 1.0 g of the sample in a weighing boat and dried in the oven at 80°C until the dried film reaches a constant weight. The weight difference of before and after were recorded, and the solid content were calculated with the formula:

$$Solid\ content\ (\%)\ = \frac{Wf}{Wi} x\ 100$$

Eq…(2)

where:
W*f* = Net weight of dry sample
W*i* = Net weight of original sample

**Preparation of PUA Film**

The samples of both WPUA 1.5 and WPUA 2.0 were placed inside a vacuum oven to release air that was trapped in the dispersion during synthesis. The two samples of WPUA were added with different photoinitiators; Darocur 1173 and Irgacure 500 and were let sit for 24 hours at room temperature. The prepared coatings were then applied to a glass substrate using a 4-sided bar coater with a thickness of 50 and 100 μm wet films. The wet films were then cured using a UV-IST, UV-curing machine equipped with a medium-pressure mercury lamp at 365 nm to induce free radical polymerization with a conveyor speed of 10 m/min. The film was checked with a thumbprint test until the film has fully cured.

**Characterisation of PUA Film**

***i. Gel Content***

The gel content was measured through Soxhlet extraction method following the works of Wang *et. al.* (2021). The cured PUA films were sliced into small pieces and weighed about 0.1 g, after which the sample was immersed in acetone for 17 h before being dried for 24 hours at 60°C until it reached a constant weight. The gel content was calculated with the formula:

$$Gel\ content(\%) = \frac{Wf}{Wi} x100 \qquad \text{Eq…(3)}$$

where:
W$f$ = Weight of gel fraction*
W$i$ = Weight of original sample
*Gel fraction refers to the weight of the cross-linked portion of the polymer that remains after the solvent extraction and drying process.

***ii. Pendulum Hardness***

The PUA films hardness with different PI and different thickness were measured through the deflection angles of pendulum oscillation on the film samples, using a Pendulum Hardness Tester, TQC Sheen, SP0500, Netherlands, using a König pendulum, in accordance with ASTM D4366.

**RESULT AND DISCUSSION**

In this study, WPUA prepolymers were synthesised by reacting polyols and diisocyanate followed by termination with an acrylate. This process provides an unsaturated carbon double bond (C=C) site from acrylate functionality. The WPUA prepolymer was then dispersed in deionized water to form WPUA dispersion.

**Properties of WPUA Dispersion**

***i. Viscosity***

The waterborne PUA dispersion was commonly used as adhesives and coatings. One of the most crucial factors influencing the workability as well as the rate of photopolymerization and properties of the cured film is the viscosity of the dispersion (Xu, J., 2013). The viscosity of WPUA dispersion

needed to be controlled to prevent sagging and difficulty to apply due to very high viscosity (Asif, A., 2004). The produced WPUA 1.5 and WPUA 2.0 are in the range of acceptable viscosity as compared to conventional WPUA coatings as shown in Table 1.

The viscosity values of both WPUA 1.5 and WPUA 2.0 dispersions shows that the NCO:OH ratio did not greatly affect the viscosity. The viscosity of the emulsion can be adjusted by controlling the volume of water added during the dispersion step.

Table 1: Comparison between in-house WPUA and commercial products

| **Company** | **Product** | **Solid content (%)** | **Viscosity (mPa·s)** | **pH** |
|---|---|---|---|---|
| Nuklear Malaysia | WPUA 1.5 | 39 | 28.16 | 7.27 |
| Nuklear Malaysia | WPUA 2.0 | 40 | 29.44 | 7.41 |
| Allnex | UCECOAT® 7230 | 40.5 to 43.5 | < 200 | 6.0 to 8.0 |
| BASF | Joncryl® HYB 6340 | 40 | 50 | 7.6 |
| UBE Corp. | UVPUD-7009E | 30 | 20 | 8.0 |
| UBE Corp. | UVPUD-7009E-C2 | 30 | 15 | 7.0 |
| Covestro | Bayhydrol® UV 2282 | 38 to 40 | < 800 | 7.8 ± 0.8 |

### *ii. pH*

According to Szycher (1999), the viscosity of the dispersion increases with increasing pH, but decreasing pH makes the dispersion unstable by causing the solids to settle. The pH of WPUA 1.5 and WPUA 2.0 are in the range of conventional coating, with 7.27 and 7.41 respectively, as shown in Table 1. The low acidity values of the resins are the result of a neutralization reaction that took place when the carboxylic acid groups were neutralized by the addition of TEA during synthesis.

### *iii. Stability of WPUA*

Zeta potential is an important indicator for assessing the stability of the WPUAs dispersions as it is a determining factor in particle dispersions for electrostatic interactions. The zeta potential values obtained for WPUA 1.5 and WPUA 2.0 were found to be -60.90 mV and -48.78 mV respectively, which indicates both dispersions are stable. These values indicate that both dispersions exhibit stable behaviour. The negative zeta potential values observed for both WPUA formulations suggest the presence of repulsive forces among the particles, which effectively prevents aggregation and ensures dispersion stability. These results demonstrate how well the WPUA formulations produce stable dispersions, which is essential for their use in a variety of industries like coatings and adhesives.

### *iv. Solid Content*

The solid content of the WPUAs were both within the expected range of 40% as displayed in Table 1. According to Nanda et al. (2005), the WPUA solid content can only be dispersed in water when the water content is equal to or greater than the solid content. Thus, the solid content range was set to about 40% as to avoid having a solid-like structure in the WPUA dispersion.

**Properties of PUA Film**

The (C=C) site from acrylate functionality was utilized for free radical polymerization when the dispersion is exposed under electron beam or ultraviolet radiation to form PUA film. The physicochemical properties of PUA films with different photoinitiators was investigated.

### *i. Curing Rate*

The amount of time needed to fully cure a sample is important especially for industrial use application. Low number of passes required to cure a sample imply higher curing and polymerization rate occurred to crosslink the PUA. The number of passes for both WPUAs with different PIs at different thickness are presented in Table 2. The performance difference between both PIs were significant at low thickness 50 μm, where PUA 2.0 film with Irgacure 500 shows higher curing rate. However, at a higher thickness of 100 μm, the curing performance for both NCO:OH ratios and PI types were almost the same. The reactivity of both PIs depends on the UV energy needed to initiate free radical polymerization, in which Irgacure 500 appeared to require less energy as compared to Darocur 1173. It was observed that the water particles slow down the curing process, thus more cycle is needed to cure the WPUA dispersion. In future study, the PUA films needed to be flashed off with a convection oven before curing to release water particles from the dispersion particularly at higher film thickness.

Table 2: Curing and mechanical properties of WPUA 1.5 and WPUA 2.0 with varying photoinitiators and film thicknesses

| **Sample** | **WPUA 1.5** | | | | **WPUA 2.0** | | | |
|---|---|---|---|---|---|---|---|---|
| | **Irgacure 500** | | **Darocur 1173** | | **Irgacure 500** | | **Darocur 1173** | |
| Film thickness (μm) | 50 | 100 | 50 | 100 | 50 | 100 | 50 | 100 |
| Curing (Number of passes) | 6 | 9 | 9 | 9 | 6 | 10 | 8 | 9 |
| Gel content (%) | 62 | 62 | 66 | 66 | 64 | 64 | 72 | 72 |
| Film hardness (Oscillation) | 28 | 18 | 29 | 18 | 46 | 26 | 44 | 23 |

### *ii. Crosslinking Density*

The gel content test was used to measure the percent of crosslinking produced in the coating after curing. The observed gel content for the WPUAs at different PI is shown in Table 2. The gel content of WPUA 2.0 is higher than WPUA 1.5, which indicates the increase in NCO: OH ratio can improve the crosslink extent of the resin.

### *iii. Pendulum Hardness*

The film hardness can be understood as the material's resistance to localized plastic deformation. Table 2 and Figure 3 shows the data on the pendulum hardness of WPUA 1.5 and WPUA 2.0 with film thickness of 50 and 100 μm as a function of photoinitiators Irgacure 500 and Darocur 1173. The data shows the pendulum hardness decreases with increasing thickness of coating. The pendulum hardness test is based on the idea that the harder the surface of the coating, the longer the pendulum will oscillate (Ma, X., 2013). In this study, WPUA 2.0 showed better hardness than WPUA 1.5. This occurrence can be linked with the high gel content and crosslinking density of WPUA 2.0 especially with Irgacure 500 that will induce high hardness (Hwang, H. D., 2011). There is no apparent

difference in the WPUAs trends between both PI as in Table 2, indicating the PUA film hardness is not affected by the types of PI.

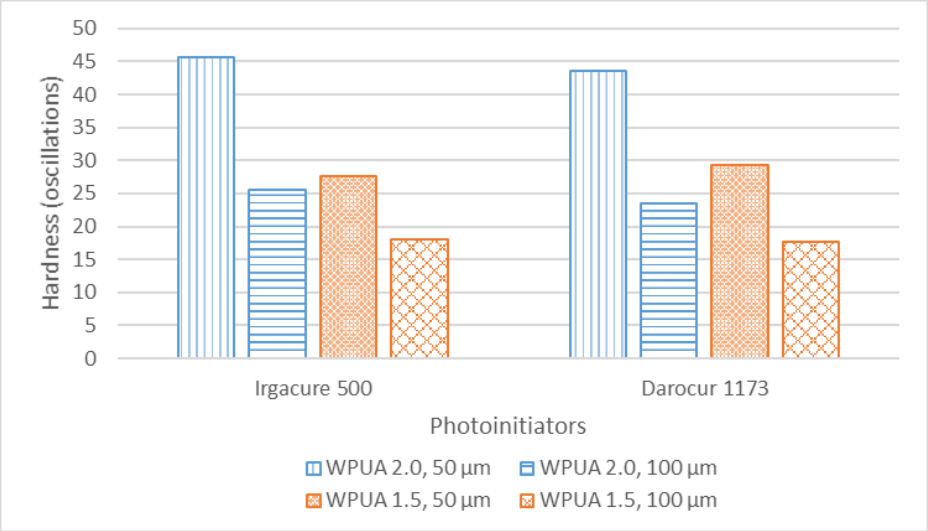


Figure 3**:** Film hardness of WPUA 1.5 and WPUA 2.0 with varying photoinitiators

## CONCLUSION

In conclusion, the experimental results highlight several features relating to the characteristics and effectiveness of the WPUA dispersions and PUA films examined in this work. According to the zeta potential measurements, both the WPUA 1.5 and WPUA 2.0 dispersions exhibit stable behaviour, which is essential for their practical application. The WPUAs' viscosity is within the permissible range of conventional PU coating which ensures adequate workability and promotes photopolymerization during curing. Furthermore, the WPUAs' solid content is within the necessary range of 40%, allowing for good dispersion in water without producing a solid-like structure. The pH values for both WPUA dispersions are within the conventional coating range, indicating the effectiveness of the neutralization reaction carried out during synthesis. The polymerization process was discovered to be influenced by the film thickness and photoinitiator selection with regards to the cure rate. In the future, especially when working with thicker films, pre-flashing the PUA films might be needed to liberate water particles from the dispersion prior to radiation curing. Based on the hardness test, it is revealed that the type of photoinitiators does not affect PUA film hardness. However, the hardness improved with increasing NCO:OH ratio. Overall, this work offers an insight towards prospective application of WPUAs as greener coatings alternatives. Future work is suggested to compare the feasibility of natural-based polyol such as palm oil in synthesizing WPUA.

## ACKNOWLEDGEMENT

The author wishes to express gratitude to the Government of Malaysia and Ministry of Science & Technology (MOSTI) for providing the facilities for this study.

**REFERENCES**

Agnol, L. D., Dias, F. T. G., Ornaghi Jr, H. L., Sangermano, M., & Bianchi, O. (2021). UV-curable waterborne polyurethane coatings: A state-of-the-art and recent advances review. Progress in Organic Coatings, 154, 106156.

Asif, A., & Shi, W. (2004). UV curable waterborne polyurethane acrylate dispersions based on hyperbranched aliphatic polyester: effect of molecular structure on physical and thermal properties. Polymers for advanced technologies, 15(11), 669-675.

Bhusari, G. S., Umare, S. S., & Chandure, A. S. (2015). Effects of NCO: OH ratio and HEMA on the physicochemical properties of photocurable poly (ester-urethane) methacrylates. Journal of Coatings Technology and Research, 12, 571-585.

Honarkar, H. (2018). Waterborne polyurethanes: A review. Journal of Dispersion Science and Technology, 39(4), 507-516.

Hwang, H. D., Park, C. H., Moon, J. I., Kim, H. J., & Masubuchi, T. (2011). UV-curing behavior and physical properties of waterborne UV-curable polycarbonate-based polyurethane dispersion. Progress in Organic Coatings, 72(4), 663-675.

Jiménez-López, A. M., & Hincapié-Llanos, G. A. (2022). Identification of factors affecting the reduction of VOC emissions in the paint industry: Systematic literature review-SLR. Progress in Organic Coatings, 170, 106945.

Kang, S. Y., Ji, Z., Tseng, L. F., Turner, S. A., Villanueva, D. A., Johnson, R., & Langer, R. (2018). Design and synthesis of waterborne polyurethanes. Advanced Materials, 30(18), 1706237.

Ma, X., Qiao, Z., Huang, Z., & Jing, X. (2013). The dependence of pendulum hardness on the thickness of acrylic coating. Journal of Coatings Technology and Research, 10, 433-439.

Nanda, A. K., Wicks, D. A., Madbouly, S. A., & Otaigbe, J. U. (2005). Effect of ionic content, solid content, degree of neutralization, and chain extension on aqueous polyurethane dispersions prepared by prepolymer method. Journal of applied polymer science, 98(6), 2514-2520.

Santamaria-Echart, A., Fernandes, I., Barreiro, F., Corcuera, M. A., & Eceiza, A. (2021). Advances in waterborne polyurethane and polyurethane-urea dispersions and their eco-friendly derivatives: A review. Polymers, 13(3), 409.

Szycher, M. (Ed.). (1999). Szycher's handbook of polyurethanes. CRC press.

Wang, X., Cui, Y., Wang, Y., Ban, T., Zhang, Y., Zhang, J., & Zhu, X. (2021). Preparation and characteristics of crosslinked fluorinated acrylate modified waterborne polyurethane for metal protection coating. Progress in Organic Coatings, 158, 106371.

Xu, J., Rong, X., Chi, T., Wang, M., Wang, Y., Yang, D., & Qiu, F. (2013). Preparation, characterization of UV-curable waterborne polyurethane-acrylate and the application in metal iron surface protection. Journal of Applied Polymer Science, 130(5), 3142-3152.

Zareanshahraki, F., Asemani, H. R., Skuza, J., & Mannari, V. (2020). Synthesis of non-isocyanate polyurethanes and their application in radiation-curable aerospace coatings. Progress in Organic Coatings, 138, 105394.

Zhou, X., Li, Y., Fang, C., Li, S., Cheng, Y., Lei, W., & Meng, X. (2015). Recent advances in synthesis of waterborne polyurethane and their application in water-based ink: a review. Journal of Materials Science & Technology, 31(7), 708-722.